

Multi-loop techniques for massless Feynman diagram calculations

A. V. KOTIKOV¹ AND S. TEBER²

¹*Bogoliubov Laboratory of Theoretical Physics, Joint Institute for Nuclear Research, 141980 Dubna, Russia.*
²*Sorbonne Université, CNRS, Laboratoire de Physique Théorique et Hautes Energies, LPTHE, F-75005 Paris, France.*

Abstract

We review several multi-loop techniques for analytical massless Feynman diagram calculations in relativistic quantum field theories: integration by parts, the method of uniqueness, functional equations and the Gegenbauer polynomial technique. A brief, historically oriented, overview of some of the results obtained over the decades for the massless 2-loop propagator-type diagram is given. Concrete examples of up to 5-loop diagram calculations are also provided.

Contents

1	Introduction	3
2	Basics of Feynman diagrams	6
2.1	Notations	6
2.2	Massless vacuum diagrams (and Mellin-Barnes transformation)	8
2.3	Massless one-loop propagator-type diagram	9
3	Massless two-loop propagator-type diagram	11
3.1	Basic definition	11
3.2	Symmetries	12
3.3	Brief historical overview of some results	14
4	Methods of calculations	21
4.1	Parametric integration	22
4.2	Integration by parts	23

4.2.1	Presentation of the method	23
4.2.2	Example of an important application	26
4.3	The method of uniqueness	27
4.4	Transformation of indices	28
4.4.1	Splitting a line into loop	29
4.4.2	Adding a new propagator and a new loop	30
4.4.3	Conformal transform of the inversion	31
4.5	Fourier transform and duality	32
4.6	Functional equations	34
4.6.1	Solution of the functional equations	35
4.6.2	Expansion of $I(1 + a_5\varepsilon)$	38
4.7	Final results for $J(D, p, 1 + a_1\varepsilon, 1 + a_2\varepsilon, 1 + a_3\varepsilon, 1 + a_4\varepsilon, 1 + a_5\varepsilon)$	39
4.8	Three-loop master integrals	40
5	More examples of calculations	42
5.1	Three and four loop calculations in the Φ^4 -model	42
5.2	Five loop calculations in the Φ^4 -model	43
5.2.1	Diagram “a”	44
5.2.2	Diagram “d”	45
6	Conclusion	47
7	Appendix A. Gegenbauer polynomial technique	48
7.1	Presentation of the method	48
7.2	One-loop integral	49
7.3	One-loop integral with traceless products	50
7.4	One-loop integral with Heaviside functions	52
7.5	Application to $I(1 + a)$	53
8	References	53

1 Introduction

In relativistic quantum field theories, the first perturbative techniques using covariance and gauge invariance were independently developed in the 1940s by Tomonaga [1], Schwinger [2] and Feynman [3] and unified by Dyson [4]. This led to the discovery of the concept of renormalization as an attempt to give a meaning to divergent integrals appearing in the perturbative series. Specific ideas of the field theoretic renormalization group (RG) were then developed starting from the 50s [5]-[11]. Early success came from their application to quantum electrodynamics (QED) with unprecedented agreement between high precision experiments and high precision theoretical computations of measurable quantities (anomalous magnetic moment, Lamb's shift, etc...). In the 50s, non-abelian gauge theories were discovered [12] and, in the 60s, the weak interaction was unified with electromagnetism (electro-weak interaction) [13]. In the 70s, 't Hooft and Veltman [14, 15] proved the renormalizability of non-abelian gauge field theories and, to this purpose, invented the dimensional regularization (DR) technique which was also independently discovered in [16, 17, 18]. Combined with the minimal subtraction (MS) scheme [19] within an RG framework, this regularization technique is particularly well suited to compute radiative corrections and we shall use it extensively in this review. In the wake of these far-reaching developments, asymptotic freedom has then been discovered [20, 21]. It eliminates the problem of the Landau poles and allows for the existence of theories which are well defined at arbitrarily low energies. The first example of such a theory is quantum chromodynamics (QCD) which describes quarks as well as their interactions (strong interaction). Contrarily to QED, a perturbative approach to QCD is possible only at high energy. At low energies, a strong coupling regime takes place corresponding to quark confinement. At this point, let us recall that, back in the 70s, 't Hooft discovered a simplification of $U(N)$ gauge theories in the limit of large N [22]. This work initiated the large- N study of gauge theories, see the monograph [23] for a review. Recently, it played an important role in examining the conjecture relating string theories in anti-de Sitter spaces to (the 't Hooft limit of) superconformal field theories in one less space-time dimension (AdS/CFT correspondence) [24]. The most prominent example of such a field theory is the $3 + 1$ -dimensional $\mathcal{N} = 4$ super-Yang-Mills theory at the conformal point which now serves as a kind of theoretical laboratory to gain insight on the beautiful and complex structure of quantum field theories.

The fundamental developments which led to the elaboration of such theories in particle/high-energy physics have had profound consequences in other fields such as statistical mechanics. Formally, a D -dimensional quantum system is equivalent to a $D + 1$ -dimensional (in Euclidean space) statistical mechanics one. Physically, complex systems composed of a large number of interacting particles are subject to emergent phenomena such as phase transitions. It is Wilson that first realized that the vicinity of a second order phase transition may be described by a continuous quantum field theory (QFT) and formulated the so-called momentum-shell RG [25, 26]. This led to the development of the small- ε expansion technique to compute critical exponents by Wilson and Fisher [27] and brought up the important notion of (non-trivial) infrared (IR) fixed points.¹ The works of the Saclay group, see, *e.g.*, [28], led to the development of the field-theoretic Wilsonian RG culminating in the book [29].

The ability to access high order corrections, and therefore achieve high precision calcula-

¹According to [23], the large- N expansion also first appeared in the context of statistical mechanics through the work of Stanley on spin systems [30].

tions, arose in the 80s with the developments of powerful methods to compute renormalization group functions, *i.e.*, β -functions and anomalous dimensions of fields, with wide applications ranging from particle physics, to statistical mechanics and condensed matter physics. These methods include, *e.g.*, the method of infra-red re-arrangement (IRR) [31] and the R^* -operation [32]-[35], the method of uniqueness [36]-[42] and (Vasil'ev's) conformal bootstrap technique [43], integration by parts (IBP) [37, 44, 45], the Gegenbauer polynomial technique [46] and the combination of these methods with symmetry arguments [47, 48]. These techniques were applied to four-dimensional relativistic theories (and their classical analogues) using RG in DR within the MS scheme which is incomparably more efficient computationally than the more physically appealing momentum-shell RG, see the classic monographs: [49, 50] and especially [51] for a beautiful historical introduction; see also the more recent books [52, 53] devoted to Feynman diagram calculations. Among their greatest early achievements, let us mention, *e.g.*, the computation of the 3-loop β -function of QCD [54] and the computation of the 5-loop β -function of Φ^4 -theory [55, 56, 57]. The following decades witnessed further ground-breaking developments, *e.g.*, in discovering dimensional recurrence relations for Feynman diagrams [58, 59], in the exact evaluation of massless Feynman diagram, *e.g.*, [60, 61, 62], in developing and applying new techniques to deal with massive ones, *e.g.*, [63]-[66], in performing high order ϵ -expansions together with understanding some intriguing relations with number theoretical issues, *e.g.*, [62]-[71], in applying such techniques to numerous models, *e.g.*, [72]-[77], in the Hopf-algebraic interpretation of the renormalization group [78, 79], in the notion of a cosmic Galois group [80, 81, 82]...

Throughout the years, there has been a dramatic increase in the complexity of the calculations. Modern challenges often require the manipulation of thousands of diagrams each one of them eventually breaking into hundreds of integrals. Some of the most complicated integrals, the so called "master integrals" [83], require human assistance for their analytic evaluation and will be the subject of this review. Other tasks, on the other hand, are rather systematic in nature as well as highly symbolic: from generating the diagrams, to performing eventual gamma matrix algebra, to reducing large numbers of diagrams to a few master integrals... This led to the automation of such tasks via the developments of powerful computer algebra systems, *e.g.*, from SCHOONSHIP [84], to REDUCE [85], FORM [86], GiNac [87] and the commercial MATHEMATICA [88], see [89] for a short review. Specific algorithms were developed to generate Feynman diagrams, *e.g.*, QGRAF [90] and EXP [91]. Others to deal with the reduction problem such as Laporta's algorithm [92], Baikov's method [93] as well as computer codes combining several algorithms to achieve this task such as REDUZE [94, 95], FIRE [96], KIRA [97] and LiteRed [98]. Some algorithms are devoted to the subtle problems of dealing with subdivergences and generating the Laurent expansion such as, *e.g.*, the sector decomposition technique [99, 100], see also the dissertation of Bogner [101], parametric integration using hyperlogarithms [102], see also the dissertation of Panzer [103] and the nice recent paper [104], the recently discovered method of graphical functions [105] and its combination with parametric integration [106] together with the automation of the R and R^* operators by Batkovich and Kompaniets [107], see also the very recent [108]. Though computer assisted, all these remarkable developments may be considered in some sense as analytical as opposed to the numerical methods only used at the final stage of the procedure in order to extract a numerical value for the coefficients of the Laurent series associated with a given diagram. Often, they involve advanced mathematical concepts from, *e.g.*, graph theory, algebraic geometry and num-

ber theory. Nowadays, computer algebra systems combined with appropriate algorithms are an integral part of the field of multi-loop calculations. For the years 2016/2017 alone, they allowed breakthrough achievements such as, *e.g.*, the 4-loop β -function calculation for the Gross-Neveu [109]², see also [110] for very recent large- N calculations, and Gross-Neveu-Yukawa models [111, 112], the 5-loop β -function calculation for QCD [113], its generalization to an arbitrary gauge group [114, 115, 116] and gauge fixing parameter [117, 118], the 6-loop [119, 120, 121] and 7-loop [122] calculations of the Φ^4 -model renormalization group functions and the 7-loop anomalous dimension calculation of twist-2 operators in planar $\mathcal{N} = 4$ super-Yang-Mills theory with the help of integrability arguments [123].

Having set the general framework, the focus of this review will be on some of the methods that we consider as being the most efficient from the point of view of the purely *analytic* computation of “master integrals”. These integrals may be viewed as basic building blocs at the *core* of multi-loop calculations. Their evaluation is therefore a fundamental task prior to any automation. Their importance is witnessed by the recent appearance of “Loopedia” [124] which attempts at providing a database for all known loop integrals. Many of such integrals related to four-dimensional models were known (but the integrals were scattered throughout various papers) before the enormous developments mentioned above concerning particle physics, statistical mechanics and (supersymmetric) gauge field theories. In other cases such as, *e.g.*, odd dimensional theories relevant to condensed matter physics systems, non-standard master integrals appear the systematic evaluation of which is more recent, see, *e.g.*, [125]-[137].

In the following, we will restrict ourselves to the case of *massless* Feynman integrals focusing in particular on the two-loop massless propagator-type integrals³ which are the most elementary ones yet highly non-trivial in some peculiar cases as we will see. The main emphasis will be on the standard rules of perturbation theory for massless Feynman diagrams as described in the pioneering work of Kazakov [56], see also the beautiful lectures [139]. As will be discussed in details in the review, such rules allow, in principle, the computation of complicated Feynman diagrams using sequences of simple transformations (without any explicit integration). A diagram is straightforwardly integrated once the appropriate sequence is found. In a sense, the method greatly simplifies multi-loop calculations. For a given diagram, the task of finding the sequence of transformations is, however, highly non-trivial. For the most complicated integrals, these rules can be supplemented with the help of the Gegenbauer x -space technique [46] and, in particular, rules for integrating massless diagrams with Heaviside theta functions and traceless products [61]. These rules provide series representation for the diagram which may be a convenient starting point for their ε -expansion.

The manuscript is organized as follows. In Sec. 2, we present the notations as well as the basics of Feynman diagram calculations at one-loop. In Sec. 3, the two-loop massless propagator-type Feynman diagram is presented and a brief historical review of the results concerning this diagram is provided. In Sec. 4, we review some methods of calculations: parametric integration, integration by parts, the method of uniqueness, Fourier transform and duality and functional equations. Excepting for the technique of parametric integration, all the mentioned

²Notice that the lower number of loops presently achieved for the Gross-Neveu model with respect to other models is related to the loss of multiplicative renormalizability of 4-fermion operators in dimensional regularization and the generation of evanescent operators; so calculations for this model are less straightforward than in other models.

³The integrals with many legs are essentially more complicated (see the recent paper [138] and references therein) and their consideration is beyond the scope of this review.

methods allow to compute Feynman integrals without any explicit integration. In Sec. 5, some concrete examples of 5-loop calculations are provided. The conclusion is given in Sec. 6. Finally, App. 7 shortly reviews the Gegenbauer polynomial technique including loop integration with Heaviside theta functions into subintegral expressions.

2 Basics of Feynman diagrams

2.1 Notations

We consider an Euclidean space-time of dimensionality D . Throughout this manuscript we shall use dimensional regularization, see the textbook [49] as well as the early reviews [140, 141] for a more complete account on dimensional regularization and the more recent [142] for a very instructive review on *conventional* dimensional regularization that we actually use, and set, *e.g.*, $D = 4 - 2\varepsilon$ in the case of $(3 + 1)$ -dimensional theories, where $\varepsilon \rightarrow 0$ is the regularization parameter. Then, the infinitesimal volume element, *e.g.*, in momentum space, can be written as:

$$d^4k = \mu^{2\varepsilon} d^Dk, \quad (2.1)$$

where μ is the so-called renormalization scale in the minimal subtraction (MS) scheme which is related to the corresponding parameter $\bar{\mu}$ in the modified minimal subtraction ($\overline{\text{MS}}$) scheme with the help of:

$$\bar{\mu}^2 = 4\pi e^{-\gamma_E} \mu^2, \quad (2.2)$$

where γ_E is Euler's constant. Our main focus will be on *massless Feynman diagrams of the propagator type* (the so called p-integrals [45]). Diagrams will be analyzed mainly in momentum space but position space will also be considered in some cases. In momentum space, Feynman diagrams are defined as integrals over dummy momentum variables or loop momenta. The dependence of these integrals on the external momentum follows from dimensional analysis and is power-like. The goal of the calculations is then to compute the dimensionless coefficient function, C_D , associated with a given diagram (see below). In some peculiar cases this function can be computed exactly. In most cases, only an approximate solution can be found. Often, it takes the form of a Laurent series in ε and of great interest are the coefficients of negative power of ε which may be related to β -functions and anomalous dimensions of fields.

In the following, for simplicity, we shall assume that all algebraic manipulations related to gamma matrices such as, *e.g.*, contraction of Lorentz indices, calculations of traces, etc... have been done.⁴ The diagrams we shall be mainly interested in are therefore expressed in terms of scalar integrals; for completeness, and because they are of practical interest in concrete calculations, we shall also consider diagrams with simple numerators such as traceless products. In reciprocal space, momentum is conserved at each vertex and integrations are over all internal momenta. This has to be contrasted with calculations in real space where integrations are over the coordinates of all vertices. In both spaces, the lines of such diagrams

⁴In some cases, *e.g.*, for n -point functions, a tensorial reduction, the so-called Passarino-Veltman reduction scheme [143], see also [144] for a review, allows to express a tensor integral in terms of scalar ones with tensor coefficients depending on the external kinematic variables and eventually the metric tensor. We assume that such a reduction has been performed and essentially focus on the computation of the scalar integrals. Notice that, at one-loop, the Passarino-Veltman reduction has been automated in packages such as FeynCalc [145, 146], LoopTools [147] and (combined with FeynArts [148]) FormCalc [149].

2.2 Massless vacuum diagrams (and Mellin-Barnes transformation)

In the frame of dimensional regularization, the one-loop massless vacuum diagram obeys the following identity [150]:

$$\textcircled{\alpha} = \int \frac{d^D k}{(k^2)^\alpha} = i\pi \Omega_D \delta(\alpha - D/2), \quad (2.9)$$

where $\Omega_D = 2\pi^{D/2}/\Gamma(D/2)$ is the surface of the unit hypersphere in D -dimensional Euclidean space-time. One way to check the consistency of this relation is to consider the Mellin-Barnes transformation of a massive scalar propagator [151, 63]:

$$\frac{1}{(k^2 + m^2)^\alpha} = \frac{1}{2i\pi\Gamma(\alpha)} \int_{-i\infty}^{i\infty} ds \frac{(m^2)^s}{(k^2)^{s+\alpha}} \Gamma(-s)\Gamma(\alpha + s). \quad (2.10)$$

Interestingly, this transformation allows to express a massive propagator in terms of a contour integral involving a massless one. As noticed by Boos and Davydychev [63], this suggests that techniques for computing massless Feynman diagrams may be of importance to compute massive ones. For our present purpose, only the expression of the massive one-loop tadpole integral will be useful.⁵ It reads:

$$\int \frac{[d^D k]}{(k^2 + m^2)^\alpha} = \frac{(m^2)^{D/2-\alpha}}{(4\pi)^{D/2}} \frac{\Gamma(\alpha - D/2)}{\Gamma(\alpha)}, \quad (2.11)$$

where the mass dependence follows from dimensional analysis and the dimensionless factor $\Gamma(\alpha - D/2)/\Gamma(\alpha)$ corresponds to the coefficient function of this simple diagram. Eq. (2.11) can be straightforwardly obtained using the standard parametric integration technique, see Sec. 4.1. It can also be obtained using the Mellin-Barnes transformation (2.10) upon assuming that Eq. (2.9) holds. This proves the consistency of Eq. (2.9).

There is a connection between v-integrals and p-integrals, see Ref. [150]. The latter may be derived by turning a p-integral into a v-integral upon multiplying it by $(p^2)^{-\sigma}$ and integrating over p .⁶ From Eq. (2.7), such a procedure yields:

$$\begin{aligned} \textcircled{\sigma} &= \frac{C_D(\vec{\alpha})}{(4\pi)^{\frac{LD}{2}}} \int \frac{d^D p}{(p^2)^{\sigma + \sum_{i=1}^N \alpha_i - \frac{LD}{2}}} \\ &= \frac{i\pi}{(4\pi)^{\frac{LD}{2}}} \Omega_D C_D(\vec{\alpha}) \delta\left(\sigma + \sum_{i=1}^N \alpha_i - \frac{LD}{2}\right) \end{aligned} \quad (2.12a)$$

$$= \frac{i\pi}{(4\pi)^{\frac{LD}{2}}} \Omega_D X_D(\vec{\alpha}, \sigma) \delta\left(\sigma + \sum_{i=1}^N \alpha_i - \frac{LD}{2}\right). \quad (2.12b)$$

Hence, the coefficient functions of the v-type diagram, X_D , and the p-type diagram, C_D , are related by:

$$C_D(\vec{\alpha}) = X_D(\vec{\alpha}, \sigma)|_{\sigma = \frac{LD}{2} - \sum_{i=1}^N \alpha_i}. \quad (2.13)$$

⁵See, *e.g.*, Refs. [151]-[155] for more examples of the use of the Mellin-Barnes transformation in Feynman diagram calculations.

⁶This is also known as gluing, see Ref. [45] and [156] for a recent review.

As can be noticed from Eq. (2.9), vacuum diagrams are rather ambiguously defined within dimensional regularization. Their scaleless nature does not provide any clue of what their actual value might be a priori: it can be zero, infinity or even some finite number, see also the review [140]. This results from a subtle interplay between infrared and ultraviolet divergences of massless diagrams. Following t'Hooft and Veltman, we shall often assume that the continuous dimension regularizes such highly divergent integrals to *zero*. Similarly, whenever a diagram contains a scaleless subdiagram, *e.g.*, such as the massless tadpole diagram, its value will be set to zero. In principle, however, care must be taken in the case where $D = 2\alpha$. On the other hand, the consequence of Eq. (2.9) is unambiguous for integrals over polynomials corresponding to the case where $\alpha < 0$ in (2.9); within dimensional regularization such integrals vanish identically. Summarizing, in the following, we shall always assume that:⁷

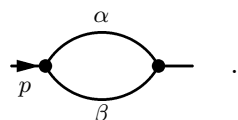
$$\int \frac{d^D k}{(k^2)^\alpha} = 0 \quad (\alpha \neq D/2). \quad (2.14)$$

2.3 Massless one-loop propagator-type diagram

The one-loop (scalar) p-type massless integral is defined as:

$$J(D, p, \alpha, \beta) = \int [d^D k] \frac{1}{k^{2\alpha}(p-k)^{2\beta}}, \quad (2.15)$$

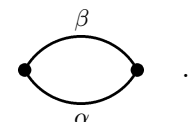
where p is the external momentum and α and β are arbitrary indices. In graphical form it is represented as:

$$J(D, p, \alpha, \beta) = \text{Diagram} \quad (2.16)$$


In Eq. (2.15), the momentum dependence is easily extracted from dimensional analysis which allows to write the diagram in the following form:

$$J(D, p, \alpha, \beta) = \frac{(p^2)^{D/2-\alpha-\beta}}{(4\pi)^{D/2}} G(D, \alpha, \beta), \quad (2.17)$$

where $G(D, \alpha, \beta)$ is the (dimensionless) coefficient function of the diagram. In graphical form, the latter is represented by a diagram similar to the one for $J(D, p, \alpha, \beta)$ but with amputated external legs:

$$G(D, \alpha, \beta) = C_D \left[\int \frac{[d^D k]}{k^{2\alpha}(p-k)^{2\beta}} \right] = \text{Diagram} \quad (2.18)$$


In the one-loop case, the so-called G -function is known exactly and reads:

$$G(D, \alpha, \beta) = \frac{a(\alpha)a(\beta)}{a(\alpha + \beta - D/2)}, \quad a(\alpha) = \frac{\Gamma(D/2 - \alpha)}{\Gamma(\alpha)}. \quad (2.19)$$

⁷In the case where $\alpha = D/2$ is encountered, it is also possible to use the following trick: introduce a regulator $\delta \rightarrow 0$ shifting the index α , *e.g.*, $\alpha \rightarrow \alpha + \delta$. The limit $\delta \rightarrow 0$ is taken at the end of the calculation. See Ref. [126] for an example.

All these results may be generalized to integrands with numerators. In particular:

$$J^{\mu_1 \cdots \mu_n}(D, p, \alpha, \beta) = \int [d^D k] \frac{k^{\mu_1 \cdots \mu_n}}{k^{2\alpha}(p-k)^{2\beta}} = \frac{(p^2)^{D/2-\alpha-\beta}}{(4\pi)^{D/2}} p^{\mu_1 \cdots \mu_n} G^{(n,0)}(D, \alpha, \beta), \quad (2.20)$$

where $k^{\mu_1 \cdots \mu_n}$ denotes the traceless product and

$$G^{(n,0)}(D, \alpha, \beta) = \frac{a_n(\alpha)a_0(\beta)}{a_n(\alpha + \beta - D/2)}, \quad a_n(\alpha) = \frac{\Gamma(n + D/2 - \alpha)}{\Gamma(\alpha)}, \quad (2.21)$$

where $G(D, \alpha, \beta) \equiv G^{(0,0)}(D, \alpha, \beta)$ and, for simplicity, the argument D is also sometimes dropped unless an ambiguity may arise. Graphically, a one-loop p-type diagram with numerator can be represented as:

$$G^{(1,0)}(D, \alpha, \beta) = C_D \left[\int \frac{[d^D k] k^\mu}{k^{2\alpha}(p-k)^{2\beta}} \right] = \begin{array}{c} \alpha^\mu \\ \curvearrowright \\ \bullet \quad \bullet \\ \beta \\ \curvearrowleft \end{array} = - \begin{array}{c} \alpha^\mu \\ \curvearrowleft \\ \bullet \quad \bullet \\ \beta \\ \curvearrowright \end{array}. \quad (2.22)$$

Whenever the integrand contains a scalar product, the corresponding lines are arrowed. As an example:

$$C_D \left[\int \frac{[d^D k] (k, p-k)}{k^{2\alpha}(p-k)^{2\beta}} \right] = \begin{array}{c} \alpha^\mu \\ \curvearrowright \\ \bullet \quad \bullet \\ \beta_\mu \\ \curvearrowleft \end{array} = \begin{array}{c} \alpha^\mu \\ \curvearrowleft \\ \bullet \quad \bullet \\ \beta_\mu \\ \curvearrowright \end{array} = - \begin{array}{c} \alpha^\mu \\ \curvearrowright \\ \bullet \quad \bullet \\ \beta_\mu \\ \curvearrowleft \end{array}, \quad (2.23)$$

where the notation $(k, p) = k^\mu p_\mu$ denotes the scalar product of the D -dimensional momenta k and p . When such a diagram is encountered, it can be evaluated as:

$$\begin{array}{c} \alpha^\mu \\ \curvearrowright \\ \bullet \quad \bullet \\ \beta_\mu \\ \curvearrowleft \end{array} = - \begin{array}{c} \alpha - 1 \\ \curvearrowright \\ \bullet \quad \bullet \\ \beta \\ \curvearrowleft \end{array} + \begin{array}{c} \alpha^\mu \\ \curvearrowright \\ \bullet \quad \bullet \\ p_\mu \\ \beta \\ \curvearrowleft \end{array} = -G(D, \alpha - 1, \beta) + G^{(1,0)}(D, \alpha, \beta), \quad (2.24)$$

where, in the third diagram, the internal momentum is dotted with an external one. Hence:

$$\int \frac{[d^D k] (k, p-k)}{k^{2\alpha}(p-k)^{2\beta}} = \frac{(p^2)^{D/2+1-\alpha-\beta}}{(4\pi)^{D/2}} \left(G^{(1,0)}(D, \alpha, \beta) - G(D, \alpha - 1, \beta) \right). \quad (2.25)$$

The expression of $G(D, \alpha, \beta)$ given above may be derived by using parametric integration, see Sec. 4.1. Following Ref. [139], an alternative simple derivation consists in first going to x -space using Eq. (2.6) and then going back to p -space:

$$\begin{aligned} \int \frac{d^D k}{k^{2\alpha}(p-k)^{2\beta}} &= \frac{a(\alpha)a(\beta)}{\pi^D 2^{2(\alpha+\beta)}} \int \frac{d^D x d^D y d^D k e^{-ikx-i(p-k)y}}{[x^2]^{D/2-\alpha} [y^2]^{D/2-\beta}} \\ &= \frac{a(\alpha)a(\beta)}{2^{2(\alpha+\beta)-D}} \int \frac{d^D x e^{-ipx}}{[x^2]^{D-\alpha-\beta}} \\ &= \pi^{D/2} \frac{a(\alpha)a(\beta)}{a(\alpha + \beta - D/2)} \frac{1}{[p^2]^{\alpha+\beta-D/2}}. \end{aligned}$$

This leads to Eq. (2.19).

An important property of the G -function is that it vanishes whenever one (or more) of the indices is zero or a negative *integer*:

$$G(D, n, m) = 0, \quad n \leq 0, \quad m \leq 0. \quad (2.26)$$

This property follows from the fact that a massless one-loop p-integral with a zero or negative integer index corresponds to a massless vacuum diagram (possibly with a polynomial numerator) which vanishes according to Eqs. (2.14) (provided the case $D = 2\alpha$ is not encountered).

Finally, the G -function informs about the singularities of Eq. (2.15). The latter can be either ultraviolet or infrared in nature. In both cases, they will appear as $1/\varepsilon$ poles in the expression of the G -function as dimensional regularization treats both types of singularities on an equal footing. In order to see that, let's note that from dimensional analysis Eq. (2.15) has an ultraviolet singularity ($k \rightarrow \infty$) for $\alpha + \beta \leq D/2$; on the other hand, it has an infrared singularity ($k \rightarrow 0$) for $\alpha \geq D/2$ and/or $\beta \geq D/2$. Then, from the explicit expression of $G(D, \alpha, \beta)$ in terms of Γ -functions:

$$G(D, \alpha, \beta) = \frac{\Gamma(D/2 - \alpha)\Gamma(D/2 - \beta)\Gamma(\alpha + \beta - D/2)}{\Gamma(\alpha)\Gamma(\beta)\Gamma(D - \alpha - \beta)}, \quad (2.27)$$

we see that poles coming from either one of the first two Γ -functions in the numerator are IR poles while those coming from the last Γ -function in the numerator are UV poles.

3 Massless two-loop propagator-type diagram

3.1 Basic definition

Central to this manuscript is the massless two-loop propagator-type diagram which is defined as:

$$J(D, p, \alpha_1, \alpha_2, \alpha_3, \alpha_4, \alpha_5) = \int \frac{[d^D k][d^D q]}{(k-p)^{2\alpha_1} (q-p)^{2\alpha_2} q^{2\alpha_3} k^{2\alpha_4} (k-q)^{2\alpha_5}}, \quad (3.28)$$

where p is the external momentum and the α_i , $i = 1 - 5$, are five arbitrary indices. In graphical form, it is represented as:

$$J(D, p, \alpha_1, \alpha_2, \alpha_3, \alpha_4, \alpha_5) = \text{Diagram} \quad (3.29)$$

Similarly to the one-loop case, the momentum dependence of Eq. (3.28) follows from dimensional analysis which allows to write this diagram in the form:

$$J(D, p, \alpha_1, \alpha_2, \alpha_3, \alpha_4, \alpha_5) = \frac{(p^2)^{D - \sum_{i=1}^5 \alpha_i}}{(4\pi)^D} G(D, \alpha_1, \alpha_2, \alpha_3, \alpha_4, \alpha_5), \quad (3.30)$$

where the (dimensionless) coefficient function of the diagram, $G(D, \{\alpha_i\})$, has been defined according to the general case Eq. (2.7). Graphically, the latter is represented as:

$$G(D, \alpha_1, \alpha_2, \alpha_3, \alpha_4, \alpha_5) = C_D [J(D, p, \alpha_1, \alpha_2, \alpha_3, \alpha_4, \alpha_5)] = \text{Diagram} \quad (3.31)$$

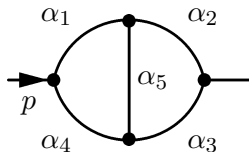


Figure 1: Two-loop scalar massless propagator-type diagram.

As in the one-loop case, whenever the integrand contains a scalar product, the corresponding lines are arrowed. As an example:

$$C_D \left[\int \frac{[d^D k][d^D q] (k - q, q - p)}{(k - p)^{2\alpha_1} (q - p)^{2\alpha_2} q^{2\alpha_3} k^{2\alpha_4} (k - q)^{2\alpha_5}} \right] = \text{Diagram} \quad (3.32)$$

As another example, we may consider the case where the scalar product involves the external momentum:

$$C_D \left[\int \frac{[d^D k][d^D q] (p, q)}{(k - p)^{2\alpha_1} (q - p)^{2\alpha_2} q^{2\alpha_3} k^{2\alpha_4} (k - q)^{2\alpha_5}} \right] = \text{Diagram} \quad (3.33)$$

Notice that there is a single topological class of two-loop propagator-type diagrams represented in Fig. 1. In some cases, two-loop diagrams may be reduced to products of one-loop diagrams (and hence products of Γ -functions) and are said to be *primitively one-loop*, or *recursively one-loop*, diagrams [45]; some examples of the later are given in Fig. 2. In general, however, no simple expression is known for the diagram of Fig. 1 with five arbitrary indices.

3.2 Symmetries

Symmetries are important because they yield identities among the coefficient functions with changed indices. We shall introduce a number of other such identities which follow from non-trivial transformations in the following sections. An appropriate use of identities among diagrams with different indices is central to multi-loop calculations and very often significantly reduces the amount of computations which has to be done. As a matter of fact, these identities, when used in an appropriate way, may reduce a considerable number of two-loop diagrams to primitively one-loop ones leaving only a small set of truly two-loop diagrams. As already mentioned in the Introduction, following Broadhurst, the set of irreducible integrals (at 1, 2 or higher loop order) is referred to as the *master integrals* [83].

We start with some basic symmetries of the diagram which follow from changing the integration variables in Eq. (3.28):

- the invariance of the integral upon changing $k \leftrightarrow q$ implies that the diagram is invariant under the change $1 \leftrightarrow 2$ and $3 \leftrightarrow 4$. Geometrically, this can be viewed as an invariance of the diagram in a reflection through the plane perpendicular to the diagram and containing the line of index α_5 . At the level of the coefficient function, Eq. (3.30), this yields the following trivial identity:

$$G(D, \alpha_1, \alpha_2, \alpha_3, \alpha_4, \alpha_5) = G(D, \alpha_2, \alpha_1, \alpha_4, \alpha_3, \alpha_5). \quad (3.34)$$

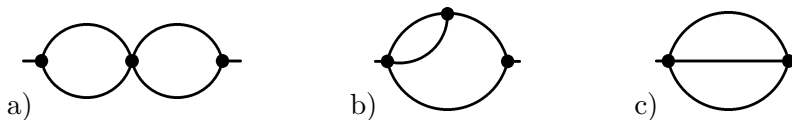


Figure 2: Two-loop primitive, or recursively one-loop, diagrams. Diagram a) corresponds to $\alpha_5 = 0$. Diagram b) corresponds to $\alpha_4 = 0$. Diagram c) corresponds to $\alpha_1 = \alpha_3 = 0$.

- the invariance of the integral upon changing $k \leftrightarrow k - p$ and $q \leftrightarrow q - p$ implies that the diagram is invariant under the change $1 \leftrightarrow 4$ and $2 \leftrightarrow 3$. Geometrically, this can be viewed as an invariance of the diagram in a reflection through the plane perpendicular to the diagram and to the line of index α_5 . This yields the following trivial identity among the coefficient functions with changed indices:

$$G(D, \alpha_1, \alpha_2, \alpha_3, \alpha_4, \alpha_5) = G(D, \alpha_4, \alpha_3, \alpha_2, \alpha_1, \alpha_5). \quad (3.35)$$

It turns out that the 2-loop diagram is invariant under a very large group: $Z_2 \times S_6$ which has 1,440 elements [47, 48]. Historically, some of the symmetry properties of the diagram were observed by the St Petersburg group [37] (see also the textbook [51]). A few years later, the study of Gorishny and Isaev [150] clearly revealed that the diagram has a full tetrahedral symmetry. To demonstrate this, they used the relation between the coefficient functions of the 2-loop p-integral and the related 3-loop v-integral. From Eq. (2.13), this relation reads:⁸

$$G(D, \alpha_1, \alpha_2, \alpha_3, \alpha_4, \alpha_5) = X_D(\vec{\alpha}, \sigma)|_{\sigma=D-\sum_{i=1}^5 \alpha_i}. \quad (3.36)$$

The 3-loop v-integral has the full tetrahedral symmetry. The coefficient function X_D is therefore invariant under the permutations of the indices corresponding to the elements of the full tetrahedral group (rotations and reflections) which is isomorphic to S_4 , the symmetric group of 4 elements (the vertices of the tetrahedron). This group has $4! = 24$ elements and 3 generators;⁹ for example: rotations around 2 axes passing by some vertex and the center of the opposite side and one reflection. The generating elements can, for example, be chosen as: the rotation axes passing through the vertices $(\alpha_1, \alpha_5, \alpha_2)$ and $(\alpha_1, \sigma, \alpha_4)$ and a reflection corresponding to the permutation of the two vertices $(\alpha_1, \alpha_2, \alpha_5)$ and $(\alpha_3, \alpha_4, \alpha_5)$ (similar to the transformation $(1 \leftrightarrow 4, 2 \leftrightarrow 3)$). For the v-integral, this yields:

$$X_D(\alpha_1, \alpha_2, \alpha_3, \alpha_4, \alpha_5, \sigma) = X_D(\alpha_4, \sigma, \alpha_2, \alpha_5, \alpha_1, \alpha_3) \quad (3.37a)$$

$$= X_D(\alpha_4, \alpha_5, \alpha_2, \sigma, \alpha_3, \alpha_1), \quad (3.37b)$$

$$= X_D(\alpha_4, \alpha_3, \alpha_2, \alpha_1, \alpha_5, \sigma). \quad (3.37c)$$

Then, cutting one line of the v-integral to transform it into a p-integral yields:

$$G(D, \alpha_1, \alpha_2, \alpha_3, \alpha_4, \alpha_5) = G(D, \alpha_2, \alpha_5, \alpha_4, \frac{3D}{2} - \sum_i \alpha_i, \alpha_1), \quad (3.38a)$$

⁸This is again the gluing (or glue and cut) method, see Ref. [45] and [156] for a recent review.

⁹There are two possible sets of generators for the symmetric group S_n :

- $n - 1$ generators formed by the transpositions $(12), (23), \dots, (n-1, n)$,
- 2 generators formed by a transposition (12) and an n-cycle: $(12 \dots n)$.

$$= G(D, \alpha_4, \alpha_5, \alpha_2, \frac{3D}{2} - \sum_i \alpha_i, \alpha_3), \quad (3.38b)$$

$$= G(D, \alpha_4, \alpha_3, \alpha_2, \alpha_1, \alpha_5). \quad (3.38c)$$

The last transformation in Eq. (3.38) is the same as the one of Eq. (3.35). Combining the 3 transformations of Eq. (3.38) one generates all the possible transformations of indices of the 2-loop diagram compatible with the tetrahedral symmetry.

Gorishny and Isaev further noted that the 2-loop diagram is invariant under another transformation which follows from the uniqueness relation (see Sec. 4.3 for more on uniqueness):

$$\begin{aligned} & C_D[J(D, p, \alpha_1, \alpha_2, \alpha_3, \alpha_4, \alpha_5)] \\ &= a(\alpha_2)a(\alpha_3)a(\alpha_5)a(D - t_2) C_D[J(D, p, \alpha_1, \tilde{\alpha}_3, \tilde{\alpha}_2, \alpha_4, t_2 - D/2)], \end{aligned} \quad (3.39)$$

where $\tilde{\alpha} = D/2 - \alpha$ and $t_2 = \alpha_2 + \alpha_3 + \alpha_5$. The existence of this additional transformation suggests that the symmetry group of the 2-loop diagram is larger than S_4 . As a matter of fact, instead of the 3 generators of Eq. (3.37) we could have chosen one transposition and a 6-cycle:

$$X_D(\alpha_1, \alpha_2, \alpha_3, \alpha_4, \alpha_5, \sigma) = X_D(\alpha_2, \alpha_1, \alpha_3, \alpha_4, \alpha_5, \sigma), \quad (3.40a)$$

$$= X_D(\sigma, \alpha_1, \alpha_2, \alpha_3, \alpha_4, \alpha_5). \quad (3.40b)$$

The transformations of Eq. (3.40) generate the group S_6 . Furthermore, the transformation of Eq. (3.39) involves dual indices $\alpha \rightarrow D/2 - \alpha$ suggesting that there might be an additional Z_2 symmetry. That the actual group is indeed $Z_2 \times S_6$, which has $2 \times 6! = 1,440$ elements, was realized by Broadhurst [47] soon after the work of Gorishny and Isaev. The 3 generators of the $Z_2 \times S_6$ group are: a transposition and a 6-cycle which generate S_6 ; and the dual transformation $\alpha_i \rightarrow D/2 - \alpha_i$ which generates Z_2 . Broadhurst [47] and then Barfoot and Broadhurst [48] not only defined the symmetry group but also gave the set of 10 group invariants. As we shall review in the next paragraph, this allowed a more accurate expansion of the massless 2-loop propagator-type diagram.

3.3 Brief historical overview of some results

The importance of the 2-loop massless propagator-type diagram of Fig. 1 comes from the fact that it is a basic building block of many multi-loop calculations. As such, it has been extensively studied during the last three decades, see Ref. [157, 69] for historical reviews. In this section, we shall review some results obtained for this diagram over the years.

Generally speaking, when all indices are integers the 2-loop massless propagator-type diagram is easily computed. One of the earliest and most well-known result is the one due to Chetyrkin, Kataev and Tkachov [46] who found an exact expression for $G(D, 1, 1, 1, 1, 1)$ with the help of the Gegenbauer polynomial technique (see App. 7 for an introduction to the latter). Soon after, the exact result for $G(D, 1, 1, 1, 1, 1)$ could be re-obtained in a much more simple and straightforward way by Vasiliev et al. [37], Tkachov [44] as well as Chetyrkin and Tkachov [45] using integration by parts (see Sec. 4.2 for more on IBP). The result reads:

$$G(D, 1, 1, 1, 1, 1) = \frac{2}{D-4} [G(D, 1, 1)G(D, 1, 2) - G(D, 1, 1)G(D, 2, 3 - D/2)], \quad (3.41)$$

where $G(D, \alpha, \beta)$ is the coefficient function of the one-loop p-type integral, Eq. (2.19). The fact that $G(D, 1, 1, 1, 1, 1)$ reduces to products of G -functions implies that this peculiar 2-loop diagram is actually primitively one-loop. It can therefore be expressed in terms of Γ -functions:

$$G(4 - 2\varepsilon, 1, 1, 1, 1, 1) = \frac{\Gamma(1 + 2\varepsilon)}{\varepsilon^3 (1 - 2\varepsilon)} \left[\frac{\Gamma^4(1 - \varepsilon)\Gamma^2(1 + \varepsilon)}{\Gamma^2(1 - 2\varepsilon)\Gamma(1 + 2\varepsilon)} - \frac{\Gamma^3(1 - \varepsilon)}{\Gamma(1 - 3\varepsilon)} \right], \quad (3.42)$$

where the case $D = 4 - 2\varepsilon$ has been considered. From dimensional analysis, $G(4 - 2\varepsilon, 1, 1, 1, 1, 1)$ is expected to be UV finite with no $1/\varepsilon$ poles. This can be checked explicitly by writing it in expanded form and keeping only the first few terms for short:¹⁰

$$G(4 - 2\varepsilon, 1, 1, 1, 1, 1) = \frac{e^{-2\gamma_E\varepsilon - \zeta_2\varepsilon^2}}{1 - 2\varepsilon} \left(6\zeta_3 + 9\zeta_4\varepsilon + 42\zeta_5\varepsilon^2 + (90\zeta_6 - 46\zeta_3^2)\varepsilon^3 + (294\zeta_7 - 135\zeta_3\zeta_4)\varepsilon^4 + \mathcal{O}(\varepsilon^5) \right), \quad (3.43)$$

where the expansion formula for Gamma functions has been used:

$$\Gamma(1 + x) = \exp \left(-\gamma_E x + \sum_{n=2}^{\infty} \frac{(-1)^n}{n} \zeta_n x^n \right), \quad (3.44)$$

and ζ_n is the Riemann zeta function which is defined as:

$$\zeta_s = \zeta(s) = \sum_{n=1}^{\infty} \frac{1}{n^s} \quad (\Re s > 1). \quad (3.45)$$

In Eq. (3.43), the $\mathcal{O}(1)$ term reduces to the celebrated ζ_3 and all coefficients of higher order ε terms can be expressed in terms of zeta functions. The authors of [45] also noticed that the functions $G(D, \alpha_1, 1, 1, \alpha_4, 1)$ as well as $G(D, \alpha_1, \alpha_2, 1, 1, 1)$, where α_1, α_2 and α_4 are arbitrary indices, can also be computed exactly using IBP. This follows from the so-called *rule of triangles* [45] whereby the 2-loop diagram can be exactly computed with the help of IBP whenever three adjacent lines have integer indices, see Fig. 3. For completeness, we give their expressions [45] (see Sec. 4.2.2 for a derivation of the first identity):

$$G(D, \alpha_1, 1, 1, \alpha_4, 1) = \frac{G(D, 1, 1)}{D - \alpha_1 - \alpha_4 - 2} \left[\alpha_1 G(D, 1 + \alpha_1, \alpha_4) - \alpha_1 G(D, 1 + \alpha_1, 2 + \alpha_4 - D/2) + \alpha_4 G(D, \alpha_1, 1 + \alpha_4) - \alpha_4 G(D, 2 + \alpha_1 - D/2, 1 + \alpha_4) \right], \quad (3.46a)$$

$$G(D, \alpha_1, \alpha_2, 1, 1, 1) = \frac{2(1 + \alpha_1 + \alpha_2 - D/2)}{(D - 3)(D - 4)} \left[\alpha_1 G(D, 1, 1 + \alpha_1) G(D, 1, \alpha_1 + \alpha_2 + 2 - D/2) + \{\alpha_2 \leftrightarrow \alpha_1\} \right] - \frac{2\alpha_1\alpha_2}{(D - 3)(D - 4)} G(D, 1, 1 + \alpha_1) G(D, 1, 1 + \alpha_2). \quad (3.46b)$$

¹⁰Notice that in Eq. (3.43), we have used a scheme in which γ_E and ζ_2 were subtracted from the remaining ε -expansion. There are several other such schemes, e.g., the G -scheme [46], see Eq. (3.65), where a factor of $G^l(\varepsilon)$ is extracted from every l -loop diagram and may be absorbed in a redefinition of the renormalization scale μ . As they resum part of the ε -expansion, these schemes appear to converge faster than the $\overline{\text{MS}}$ scheme.



Figure 3: Some simple two-loop massless propagator diagrams which satisfy the rule of triangle and can be computed exactly using IBP identities.

These functions can be expanded for arbitrary indices α_1 , α_2 and α_4 in $D = n - 2\varepsilon$ ($n \in \mathbb{N}^*$) with the help of:

$$\Gamma(x + \varepsilon) = \Gamma(x) \exp \left[\sum_{k=1}^{\infty} \psi^{(k-1)}(x) \frac{\varepsilon^k}{k!} \right], \quad (3.47)$$

where $\psi^{(k)}$ is the polygamma function of order k :

$$\psi(x) = \psi^{(0)}(x) = \frac{\Gamma'(x)}{\Gamma(x)}, \quad \psi^{(k)}(x) = \frac{d^k}{dx^k} \psi(x), \quad (3.48)$$

$\psi(x)$ being the digamma function and $\psi'(x) = \psi^{(1)}(x)$ the trigamma function.

On the other hand, for arbitrary (non-integer) values of all the indices, the evaluation of the massless 2-loop p-type integral is highly non-trivial (even for the lowest order coefficients of the ε -expansion) and peculiar cases have to be considered, see, *e.g.*, Refs. [46]-[69]. In the case where all the indices take the form:¹¹ $\alpha_i = n_i + a_i\varepsilon$, where the n_i are positive integers and the a_i are non-negative real numbers, the diagram is known only in the form of an ε -expansion. For $n_i = 1$, arbitrary a_i and $D = 4 - 2\varepsilon$, an expansion to order ε^3 could be carried out in the seminal paper of Kazakov using the method of uniqueness [39], see also Sec. 4. Using functional identities among complicated diagrams, Kazakov further managed to extend his computation to order ε^4 [56, 57]. Then, using the symmetry arguments outlined in Sec. 3.2, Broadhurst [47] and then Barfoot and Broadhurst [48] managed to extend the computation to order ε^5 and then ε^6 , respectively. Subsequently, the orders ε^7 and ε^8 were computed by Broadhurst, Gracey and Kreimer [62]. After two decades of calculations, an expansion to order ε^9 was achieved in Ref. [68]. At this point, number theoretical issues were raised, see, *e.g.*, [68] and references therein. It was known since the early days of quantum field theory that the Riemann zeta function, Eq. (3.45), often arises in Feynman diagram computations. More complicated diagrams depending on an additional scale, such as massive propagator-type Feynman diagrams, were also known to be expressed in terms of the polylogarithm. This function is a generalization of the zeta function and is defined as:

$$\text{Li}_s(z) = \sum_{n=1}^{\infty} \frac{z^n}{n^s}, \quad (3.49)$$

where $\text{Li}_1(z) = -\log(1 - z)$ and $\text{Li}_s(1) = \zeta_s$ with $s \geq 2$. Other generalizations relevant to multi-loop massless Feynman diagrams include multiple zeta functions, also known as multiple

¹¹Indices of this kind appear when considering multi-loop Feynman diagrams with integer indices. Upon integrating some of the subdiagrams using, *e.g.*, IBP or another technique, the diagram transforms into a diagram with less loops but having lines where the integer indices are shifted by ε quantities.

zeta values (MZV) or Euler sums; they are defined as:

$$\zeta_{s_1, s_2, \dots, s_l} = \zeta(s_1, s_2, \dots, s_l) = \sum_{n_1 > n_2 > \dots > n_l > 0} \frac{1}{n_1^{s_1} n_2^{s_2} \dots n_l^{s_l}} \quad (s_1 > 1, s_2, \dots, s_l \in \mathbb{N}), \quad (3.50)$$

where the integer l is referred to as the *length* of the multiple zeta value and $s = \sum_{i=1}^l s_i$ to its *weight*. In general, they reduce to zeta functions, *e.g.*, $\zeta(2, 2) = (3/4)\zeta(4)$, $\zeta(3, 2) = 3\zeta(2)\zeta(3) - (11/2)\zeta(5)$, etc... In some cases they are irreducible, *e.g.*, at length 2 and weight 8, $\zeta(6, 2)$ cannot be written in terms of zeta functions. Multiple zeta functions are themselves a peculiar case of the multiple polylogarithm:

$$\text{Li}_{s_1, s_2, \dots, s_l}(z_1, z_2, \dots, z_l) = \sum_{n_1 > n_2 > \dots > n_l > 0} \frac{z_1^{n_1} z_2^{n_2} \dots z_l^{n_l}}{n_1^{s_1} n_2^{s_2} \dots n_l^{s_l}}, \quad (3.51)$$

which appears in multi-scale Feynman diagrams. The important question that is then asked is whether Feynman diagrams (and in particular the coefficients of the ε expansion) can be fully expressed in terms of the zeta functions, Eq. (3.45), or generalization of these functions such as the multiple zeta functions and multiple polylogarithms? In the general case, this question is very difficult to answer. At this point, let's note that in the case of massive propagator-type diagrams, it is well known that, starting from two-loops, there are integrals which cannot be expressed in terms of multiple polylogarithms. The simplest examples are given by the two-loop sunrise and kite integrals, which can be expressed in terms of Elliptic polylogarithms, see the recent review [158] and references therein. Even more complicated integrals containing structures beyond multiple polylogarithms have been considered recently in [159].

Returning to the massless two-loop p-type integral $J(D, p, \alpha_1, \alpha_2, \alpha_3, \alpha_4, \alpha_5)$ of Eq. (3.28), shown in Fig. 1, we would like to note that progress appeared in 2003 with the work of Bierenbaum and Weinzierl [69]. For $\alpha_i = n_i + a_i\varepsilon$ and $D = 2m - 2\varepsilon$ ($m \in \mathbb{N}$), they managed to automate its ε -expansion; in principle, their computer assisted method allows an expansion to arbitrary order in ε the only restrictions arising from hardware constraints. Furthermore, they proved the following important theorem [69]:¹²

Theorem 1 (Bierenbaum and Weinzierl (2003)) *Multiple zeta values are sufficient for the Laurent expansion of the two-loop integral, $G(D, \alpha_1, \alpha_2, \alpha_3, \alpha_4, \alpha_5)$, with $D = 2m - 2\varepsilon$ ($m \in \mathbb{N}$) if all powers of the propagators are of the form $\alpha_i = n_i + a_i\varepsilon$ where the n_i are positive integers and the a_i are non-negative real numbers.*

On a more “phenomenological” level, a principle of “maximum weight” or “maximal transcendentality” was discovered in Refs. [62], [160]-[163]¹³ (some reviews can be found in [164]). In very simple terms, this property can be checked at the level of the elementary example provided by Eq. (3.43). For this, let's assume that the transcendentality level of ζ_s is s and the one of ε is -1 . Then, we see that all displayed terms of the ε -expansion have transcendentality 3. Such an observation strongly constrains the coefficients of the series and, when judiciously used, sometimes allows to reconstruct a whole series from the knowledge of the first few terms, see examples in [160].

¹²Some generalization of the theorem appeared in Refs. [70, 71].

¹³We were informed by David Broadhurst that this principle appears to be first due to John Gracey in an example of supersymmetric nonlinear sigma model preceding Ref. [62].

It turns out that, unfortunately, none these powerful theorems and beautiful observations hold in the case of odd-dimensional field theories and related expansions in the vicinity of non-integer indices that we will be concerned with in the following. From the few existing studies, one may anticipate that odd-dimensional theories are “transcendentally” more complex than even dimensional ones [67]. As a simple example, let’s reconsider Eq. (3.41) in $D = 3 - 2\varepsilon$. In this case:

$$G(3 - 2\varepsilon, 1, 1, 1, 1, 1) = -2 \frac{\Gamma(1 + 2\varepsilon)}{1 + 2\varepsilon} \left[2\varepsilon \frac{\Gamma^4(1/2 - \varepsilon)\Gamma^2(1/2 + \varepsilon)}{\Gamma^2(1 - 2\varepsilon)\Gamma(1 + 2\varepsilon)} + \frac{1 + 6\varepsilon}{\varepsilon(1 + 2\varepsilon)} \frac{\Gamma^3(1/2 - \varepsilon)}{\Gamma(1/2 - 3\varepsilon)} \right], \quad (3.52)$$

where the first argument in G emphasizes that we work near 3 dimensions. From Eq. (3.52), we first see the appearance of a $1/\varepsilon$ -pole. The latter is of IR nature and arises from the last G -function in Eq. (3.41). Moreover, as G -functions in D -dimensions are expressed in terms of Γ -functions with arguments depending on $D/2$, we see the appearance of half-integer indices in Eq. (3.52) around which the expansion has to be made. With the help of Eq. (3.47), this leads to:

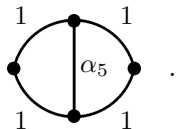
$$G(3 - 2\varepsilon, 1, 1, 1, 1, 1) = -2\pi \frac{e^{-2\gamma_E\varepsilon + \zeta_2\varepsilon^2}}{1 + 2\varepsilon} \left[\frac{1}{\varepsilon} + 4 + (2\pi^2 - 9\zeta_2 - 8)\varepsilon + \frac{4}{3} (12 - 44\zeta_3 - 27\zeta_2 + 6\pi^2 \log 2) \varepsilon^2 + O(\varepsilon^3) \right], \quad (3.53)$$

where we have used the fact that $\psi(1/2) = -\gamma_E - 2\log 2$, $\psi'(1/2) = 3\zeta_2$ and $\psi''(1/2) = -14\zeta_3$.¹⁴ As anticipated, Eq. (3.53) has no property of “maximal transcendentality”. It also features numbers such as π and $\log 2$ which arise from derivatives of the Γ -function at half-integer argument. In principle, according to [67], even more complicated numbers may appear at a higher number of loops, the first of which is:

$$U(3, 1) = \sum_{m>n>0} \frac{(-1)^{m+n}}{m^3 n} = \frac{1}{2} \zeta(4) - 2 \left\{ \text{Li}_4(1/2) + \frac{1}{24} \log^2 2 (\log^2 2 - \pi^2) \right\}, \quad (3.54)$$

with a non-trivial, *e.g.*, beyond MZV, $\text{Li}_4(1/2)$.

Pursuing with our historical overview, there are some specific cases where an exact evaluation of the diagram can be found. One of the simplest non-trivial, *i.e.*, beyond the rules of triangle see Fig. 4, diagram which may be considered is the one with an arbitrary index on the central line:

$$G(D, 1, 1, 1, 1, \alpha_5) = \text{Diagram} . \quad (3.55)$$


Early calculations by Vasil’ev, Pis’mak and Khonkonen [37] focused on the case where the index α_5 is related to the dimensionality of the system as follows: $\alpha_5 = \lambda = D/2 - 1$. Using

¹⁴We have: $\psi^{(n)}(1/2) = (-1)^{n+1} n! (2^{n+1} - 1) \zeta_{n+1}$ for $n \in \mathbb{N}^*$.

the method of uniqueness in real space, they have shown that [37] (see also discussions in Refs. [74, 76]):

$$G(D = 2\lambda + 2, 1, 1, 1, 1, \lambda) = 3 \frac{\Gamma(\lambda)\Gamma(1-\lambda)}{\Gamma(2\lambda)} \left[\psi'(\lambda) - \psi'(1) \right], \quad (3.56)$$

where $\psi'(x)$ is the trigamma function. Notice that this result has been recently recovered, hopefully in a simpler way, in Ref. [126] using the method of uniqueness in momentum space. For an arbitrary index α_5 , the diagram is beyond IBP as well as uniqueness. A one-fold series representation of Eq. (3.55) has first been given by Kazakov in Ref. [57]. His expression reads:

$$G(2\lambda + 2, 1, 1, 1, 1, \alpha_5) = -2 \frac{\Gamma^2(\lambda)\Gamma(1-\lambda)\Gamma(\lambda-\alpha_5)\Gamma(1-2\lambda+\alpha_5)}{\Gamma(2\lambda)} \left[\frac{1}{\Gamma(\alpha_5)\Gamma(3\lambda-\alpha_5-1)} \right. \\ \left. \times \sum_{n=1}^{\infty} (-1)^n \frac{\Gamma(n+2\lambda-1)}{\Gamma(n+1-\lambda)} \left(\frac{1}{n-\lambda+\alpha_5} + \frac{1}{n-1+2\lambda-\alpha_5} \right) - \cos[\pi\lambda] \right], \quad (3.57)$$

where the one-fold series can be represented as a combination of two ${}_3F_2$ -hypergeometric functions of argument -1 (see Sec. 4.6 for a proof via functional equations).¹⁵

Later, a whole class of complicated diagrams where two adjacent indices are integers and the three others are arbitrary, see Fig. 5, could be computed exactly by Kotikov [61] on the basis of a new development of the Gegenbauer polynomial technique. For this class of diagrams, similar results have been obtained in Ref. [62] using an Ansatz to solve the recurrence relations arising from IBP for the 2-loop diagram. All these results are expressed in terms of (combinations of) generalized hypergeometric functions, ${}_3F_2$ with argument 1. As a matter of fact, from [61], the diagram of Eq. (3.55) could be expressed as:

$$G(2\lambda + 2, 1, 1, 1, 1, \alpha_5) = -2 \Gamma(\lambda)\Gamma(\lambda-\alpha_5)\Gamma(1-2\lambda+\alpha_5) \times \quad (3.58) \\ \times \left[\frac{\Gamma(\lambda)}{\Gamma(2\lambda)\Gamma(3\lambda-\alpha_5-1)} \sum_{n=0}^{\infty} \frac{\Gamma(n+2\lambda)\Gamma(n+1)}{n!\Gamma(n+1+\alpha_5)} \frac{1}{n+1-\lambda+\alpha_5} + \frac{\pi \cot \pi(2\lambda-\alpha_5)}{\Gamma(2\lambda)} \right],$$

see Sec. 7 for more details. Notice that the equality of the two representations (3.57) and (3.58) was proven only recently [137], see also this reference for other representations of this diagram. This proof provides the following relation, conjectured in Ref. [61], between two ${}_3F_2$ -hypergeometric functions of argument -1 and a single ${}_3F_2$ -hypergeometric function of argument 1:

$${}_3F_2(2A, B, 1; B+1, 2-A; -1) + \frac{B}{1+A-B} {}_3F_2(2A, 1+A-B, 1; 2+A-B, 2-A; -1) \\ = B \cdot \frac{\Gamma(2-A)\Gamma(B+A-1)\Gamma(B-A)\Gamma(1+A-B)}{\Gamma(2A)\Gamma(1+B-2A)} - \frac{1-A}{B+A-1} {}_3F_2(2A, B, 1; B+1, A+B; 1), \quad (3.59)$$

where A , B and C are arbitrary. As far as we know, such a relation does not appear in standard textbooks.

¹⁵According to [165], Regge proposed that any Feynman diagram can be understood in terms of some hypergeometric functions, see [165] and references therein for more on the hypergeometric function approach to Feynman diagrams.

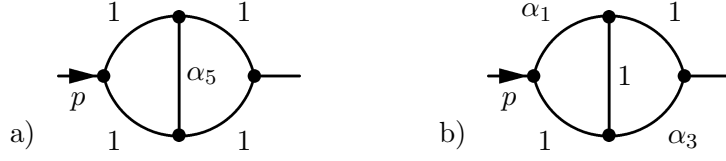


Figure 4: Examples of two-loop massless p-type diagrams which are beyond IBP identities and uniqueness.

On the basis of Ref. [61], the case of:

$$G(D, \alpha_1, 1, \alpha_3, 1, 1) = \text{Diagram} \quad , \quad (3.60)$$

could also be computed explicitly [127]. It was shown to be expressed in terms of two generalized hypergeometric functions, ${}_3F_2$ with argument 1 [127]. The result reads [127]:

$$G(D, \alpha_1, 1, \alpha_3, 1, 1) = \frac{1}{\tilde{\alpha}_1 - 1} \frac{1}{1 - \tilde{\alpha}_3} \frac{\Gamma(\tilde{\alpha}_1)\Gamma(\tilde{\alpha}_3)\Gamma(3 - \tilde{\alpha}_1 - \tilde{\alpha}_3)}{\Gamma(\alpha_1)\Gamma(\lambda - 2 + \tilde{\alpha}_1 + \tilde{\alpha}_3)} \frac{\Gamma(\lambda)}{\Gamma(2\lambda)} I(\tilde{\alpha}_1, \tilde{\alpha}_3), \quad (3.61)$$

where $\tilde{\alpha} = D/2 - \alpha$, $\lambda = D/2 - 1$, $D = 4 - 2\varepsilon$ and the function $I(\tilde{\alpha}_1, \tilde{\alpha}_3)$ can be written in four different forms; for example:

$$I(\tilde{\alpha}_1, \tilde{\alpha}_3) = \frac{\Gamma(1 + \lambda - \tilde{\alpha}_1)}{\Gamma(3 - \tilde{\alpha}_1 - \tilde{\alpha}_3)} \frac{\pi \sin[\pi(\tilde{\alpha}_3 - \tilde{\alpha}_1 + \lambda)]}{\sin[\pi(\lambda - 1 + \tilde{\alpha}_3)] \sin[\pi\tilde{\alpha}_1]} + \sum_{n=0}^{\infty} \frac{\Gamma(n + 2\lambda)}{n!(n + \lambda + \tilde{\alpha}_1 - 1)} \quad (3.62)$$

$$\times \left(\frac{\Gamma(n + 1)}{\Gamma(n + 2 + \lambda - \tilde{\alpha}_3)} - \frac{\Gamma(n - 2 + \lambda + \tilde{\alpha}_1 + \tilde{\alpha}_3)\Gamma(2 - \tilde{\alpha}_3)\Gamma(\lambda)}{\Gamma(n - 1 + 2\lambda + \tilde{\alpha}_1)\Gamma(3 - \tilde{\alpha}_1 - \tilde{\alpha}_3)\Gamma(\lambda + \tilde{\alpha}_1 - 1)} \frac{\sin[\pi(\tilde{\alpha}_3 + \lambda - 1)]}{\sin[\pi\tilde{\alpha}_1]} \right),$$

$$I(\tilde{\alpha}_1, \tilde{\alpha}_3) = \frac{\Gamma(1 + \lambda - \tilde{\alpha}_1)}{\Gamma(3 - \tilde{\alpha}_1 - \tilde{\alpha}_3)} \frac{\pi \sin[\pi\tilde{\alpha}_1]}{\sin[\pi(\lambda - 1 + \tilde{\alpha}_3)] \sin[\pi(\tilde{\alpha}_1 + \tilde{\alpha}_3 + \lambda - 1)]} \quad (3.63)$$

$$+ \sum_{n=0}^{\infty} \frac{\Gamma(n + 2\lambda)}{n!} \left(\frac{1}{n + \lambda + \tilde{\alpha}_1 - 1} \frac{\Gamma(n + 1)}{\Gamma(n + 2 + \lambda - \tilde{\alpha}_3)} \right.$$

$$\left. + \frac{1}{n + \lambda + 1 - \tilde{\alpha}_1} \frac{\Gamma(n + 2 - \tilde{\alpha}_1)\Gamma(2 - \tilde{\alpha}_3)\Gamma(\lambda)}{\Gamma(n + 3 + \lambda - \tilde{\alpha}_1 - \tilde{\alpha}_3)\Gamma(3 - \tilde{\alpha}_1 - \tilde{\alpha}_3)\Gamma(\lambda + \tilde{\alpha}_1 - 1)} \frac{\sin[\pi(\tilde{\alpha}_3 + \lambda - 1)]}{\sin[\pi(\tilde{\alpha}_1 + \tilde{\alpha}_3 + \lambda - 1)]} \right),$$

see [127] for other representations in terms of ψ -functions. Of course, Eq. (3.61) allows to recover all previously known cases for integer indices.

As an application, we may consider the peculiar case where $\alpha_1 = \varepsilon$ and $\alpha_3 = 2\varepsilon$ which appears in the computation of the renormalization group function of the Φ^4 -model at 6 loops [120, 121]. Using Eqs. (3.61) and (3.63), the first terms of the expansion are easily found and read:

$$G(4 - 2\varepsilon, \varepsilon, 1, 2\varepsilon, 1, 1) = G^2(\varepsilon) \left[-\frac{7}{30\varepsilon} - \frac{9}{5} - \frac{367}{30} \varepsilon + \left(\frac{239}{15} \zeta_3 - \frac{1187}{15} \right) \varepsilon^2 \right]$$

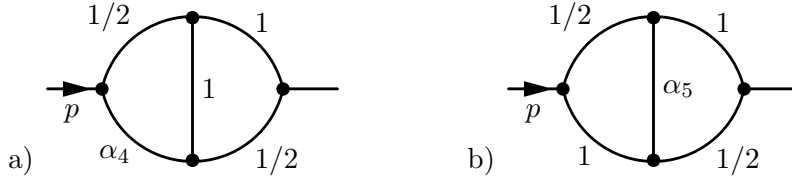


Figure 6: Examples of complicated diagrams appearing in Refs. [134, 135].

technique) involve explicit integrations. Other methods are *algebraic* and involve identities between different diagrams which are conveniently expressed in graphical form. These identities transform a diagram into another one (with different indices) and sometimes allow its exact computation without performing any explicit integration (assuming we know the one-loop G -functions). We shall refer to them as the *standard rules of perturbation theory for massless Feynman diagrams* [56].

4.1 Parametric integration

This is probably one of the oldest techniques known in Feynman diagram calculation, see, *e.g.*, the textbooks [52, 53]. It is based on so-called *Schwinger-trick* (see below) and amounts to represent a diagram, originally expressed in position or momentum space, in the space of *Feynman parameters* (or parametric space). The method is very useful in the case of massive Feynman diagrams. Many recent developments, even for massless multi-loop diagrams, are based on this technique, see, *e.g.*, [70, 71], [99]-[106],[120, 121].

The Schwinger-trick is based on the integral representation of the Γ -function:

$$\frac{1}{A_j^{\alpha_j}} = \frac{1}{\Gamma(\alpha_j)} \int_0^{+\infty} dt e^{-A_j t} t^{\alpha_j-1}, \quad (4.68)$$

where $A_j = k_j^2 + m_j^2$ and α_j is the index of the propagator. It immediately allows to compute the massive tadpole diagram, Eq. (2.11). Its generalization to the product of an arbitrary number of propagators with arbitrary exponents can be written as:

$$\frac{1}{A_1^{\alpha_1} \cdots A_N^{\alpha_N}} = \frac{\Gamma(\alpha)}{\Gamma(\alpha_1) \cdots \Gamma(\alpha_N)} \int_0^1 du_1 \cdots \int_0^1 du_N \frac{\delta(1 - \sum_{j=1}^N u_j) u_1^{\alpha_1-1} \cdots u_N^{\alpha_N-1}}{(u_1 A_1 + \cdots + u_N A_N)^\alpha}, \quad (4.69)$$

where $\alpha = \sum_{j=1}^N \alpha_j$ and the u_i are the so-called Feynman parameters. The one-loop p-type integral can be computed straightforwardly using Eq. (4.69) yielding Eq. (2.19).

Let's consider an L -loop diagram with external momenta collected in the vector \vec{p} and N internal propagators whose indices are collected in the vector $\vec{\alpha}$. In momentum space, this diagram reads:

$$J_L(D, \vec{p}, \vec{\alpha}) = \int \frac{[d^D k_1] \cdots [d^D k_L]}{A_1^{\alpha_1} \cdots A_N^{\alpha_N}}. \quad (4.70)$$

Using Eq. (4.69), Eq. (4.70) can then be represented in parametric space under the general

form:

$$J_L(D, \vec{p}, \vec{\alpha}) = (4\pi)^{-LD} \frac{\Gamma(\alpha)}{\Gamma(\alpha_1) \cdots \Gamma(\alpha_N)} \int_0^1 d^N u \delta \left(1 - \sum_{j=1}^N u_j \right) \prod_{j=1}^N u_j^{\alpha_j - 1} \frac{\mathcal{U}^{\alpha - (L+1)D/2}}{\mathcal{F}(\vec{p})^{\alpha - LD/2}}, \quad (4.71)$$

where \mathcal{U} and \mathcal{F} are polynomials in the Feynman parameters and \mathcal{F} also depends on the external momenta and masses. For an arbitrary Feynman diagram, the Symanzik polynomials \mathcal{U} and \mathcal{F} are not so easy to compute starting from the momentum representation. Some more efficient derivations are based on the topology of the diagram under consideration, see, *e.g.*, [100]. Let's mention that in the case of the massless 2-loop p-type integral, these polynomials read:

$$\mathcal{U} = (u_1 + u_2 + u_3 + u_4)u_5 + (u_1 + u_4)(u_2 + u_3), \quad (4.72a)$$

$$\mathcal{F} = \left((u_1 + u_4)u_2u_3 + (u_2 + u_3)u_1u_4 + (u_1 + u_2)(u_3 + u_4)u_5 \right) p^2. \quad (4.72b)$$

4.2 Integration by parts

Thanks to its simplicity and efficiency, integration by parts (IBP) is one of the most widely used methods in multi-loop calculations. It has been introduced by Vasil'ev, Pis'mak and Khonkonen [37], Tkachov [44] and Chetyrkin and Tkachov [45]. It allows to reduce a complicated Feynman diagram in terms of a limited number of master integrals; such reduction is now automated via its implementation in computer programs with the help of various algorithms, see, *e.g.*, [92]-[98]. As reviewed in Sec. 3.3, in some simple cases, the master integrals themselves can be computed from IBP alone. In general, however, other methods have to be used often in combination with IBP (see next items).

4.2.1 Presentation of the method

IBP recurrence relations in momentum-space are essentially based on the translational invariance of dimensionally regularized integrals:

$$\int d^D k f(k) = \int d^D k f(k+q) \quad \Rightarrow \quad 0 = \int d^D k \frac{\partial}{\partial k^\mu} f(k). \quad (4.73)$$

In the following, we shall mainly be concerned with the application of the IBP procedure to the 2-loop massless p-type diagram of Eq. (3.28).¹⁸ The IBP relations for this diagram then follow from:

$$0 = (\partial_{\mathcal{C}} \cdot P) J(D, p, \alpha_1, \alpha_2, \alpha_3, \alpha_4, \alpha_5), \quad (4.74)$$

where \mathcal{C} is a closed oriented contour and P some momentum. In the above identity it is understood that differentiation goes before integration. Let's define p_i as the momentum carried by the line of index α_i :

$$p_1 = k - p, \quad p_2 = q - p, \quad p_3 = q, \quad p_4 = k, \quad p_5 = k - q, \quad (4.75)$$

where p is the external momentum. Different IBP relations come from different choices for the contour \mathcal{C} and the momentum P (in the following, the line carrying momentum P will be

¹⁸The original references [44, 45] were actually focusing on IBP relations for 3-loop massless p-type diagrams.

referred to as the *distinguished line*). According to Chetyrkin and Tkachov [45], for an L -loop p -integral one can write down $(L + 1)^2$ independent IBP identities. This comes from the fact that there are $L + 1$ possible choices for \mathcal{C} (L internal and 1 external) and a similar number for P (L loop momenta and one external momentum). So, for the 2-loop massless p -type diagram there are *a priori* 9 IBP relations.

Let's first consider the case corresponding to $P = p_5$ and $\mathcal{C} = \{+p_1, +p_4, +p_5\}$. Along this contour the derivative reads:

$$\partial_{\mathcal{C}} = +\frac{\partial}{\partial p_1} + \frac{\partial}{\partial p_4} + \frac{\partial}{\partial p_5}, \quad (4.76)$$

where the sign before p_i or $\partial/\partial p_i$ is plus if p_i flows in the direction of \mathcal{C} and minus otherwise. With the help of Eq. (4.74), this leads to:

$$\int \int d^D k d^D q \frac{\partial}{\partial k^\mu} \left\{ \frac{1}{(k-p)^{2\alpha_1} (q-p)^{2\alpha_2} q^{2\alpha_3} k^{2\alpha_4} (k-q)^{2\alpha_5}} \right\} = 0. \quad (4.77)$$

Using equalities of the type:

$$\frac{\partial k^\nu}{\partial k^\mu} = \delta_\mu^\nu \quad (\delta_\mu^\mu = D), \quad \frac{\partial (k-p)^{-2\alpha}}{\partial k^\mu} = -2\alpha \frac{(k-p)_\mu}{(k-p)^{2\alpha+2}}, \quad (4.78)$$

and canceling squared combinations of momentum in the numerator and denominator yields, in graphical form:

$$\begin{aligned} (D - \alpha_1 - \alpha_4 - 2\alpha_5) \text{Diagram} &= \alpha_1 \left[\text{Diagram}_1^+ - \text{Diagram}_2^+ \right] + \\ &+ \alpha_4 \left[\text{Diagram}_3^+ - \text{Diagram}_4^+ \right], \end{aligned} \quad (4.79)$$

where \pm on the right-hand side of the equation denotes the increase or decrease of a line index by 1 with respect to its value on the left-hand side. Similarly, for $P = p_5$ but a contour running along the right triangle, the following identity is obtained:

$$\begin{aligned} (D - \alpha_2 - \alpha_3 - 2\alpha_5) \text{Diagram} &= \alpha_2 \left[\text{Diagram}_1^- - \text{Diagram}_2^- \right] + \\ &+ \alpha_3 \left[\text{Diagram}_3^- - \text{Diagram}_4^- \right]. \end{aligned} \quad (4.80)$$

Actually, Eqs. (4.80) and Eq. (4.79) are related to each other by using the symmetries of the diagram. As can be seen from Eqs. (4.79) and (4.80), the distinguished line in the above examples is the vertical one.

As another example, we may take $P = p_4$ (*i.e.*, the distinguished line now becomes the one with index α_4) and a contour running along the left triangle; this yields:

$$\begin{aligned}
 (D - \alpha_1 - \alpha_5 - 2\alpha_4) \begin{array}{c} \alpha_1 \quad \alpha_2 \\ \bullet \quad \bullet \\ | \\ \alpha_4 \quad \alpha_3 \\ \bullet \quad \bullet \end{array} &= \alpha_1 \left[\begin{array}{c} + \\ \bullet \quad \bullet \\ | \\ \bullet \quad \bullet \\ - \end{array} - (p^2) \times \begin{array}{c} + \\ \bullet \quad \bullet \\ | \\ \bullet \quad \bullet \\ \bullet \end{array} \right] + \\
 &+ \alpha_5 \left[\begin{array}{c} \bullet \quad \bullet \\ | \\ + \\ \bullet \quad \bullet \\ - \end{array} - \begin{array}{c} \bullet \quad \bullet \\ | \\ + \\ \bullet \quad \bullet \\ - \end{array} \right]. \quad (4.81)
 \end{aligned}$$

Other identities can be obtained from Eq. (4.81) by using the symmetries of the diagrams and will not be displayed.

Another set of useful identities, the so-called ‘‘homogeneity’’ relations [45], follow from the fact that the dimensionality d_F of J (in units of momentum) is known in terms of the α_i and D from simple dimensional analysis:

$$d_F = 2 \left(D - \sum_{j=1}^5 \alpha_j \right). \quad (4.82)$$

These relations read [45]:

$$d_F J = \left(p \cdot \frac{d}{dp} \right) J = -p \cdot \left(\frac{\partial}{\partial p_1} + \frac{\partial}{\partial p_2} \right) J, \quad (4.83a)$$

$$(D + d_F) \frac{p_1 \cdot p}{p^2} J = \left(\frac{d}{dp} \cdot p_1 \right) J = - \left(\frac{\partial}{\partial p_1} + \frac{\partial}{\partial p_2} \right) \cdot p_1 J, \quad (4.83b)$$

$$(D + d_F) \frac{p_2 \cdot p}{p^2} J = \left(\frac{d}{dp} \cdot p_2 \right) J = - \left(\frac{\partial}{\partial p_1} + \frac{\partial}{\partial p_2} \right) \cdot p_2 J, \quad (4.83c)$$

where the chosen circuit is $\mathcal{C} = \{p, p_1, p_2\}$ and successive relations correspond to $P = p$, $P = p_1$ and $P = p_2$, respectively. In graphical notations, Eq. (4.83c) reads:

$$\begin{aligned}
 \left(\frac{D}{2} + \alpha_1 - \alpha_3 - \alpha_4 - \alpha_5 \right) \begin{array}{c} \alpha_1 \quad \alpha_2 \\ \bullet \quad \bullet \\ | \\ \alpha_4 \quad \alpha_3 \\ \bullet \quad \bullet \end{array} &= \alpha_2 \left[\begin{array}{c} \bullet \quad \bullet \\ | \\ + \\ \bullet \quad \bullet \\ - \end{array} - \begin{array}{c} - \\ \bullet \quad \bullet \\ | \\ \bullet \quad \bullet \\ + \end{array} \right] + \\
 &+ \left(\frac{3D}{2} - \sum_{i=1}^5 \alpha_i \right) (k^2)^{-1} \left[\begin{array}{c} \bullet \quad \bullet \\ | \\ - \\ \bullet \quad \bullet \\ - \end{array} - \begin{array}{c} - \\ \bullet \quad \bullet \\ | \\ \bullet \quad \bullet \\ - \end{array} \right]. \quad (4.84)
 \end{aligned}$$

This identity is particularly useful in order to express a diagram as a function of another diagram with one index decreased.

Other relations follow from double differentiation with respect to the external momentum:

$$d_F(d_F + D - 2) J = p^2 \frac{d^2 J}{dp_\mu dp^\mu} = p^2 \left(\frac{\partial}{\partial p_1} + \frac{\partial}{\partial p_2} \right)^2 J. \quad (4.85)$$

$$+ \left[A_5 \zeta_7 - A_6 \zeta_3 \zeta_4 \right] \varepsilon^4 + O(\varepsilon^5) \Big], \quad (4.90)$$

with

$$\begin{aligned} A_0 &= 6, \\ A_1 &= 9, \\ A_2 &= 42 + 30 \bar{a} + 10 \bar{a}^2 - 10 a_1 a_4, \\ A_3 &= \frac{5}{2} (A_2 - 6), \\ A_4 &= 46 + 42 \bar{a} + 14 \bar{a}^2 - 14 a_1 a_4, \\ A_5 &= 294 + 402 \bar{a} + 260 \bar{a}^2 - 134 a_1 a_4 + 84 \bar{a}^3 - 84 \bar{a} a_1 a_4 + 14 \bar{a}^4 - 28 \bar{a}^2 a_1 a_4 + 14 a_1^2 a_4^2, \\ A_6 &= 3 (A_4 - 1), \end{aligned} \quad (4.91)$$

where

$$\bar{a} = a_1 + a_4, \quad \hat{K}_n = \exp \left[-n \left(\gamma_E \varepsilon + \frac{\zeta_2}{2} \varepsilon^2 \right) \right]. \quad (4.92)$$

Notice that, for $a_1 = a_4 = 0$, we recover the result in (3.43).

4.3 The method of uniqueness

The method of uniqueness is a powerful (but not very well known) technique devoted to the computation of *massless* multi-loop Feynman diagrams. This method owes its name to the so-called *uniqueness relation*, otherwise known as the *star-triangle* or *Yang-Baxter relation*, which is used in theories with conformal symmetry. Historically, such relation was probably first used to compute three-dimensional integrals by D'Eramo, Peleti and Parisi [36]. Within the framework of multi-loop calculations, the method has first been introduced by Vasil'ev, Pis'mak and Khonkonen [37]. It allows, in principle, the computation of complicated Feynman diagrams using sequences of simple transformations (including integration by parts) without performing any explicit integration. A diagram is straightforwardly integrated once the appropriate sequence is found. In a sense, the method greatly simplifies multi-loop calculations [37]-[57]. As a matter of fact, the first analytical expression for the five-loop β -function of the Φ^4 -model was derived by Kazakov using this technique [56, 57]. For a given diagram, the task of finding the sequence of transformations is, however, highly non-trivial. In the following, we will briefly present the method in momentum space in very close analogy with the beautiful lectures of Kazakov [139] where the method was presented in coordinate space, see also [166] for a recent short review.

In momentum space, a triangle made of scalar propagators with three arbitrary indices is defined as:

$$\begin{array}{c} p_2 \\ | \\ \alpha_3 \bullet \quad \alpha_1 \\ \diagdown \quad \diagup \\ \alpha_2 \\ \bullet \\ / \quad \backslash \\ p_1 \quad p_3 = -p_1 - p_2 \end{array} = \int \frac{[d^D k]}{k^{2\alpha_2} (k - p_1)^{2\alpha_3} (k - p_1 - p_2)^{2\alpha_1}}. \quad (4.93)$$

	Line	Triangle	Vertex
Arbitrary	α	$\sum_{j=1}^3 \alpha_j$	$\sum_{j=1}^3 \alpha_j$
Ordinary	1	3	3
Unique	$D/2$	D	$D/2$

Table 1: Indices of lines, triangles and vertices in p -space.

On the other hand, a vertex made of scalar propagators with three arbitrary indices is defined as:

$$\begin{array}{c} \beta_2 \\ | \\ \bullet \\ / \quad \backslash \\ \beta_1 \quad \beta_3 \end{array} = \frac{1}{p_1^{2\beta_1} p_2^{2\beta_2} (p_1 + p_2)^{2\beta_3}}. \quad (4.94)$$

Both triangle and vertex diagrams have indices $\sum_{j=1}^3 \alpha_j$, corresponding to the sum of the indices of their constituent lines. In momentum space, *ordinary* triangles and vertices, that is triangle and vertices made of ordinary lines, have index 3. Of great importance in the following will be the notion of a *unique* triangle and a *unique* vertex. In momentum space, these diagrams are said to be *unique* if their indices are equal to D and $D/2$, respectively; see Tab. 1 for a summary.

The uniqueness (or star-triangle) relation connects a unique triangle to a unique vertex and reads:

$$\begin{array}{c} \alpha_2 \\ | \\ \bullet \\ / \quad \backslash \\ \alpha_1 \quad \alpha_3 \end{array} \stackrel{\sum_j \alpha_j = D/2}{=} \frac{(4\pi)^{D/2}}{G(\tilde{\alpha}_1, \tilde{\alpha}_2)} \begin{array}{c} \tilde{\alpha}_3 \\ \bullet \\ \backslash \quad / \\ \tilde{\alpha}_1 \\ \bullet \\ \backslash \quad / \\ \tilde{\alpha}_2 \end{array}, \quad (4.95)$$

where $\tilde{\alpha}_i = D/2 - \alpha_i$ is the index dual to α_i and the condition $\sum_{j=1}^3 \alpha_j = D/2$ implies that the vertex is unique. This relation can be proved by performing an inversion of all integration variables in the triangle: $k_\mu \rightarrow k_\mu/(k)^2$, keeping the external momenta fixed. Upon using the fact that the triangle is unique, $\sum_j \tilde{\alpha}_j = D$, the integral simplifies and reduces to a simple vertex.

4.4 Transformation of indices

In order to illustrate the power of the method of uniqueness, we now proceed on giving several useful transformations of indices. Following Kazakov (see also Sec. 3.2) and considering the general massless two-loop p-type diagram with arbitrary indices, *e.g.*, Eq. (3.28), we shall denote the index of the left (right) triangle as: $t_1 = \alpha_1 + \alpha_4 + \alpha_5$ ($t_2 = \alpha_2 + \alpha_3 + \alpha_5$) and the index of the upper (lower) vertex as: $v_1 = \alpha_1 + \alpha_2 + \alpha_5$ ($v_2 = \alpha_3 + \alpha_4 + \alpha_5$). The following notations will also be useful: $\bar{t}_i = t_i - D/2$, $\bar{v}_i = v_i - D/2$ ($i = 1, 2$) and, as previously defined, $\tilde{\alpha}_j = D/2 - \alpha_j$ ($j = 1, \dots, 5$).

4.4.1 Splitting a line into loop

This transformation allows to derive Eq. (3.39) which was first obtained by Gorishny and Isaev [150]. From the two-loop p-type diagram with arbitrary indices, we start by replacing the central line by a loop¹⁹ in such a way that the right triangle is unique. This yields:

$$\begin{array}{c} \alpha_1 \qquad \alpha_2 \\ \bullet \qquad \bullet \\ \diagdown \quad \diagup \\ \alpha_5 \\ \diagup \quad \diagdown \\ \bullet \qquad \bullet \\ \alpha_4 \qquad \alpha_3 \end{array} = \frac{(4\pi)^{D/2}}{G(D, \beta, \gamma)} \begin{array}{c} \alpha_1 \qquad \alpha_2 \\ \bullet \qquad \bullet \\ \diagdown \quad \diagup \\ \beta \quad \gamma \\ \diagup \quad \diagdown \\ \bullet \qquad \bullet \\ \alpha_4 \qquad \alpha_3 \end{array}, \quad (4.96)$$

where $\beta = t_2 - D/2 \equiv \bar{t}_2$ and $\gamma = D - \alpha_2 - \alpha_3 \equiv \tilde{\alpha}_2 + \tilde{\alpha}_3$. The right triangle being unique, we can use Eq. (4.95) to simplify the diagram:

$$\begin{array}{c} \alpha_1 \qquad \alpha_2 \\ \bullet \qquad \bullet \\ \diagdown \quad \diagup \\ \alpha_5 \\ \diagup \quad \diagdown \\ \bullet \qquad \bullet \\ \alpha_4 \qquad \alpha_3 \end{array} = \frac{G(D, \alpha_2, \gamma)}{G(D, \bar{t}_2, \gamma)} (p^2)^{D/2 - \alpha_2 - \alpha_3} \begin{array}{c} \alpha_1 \qquad \tilde{\alpha}_3 \\ \bullet \qquad \bullet \\ \diagdown \quad \diagup \\ \bar{t}_2 \\ \diagup \quad \diagdown \\ \bullet \qquad \bullet \\ \alpha_4 \qquad \tilde{\alpha}_2 \end{array}. \quad (4.97)$$

Focusing for simplicity on the coefficient functions, all the dependence on the external momentum disappears. Together with the simplification of the G -functions this yields the advertised Eq. (3.39) that we reproduce for clarity:

$$C_D[J(D, p, \alpha_1, \alpha_2, \alpha_3, \alpha_4, \alpha_5)] = a(\alpha_2)a(\alpha_3)a(\alpha_5)a(D - t_2) C_D[J(D, p, \alpha_1, \tilde{\alpha}_3, \tilde{\alpha}_2, \alpha_4, \bar{t}_2)].$$

Notice that, for $\alpha_1 = \alpha_4 = \bar{t}_2 = 1$, *i.e.*, $\alpha_1 = \alpha_4 = 1$ and $t_2 = 1 + D/2$ (that is, the sum of indices α_2, α_3 and α_5 is equal to $D/2 + 1$), the left triangle on the rhs of Eq. (4.97) corresponds to the ordinary one, see Tab. 1. Moreover, for $\tilde{\alpha}_2 = \tilde{\alpha}_3 = \bar{t}_2 = 1$, *i.e.*, $\alpha_2 = \alpha_3 = D/2 - 1 = 1 - \varepsilon$ and $\alpha_5 = 3 - D/2 = 1 + \varepsilon$, it is the right triangle on the rhs of Eq. (4.97) that corresponds to the ordinary one. In these cases, the diagrams can be evaluated with the help of the IBP relations and expressed in terms of Γ -functions in agreement with subsection 4.2.2.

We can now repeat the above manipulations with a lateral line (we use the one having the index α_1), *i.e.*,

$$\begin{array}{c} \alpha_1 \qquad \alpha_2 \\ \bullet \qquad \bullet \\ \diagdown \quad \diagup \\ \alpha_5 \\ \diagup \quad \diagdown \\ \bullet \qquad \bullet \\ \alpha_4 \qquad \alpha_3 \end{array} = \frac{(4\pi)^{D/2}}{G(D, \beta_1, \gamma_1)} \begin{array}{c} \beta_1 \qquad \alpha_2 \\ \bullet \qquad \bullet \\ \diagdown \quad \diagup \\ \gamma_1 \quad \alpha_5 \\ \diagup \quad \diagdown \\ \bullet \qquad \bullet \\ \alpha_4 \qquad \alpha_3 \end{array}, \quad (4.98)$$

where $\beta_1 = t_1 - D/2 = \bar{t}_1$ and $\gamma_1 = D - \alpha_4 - \alpha_5 = \tilde{\alpha}_4 + \tilde{\alpha}_5$. The triangle having the lines with the indices γ_1, α_4 and α_5 , is unique so we can use Eq. (4.95) to simplify the diagram:

$$\begin{array}{c} \alpha_1 \qquad \alpha_2 \\ \bullet \qquad \bullet \\ \diagdown \quad \diagup \\ \alpha_5 \\ \diagup \quad \diagdown \\ \bullet \qquad \bullet \\ \alpha_4 \qquad \alpha_3 \end{array} = \frac{G(D, \alpha_4, \gamma_1)}{G(D, \bar{t}_1, \gamma_1)} \begin{array}{c} \bar{t}_1 \qquad \alpha_2 \\ \bullet \qquad \bullet \\ \diagdown \quad \diagup \\ \tilde{\alpha}_4 \\ \diagup \quad \diagdown \\ \bullet \qquad \bullet \\ \tilde{\alpha}_5 \qquad \tilde{\alpha}_3 \end{array}, \quad (4.99)$$

where $\bar{\alpha}_3 = \alpha_3 + D/2 - \gamma_1 = \alpha_3 + \alpha_4 + \alpha_5 - D/2 = v_2 - D/2 \equiv \bar{v}_2$. Eq. (4.99) gives for the corresponding coefficient function:

$$C_D[J(D, p, \alpha_1, \alpha_2, \alpha_3, \alpha_4, \alpha_5)] = a(\alpha_1)a(\alpha_4)a(\alpha_5)a(D - t_1) C_D[J(D, p, \bar{t}_1, \alpha_2, \bar{v}_2, \tilde{\alpha}_5, \tilde{\alpha}_4)].$$

¹⁹In coordinate space, it corresponds to the insertion of a point into this line (see the table of such transformations in Ref. [37] and also Ref. [139] for a review).

In this example, we have now an ordinary left triangle when: $\tilde{\alpha}_4 = \tilde{\alpha}_5 = \bar{t}_1 = 1$, *i.e.*, $\alpha_2 = \alpha_5 = D/2 - 1 = 1 - \varepsilon$ and $\alpha_1 = 3 - D/2 = 1 + \varepsilon$. On the other hand, the right triangle becomes ordinary when: $\alpha_2 = \tilde{\alpha}_3 = \tilde{\alpha}_4 = 1$, *i.e.*, $\tilde{\alpha}_4 = \alpha_2 = 1$ and $v_2 = \alpha_3 + \alpha_4 + \alpha_5 = D/2 + 1$, and, finally, $\alpha_2 = 1$, $\alpha_4 = D/2 - 1 = 1 - \varepsilon$ and $\alpha_3 + \alpha_5 = 2$. In all these cases, the diagrams may again be evaluated with the help of the IBP relations and expressed in terms of Γ -functions in agreement with subsection 4.2.2.

4.4.2 Adding a new propagator and a new loop

Another transformation allowing to change the indices of the two-loop p-type diagram (see also Eq. (3.30)):

$$\begin{array}{c} \alpha_1 \\ \bullet \\ \text{---} \bullet \quad \bullet \quad \text{---} \\ \alpha_4 \quad \alpha_5 \quad \alpha_3 \\ \bullet \\ \alpha_2 \end{array} = \frac{p^{-2\delta}}{(4\pi)^D} C_D[J(D, p, \alpha_1, \alpha_2, \alpha_3, \alpha_4, \alpha_5)], \quad (4.100)$$

where $\delta = \sum_{i=1}^5 \alpha_i - D$, consists in adding an additional propagator with index $\tilde{\alpha}_2 - \alpha_3$ to both its lhs and rhs. This leads to:

$$\frac{p^{-2\delta}}{(4\pi)^D} C_D[J(D, p, \alpha_1, \alpha_2, \alpha_3, \alpha_4, \alpha_5)] \frac{1}{p^{2(\tilde{\alpha}_2 - \alpha_3)}} = \begin{array}{c} \alpha_1 \\ \bullet \\ \text{---} \bullet \quad \bullet \quad \text{---} \\ \alpha_4 \quad \alpha_5 \quad \alpha_3 \\ \bullet \\ \tilde{\alpha}_2 - \alpha_3 \end{array}, \quad (4.101)$$

with the vertex of indices α_2 , α_3 and $\tilde{\alpha}_2 - \alpha_3$ being unique. We can therefore use Eq. (4.95) from right to left in order to obtain:

$$\text{rhs of Eq. (4.101)} = \frac{(4\pi)^{D/2}}{G(D, \tilde{\alpha}_2, \tilde{\gamma})} \begin{array}{c} \alpha_1 \\ \bullet \\ \text{---} \bullet \quad \bullet \quad \text{---} \\ \alpha_4 \quad \alpha_5 \quad \tilde{\alpha}_3 \\ \bullet \\ \tilde{\gamma} \\ \bullet \\ \tilde{\alpha}_2 \end{array}, \quad (4.102)$$

where $\tilde{\gamma} = D/2 - \tilde{\alpha}_2 + \alpha_3 = \alpha_2 + \alpha_3$. Finally, calculating the internal loop, yields:

$$\frac{p^{-2\delta}}{(4\pi)^D} C_D[J(D, p, \alpha_1, \alpha_2, \alpha_3, \alpha_4, \alpha_5)] \frac{1}{p^{2(\tilde{\alpha}_2 - \alpha_3)}} = \frac{G(D, \alpha_5, \alpha_2 + \alpha_3)}{G(D, \tilde{\alpha}_2, \alpha_2 + \alpha_3)} \begin{array}{c} \alpha_1 \\ \bullet \\ \text{---} \bullet \quad \bullet \quad \text{---} \\ \alpha_4 \quad \alpha_5 \quad \tilde{\alpha}_3 \\ \bullet \\ \beta \\ \bullet \\ \tilde{\alpha}_2 \end{array}, \quad (4.103)$$

with $\beta = t_2 - D/2 \equiv \bar{t}_2$ (see the previous subsection). Hence, for the corresponding coefficient function, we have:

$$C_D[J(D, p, \alpha_1, \alpha_2, \alpha_3, \alpha_4, \alpha_5)] = a(\alpha_2)a(\alpha_3)a(\alpha_5)a(D - t_2) C_D[J(D, p, \alpha_1, \tilde{\alpha}_3, \tilde{\alpha}_2, \alpha_4, \bar{t}_2)].$$

In a sense, the procedure of adding an additional propagator can be considered as the inverse of the transform given in the previous subsection, see Eq. (4.96). From Eq. (4.103), we can then see that the left triangle becomes the ordinary one when $\alpha_1 = \alpha_4 = \bar{t}_2 = 1$, *i.e.*, $\alpha_1 = \alpha_4 = 1$ and $t_2 = 1 + D/2$ (so the sum of the indices α_2 , α_3 and α_5 is equal to $D/2 + 1$). Moreover, the right triangle becomes the ordinary one when $\tilde{\alpha}_2 = \tilde{\alpha}_3 = \bar{t}_2 = 1$, *i.e.*, $\alpha_2 = \alpha_3 = D/2 - 1 = 1 - \varepsilon$ and $\alpha_5 = 3 - D/2 = 1 + \varepsilon$. In all these cases, the diagrams may

again be evaluated with the help of the IBP relations and expressed in terms of Γ -functions in agreement with subsection 4.2.2.

Now let's add an additional line of index $\tilde{\alpha}_1 + \tilde{\alpha}_2$ to both sides of Eq. (4.100). This yields:

$$\frac{p^{-2\bar{v}_2}}{(4\pi)^{3D/2}} C_D[J(D, p, \alpha_1, \alpha_2, \alpha_3, \alpha_4, \alpha_5)] G(D, \delta, \tilde{\alpha}_1 + \tilde{\alpha}_2) = \text{Diagram} \quad (4.104)$$

The upper triangle is unique which leads to the replacement of the rhs by the diagram:

$$\frac{1}{(4\pi)^{D/2}} G(D, \alpha_1, \alpha_2) \text{Diagram} \quad (4.105)$$

This finally leads to the identity:

$$C_D[J(D, p, \alpha_1, \alpha_2, \alpha_3, \alpha_4, \alpha_5)] = \frac{G(\alpha_1, \alpha_2)}{G(\delta, \tilde{\alpha}_1 + \tilde{\alpha}_2)} C_D[J(D, p, \tilde{\alpha}_2, \tilde{\alpha}_1, \alpha_3, \alpha_4, \bar{v}_1)],$$

and

$$C_D[J(D, p, \alpha_1, \alpha_2, \alpha_3, \alpha_4, \alpha_5)] = a(\alpha_1)a(\alpha_2)a(\bar{v}_2)a(3D/2 - \sum_{i=1}^5 \alpha_i) C_D[J(D, p, \tilde{\alpha}_2, \tilde{\alpha}_1, \alpha_3, \alpha_4, \bar{v}_1)].$$

From these results, we observe that the left triangle becomes an ordinary one for $\tilde{\alpha}_2 = \alpha_4 = \bar{v}_1 = 1$, *i.e.*, $\alpha_4 = 1$, $\alpha_2 = D/2 - 1 = 1 - \varepsilon$ and $\alpha_1 + \alpha_5 = 2$. Moreover, the right triangle becomes an ordinary one for $\tilde{\alpha}_1 = \alpha_3 = \bar{v}_1 = 1$, *i.e.*, $\alpha_3 = 1$, $\alpha_1 = D/2 - 1 = 1 - \varepsilon$ and $\alpha_2 + \alpha_5 = 2$. Once again, in all these cases, the final results may be evaluated with the help of the IBP relations and expressed in terms of Γ -functions in agreement with subsection 4.2.2.

Let's add that similar transformations but for diagrams containing lines with arrows (see definition of such line in (2.3) can be found in [42].²⁰

4.4.3 Conformal transform of the inversion

In order to implement this transformation, we perform the inversion:

$$k_i^\mu \rightarrow \frac{k_i^\mu}{k_i^2}, \quad (4.106)$$

of the integration variables and the external momenta. So, we have:

$$k_i^2 \rightarrow \frac{1}{k_i^2}, \quad (k_i - k_j)^2 \rightarrow \frac{(k_i - k_j)^2}{k_i^2 k_j^2}, \quad d^D k_i \rightarrow \frac{d^D k_i}{k_i^{2D}}, \quad (4.107)$$

²⁰The journal version of [42] contains mostly the formulas without graphics. The corresponding graphical representations can be found in the preprint version of [42] (see, for example, the corresponding KEK scanned document).

and, thus,

$$\int \frac{[d^D k_1][d^D k_2]}{k_1^{2\alpha_1} k_2^{2\alpha_2} (k_1 - k_2)^{2\alpha_5} (p - k_1)^{2\alpha_4} (p - k_2)^{2\alpha_3}} \rightarrow \int [d^D k_1][d^D k_2] \frac{k_1^{2\alpha_1} k_2^{2\alpha_2} (k_1^2 k_2^2)^{2\alpha_5} (p^2 k_1^2)^{2\alpha_4} (p^2 k_2^2)^{2\alpha_3}}{k_1^{2D} k_2^{2D} (k_1 - k_2)^{2\alpha_5} (p - k_1)^{2\alpha_4} (p - k_2)^{2\alpha_3}}, \quad (4.108)$$

or, graphically:



$$\rightarrow \quad (4.109)$$

The last result can be rewritten as:

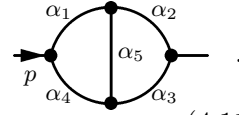
$$C_D[J(D, p, \alpha_1, \alpha_2, \alpha_3, \alpha_4, \alpha_5)] \stackrel{(In)}{=} C_D[J(D, p, D - t_1, D - t_2, \alpha_3, \alpha_4, \alpha_5)].$$

This equation shows that the left triangle becomes an ordinary one for $\alpha_4 = \alpha_5 = D - t_1 = 1$, *i.e.*, $\alpha_4 = \alpha_5 = 1$ and $\alpha_1 = D - 3 = 1 - 2\varepsilon$. Moreover, the right triangle becomes an ordinary one for $\alpha_3 = \alpha_5 = D - t_2 = 1$, *i.e.*, $\alpha_3 = \alpha_5 = 1$ and $\alpha_2 = D - 3 = 1 - 2\varepsilon$. In these cases, the final results may be evaluated with the help of the IBP relations and expressed in terms of Γ -functions in agreement with subsection 4.2.2.

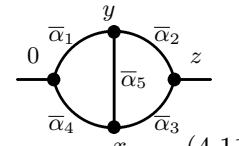
4.5 Fourier transform and duality

Up to now, all diagrams were expressed in momentum space. Useful identities can be obtained by relating p -space and x -space diagrams. Following [139], we briefly present them in this paragraph.

Recall, from Eq. (3.28), that the 2-loop massless propagator-type diagram in p -space was defined as:

$$J(D, p, \{\alpha_i\}) = \int \frac{[d^D k][d^D q]}{[(k - p)^2]^{\alpha_1} [(q - p)^2]^{\alpha_2} [q^2]^{\alpha_3} [k^2]^{\alpha_4} [(k - q)^2]^{\alpha_5}} = \text{Diagram} \quad (4.110)$$


Equivalently, all calculations may be done in position space. In x -space, the 2-loop massless propagator-type diagram is defined as:

$$J(D, z, \{\bar{\alpha}_i\}) = \int \frac{[d^D x][d^D y]}{[y^2]^{\bar{\alpha}_1} [(y - z)^2]^{\bar{\alpha}_2} [(z - x)^2]^{\bar{\alpha}_3} [x^2]^{\bar{\alpha}_4} [(x - y)^2]^{\bar{\alpha}_5}} = \text{Diagram} \quad (4.111)$$


where 0 denotes the so-called “root vertex” and the $\bar{\alpha}_i$ are arbitrary indices. It is actually straightforward to show that the p -space and x -space diagrams are related provided that $\bar{\alpha}_i = \tilde{\alpha}_i$ where $\tilde{\alpha} = D/2 - \alpha$ is the index which is dual (in the sense of Fourier transform) to α . This follows from the Fourier transform, Eq. (2.6), that we reproduce here for clarity:

$$\frac{1}{[k^2]^\alpha} = \frac{a(\alpha)}{(2\pi)^{D/2}} \int d^D x \frac{e^{ikx}}{[x^2]^{D/2 - \alpha}}, \quad a(\alpha) = \frac{\Gamma(D/2 - \alpha)}{\Gamma(\alpha)}. \quad (4.112)$$

Hence, for a given diagram, the Fourier transform allows to relate its p -space and x -space coefficient functions and the relation reads:

$$C_D[J(D, p, \alpha_1, \alpha_2, \alpha_3, \alpha_4, \alpha_5)] \stackrel{\text{(FT)}}{=} \frac{\prod_{j=1}^5 a(\alpha_j)}{a\left(\sum_{j=1}^5 \alpha_j - D\right)} C_D[J(D, z, \tilde{\alpha}_1, \tilde{\alpha}_2, \tilde{\alpha}_3, \tilde{\alpha}_4, \tilde{\alpha}_5)]. \quad (4.113)$$

Graphically, this can be represented as:

$$\begin{array}{c} \alpha_1 \\ \bullet \\ \alpha_2 \\ \bullet \\ \alpha_5 \\ \bullet \\ \alpha_4 \\ \bullet \\ \alpha_3 \end{array} = \frac{\prod_{j=1}^5 a(\alpha_j)}{a\left(\sum_{j=1}^5 \alpha_j - D\right)} \begin{array}{c} \tilde{\alpha}_1 \\ \bullet \\ \tilde{\alpha}_2 \\ \bullet \\ \tilde{\alpha}_5 \\ \bullet \\ \tilde{\alpha}_4 \\ \bullet \\ \tilde{\alpha}_3 \end{array} z, \quad (4.114)$$

where all external legs were amputated as the diagrams correspond to coefficient functions but we have explicitly indicated the location of the external vertices in the x -space function to distinguish it from its p -space counterpart.

Another useful transformation is the so-called duality transformation. It is based on the fact that the loop momenta are dummy integration variables. They can therefore be replaced by dummy coordinate integration variables. Such an innocent looking change of variables yields a dual diagram with some indices exchanged with respect to the original diagram. At the level of coefficient functions, the relation is given by:

$$\begin{aligned} C_D[J(D, p, \alpha_1, \alpha_2, \alpha_3, \alpha_4, \alpha_5)] &\stackrel{\text{(Du)}}{=} C_D[J(D, z, \alpha_1, \alpha_4, \alpha_3, \alpha_2, \alpha_5)] \\ &\stackrel{\text{(Du)}}{=} C_D[J(D, z, \alpha_3, \alpha_2, \alpha_1, \alpha_4, \alpha_5)] \\ &\stackrel{\text{(Du)}}{=} C_D[J(D, z, \alpha_2, \alpha_3, \alpha_4, \alpha_1, \alpha_5)]. \end{aligned} \quad (4.115)$$

Notice that in the first line, the duality transformation exchanges indices 2 and 4. The two other equalities follow from the symmetries of the diagram ($1 \leftrightarrow 2$, $3 \leftrightarrow 4$ and $1 \leftrightarrow 4$, $2 \leftrightarrow 3$).

For later purposes, let's add that, for an arbitrary planar propagator-type diagram, the dual one can be constructed by first putting a point in every loop of the diagram and two points outside of it. Then, one has to connect all the points by lines such that every line of the initial diagram is crossed once. The new lines produce the dual diagram with indices equal ²¹ to that of the crossed old lines. This is demonstrated by considering the following cases:

$$\begin{array}{c} \alpha_i \\ \bullet \\ \bullet \\ \bullet \\ \bullet \\ \bullet \\ \alpha_i \end{array} \Rightarrow \begin{array}{c} \bullet \\ \bullet \\ \bullet \\ \bullet \\ \bullet \\ \bullet \\ \bullet \end{array} \Rightarrow \begin{array}{c} \alpha_i \\ \bullet \\ \bullet \\ \bullet \\ \bullet \\ \bullet \\ \alpha_i \end{array}, \quad (4.116a)$$

$$\begin{array}{c} \alpha_i \\ \bullet \\ \bullet \\ \bullet \\ \bullet \\ \bullet \\ \alpha_i \end{array} \Rightarrow \begin{array}{c} \bullet \\ \bullet \\ \bullet \\ \bullet \\ \bullet \\ \bullet \\ \bullet \end{array} \Rightarrow \begin{array}{c} \alpha_i \\ \bullet \\ \bullet \\ \bullet \\ \bullet \\ \bullet \\ \alpha_i \end{array}. \quad (4.116b)$$

²¹The duality transformation defined here follows from Kotikov [42, 61] and Kazakov and Kotikov ([40]) and differs from the duality transformation considered by Kazakov [139] which corresponds to duality plus Fourier transform, see Eq. (4.117)

These examples show that, in the general case, not only indices are changed but also the topology of the diagram. Hence, the fact that the 2-loop p-type diagram preserves its topology under the duality transformation is a rather special case.

Both Fourier transform and duality transform relate diagrams which are in different spaces with different integration rules. By combining them, it is possible to relate the coefficient functions of two p -space diagrams with changed indices:

$$C_D[J(D, p, \alpha_1, \alpha_2, \alpha_3, \alpha_4, \alpha_5)] \stackrel{(\text{FT+Du})}{=} \frac{\prod_i a(\alpha_i)}{a(\sum_i \alpha_i - D)} C_D[J(D, p, \tilde{\alpha}_2, \tilde{\alpha}_3, \tilde{\alpha}_4, \tilde{\alpha}_1, \tilde{\alpha}_5)]. \quad (4.117)$$

Other similar transformations can be obtained from the symmetries of the diagram.

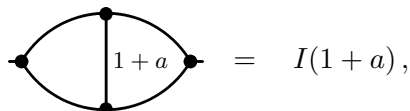
To conclude this section, it is in practice often convenient to perform calculations in dual x -space (see [40, 41, 42]), because the dual transform does not change the indices of the considered diagrams and does not introduce any additional coefficient in front of the diagram. Such type of calculations have been carried out [40, 41, 42] in order to evaluate two-loop four-point diagrams, in a special kinematics, which contribute to the cross-sections of the deep-inelastic scattering at parton level (see [41, 167]). Nowadays, the dual transform is very popular for the evaluation of the so-called conformal integrals (see [168] and references therein).

We would also like to note that it is convenient [169, 170] to use the dual transform even for diagrams having massive propagators, where the mass has formally inverse-mass dimensionality. The recent application of the dual transform to such type of diagrams can be found in the review [171].

4.6 Functional equations

Up to now, all calculations could be performed exactly due to the fact that after some transformations, *e.g.*, integration by parts, uniqueness relation and transformation of indices, the diagrams on the rhs could be reduced to sequences of chains and simple loops. Using the results of Eqs. (4.90) and (4.91) we are for example in a position to compute the expansion for the rather general integral corresponding to $\alpha_i = 1 + a_i \varepsilon$ ($i = 1, 2, 3, 4$) and $\alpha_5 = 1$. However, sometimes, this cannot be achieved, especially when the number of loops is large enough (≥ 5). Actually, as discussed in previous sections, even the 2-loop massless propagator type diagram is beyond IBP and uniqueness for arbitrary values of indices. This is already the case for: $\alpha_i = 1$ ($i = 1, 2, 3, 4$) and $\alpha_5 = 1 + a_5 \varepsilon$ that we shall now proceed on investigating with the help of the so-called functional equations [57, 139].

Let's then consider the simplest non-trivial case previously discussed of a two-loop p-type diagram with an arbitrary index on the central line $I(\alpha_5) = J(D, p, 1, 1, 1, 1, \alpha_5)$ (see Fig. 4a):



$$\text{Diagram} = I(1 + a),$$

where we have chosen $\alpha_5 = 1 + a$. We start by implementing the following sequence of transformations (here In denotes inversion transformation and AL the addition of a new loop):

$$\begin{array}{c} \bullet \\ \diagup \\ \text{---} \\ \diagdown \\ \bullet \end{array} \begin{array}{c} \bullet \\ \diagdown \\ \text{---} \\ \diagup \\ \bullet \end{array} \stackrel{(In)}{=} \begin{array}{c} \bar{\alpha} \\ \bullet \\ \diagup \\ \text{---} \\ \diagdown \\ \bullet \end{array} \begin{array}{c} \bullet \\ \diagdown \\ \text{---} \\ \diagup \\ \bar{\alpha} \\ \bullet \end{array} \stackrel{(AL)}{=} \begin{array}{c} D/2 - \bar{\alpha} \\ \bullet \\ \diagup \\ \text{---} \\ \diagdown \\ \bullet \end{array} \begin{array}{c} \bullet \\ \diagdown \\ \text{---} \\ \diagup \\ D/2 - \bar{\alpha} \\ \bullet \end{array} ,$$

where $\bar{\alpha} = D - t_1 = D - 3 - a$, $v_1 = 1 + a + 2\bar{\alpha}$ and, thus, $\bar{v}_1 = v_1 - D/2 = 1 - 3\varepsilon - a$. This yields the first equation for $I(1+a)$:

$$I(1+a) = I(1-a-3\varepsilon). \quad (4.118)$$

In order to get another equation, we start by applying integration by parts to the right triangle with the vertical distinguished line. This yields:

$$I(1+a)(D-4-2a) = 2 \left[\begin{array}{c} 2 \\ \bullet \\ \diagup \\ \text{---} \\ \diagdown \\ \bullet \end{array} \begin{array}{c} \bullet \\ \diagdown \\ \text{---} \\ \diagup \\ a \\ \bullet \end{array} - \begin{array}{c} 2 \\ \bullet \\ \diagup \\ \text{---} \\ \diagdown \\ \bullet \end{array} \begin{array}{c} \bullet \\ \diagdown \\ \text{---} \\ \diagup \\ 1+a \\ \bullet \end{array} \right]. \quad (4.119)$$

Similarly, using the integration by parts to the right triangle with the lateral distinguished line for the diagram $I(a)$, we obtain:

$$I(a)(D-3-a) = \begin{array}{c} \bullet \\ \diagup \\ \text{---} \\ \diagdown \\ 2 \\ \bullet \end{array} \begin{array}{c} \bullet \\ \diagdown \\ \text{---} \\ \diagup \\ a \\ \bullet \end{array} - p^2 \begin{array}{c} \bullet \\ \diagup \\ \text{---} \\ \diagdown \\ 2 \\ \bullet \end{array} \begin{array}{c} \bullet \\ \diagdown \\ \text{---} \\ \diagup \\ a \\ \bullet \end{array} + a \left[\begin{array}{c} \bullet \\ \diagup \\ \text{---} \\ \diagdown \\ \bullet \end{array} \begin{array}{c} \bullet \\ \diagdown \\ \text{---} \\ \diagup \\ 1+a \\ \bullet \end{array} - \begin{array}{c} \bullet \\ \diagup \\ \text{---} \\ \diagdown \\ \bullet \end{array} \begin{array}{c} \bullet \\ \diagdown \\ \text{---} \\ \diagup \\ 1+a \\ \bullet \end{array} \right], \quad (4.120)$$

where the last two diagrams in the rhs cancel each other. Combining Eqs. (4.119) and (4.120), we come to the equation:

$$\begin{aligned}
-(a+\varepsilon)I(1+a)p^2 + (1-a-2\varepsilon)I(a) &= \begin{array}{c} \bullet \\ \diagup \\ \text{---} \\ \diagdown \\ 2 \\ \bullet \end{array} \begin{array}{c} \bullet \\ \diagdown \\ \text{---} \\ \diagup \\ a \\ \bullet \end{array} - p^2 \begin{array}{c} \bullet \\ \diagup \\ \text{---} \\ \diagdown \\ 2 \\ \bullet \end{array} \begin{array}{c} \bullet \\ \diagdown \\ \text{---} \\ \diagup \\ 1+a \\ \bullet \end{array} \\
&= \frac{p^{-2(a+2\varepsilon)}}{(4\pi)^D} [G(D, 2, a)G(D, 1, 1+a+\varepsilon) - G(D, 1, a+1)G(D, 2, 1+a+\varepsilon)]. \quad (4.121)
\end{aligned}$$

After some little algebra, we have for the coefficient function:

$$C_D[I(1+a)] = \frac{1-a-2\varepsilon}{a+\varepsilon} C_D[I(a)] + \frac{2(2a-1+3\varepsilon)\Gamma(-a-\varepsilon)\Gamma(a-1+2\varepsilon)\Gamma^2(1-\varepsilon)}{(a+\varepsilon)\Gamma(a+1)\Gamma(2-3\varepsilon-a)}. \quad (4.122)$$

Eqs. (4.118) and (4.122) are the desired functional equations for $I(1+a)$.

4.6.1 Solution of the functional equations

To simplify the inhomogeneous part of Eq. (4.122), we make the substitution:

$$C_D[I(1+a)] = 2 \frac{\Gamma^2(1-\varepsilon)\Gamma(-a-\varepsilon)\Gamma(a+2\varepsilon)}{\Gamma(a+1)\Gamma(1-3\varepsilon-a)} F(1+a), \quad (4.123)$$

where the function $F(1+a)$ obeys the following equations: ²²

$$F(1+a) = F(1-a-3\varepsilon), \quad (4.124a)$$

$$F(1+a) = -\frac{a}{a-1+3\varepsilon} F(a) - \frac{1}{a-1+3\varepsilon} \left[\frac{1}{a+\varepsilon} + \frac{1}{a-1+2\varepsilon} \right]. \quad (4.124b)$$

The solution of Eqs. (4.124a) and (4.124b) has been found by D. Kazakov in Refs. [56, 139]. In order to do so, he used the analytic properties of $I(1+a)$ which can be obtained from, *e.g.*, its α -representation (see Eq. (12) in [56]), and are such that the function $I(1+a)$ is a meromorphic function, regular at $a=0$ with simple poles at $a=\pm n-2\varepsilon$ and $a=\pm n-\varepsilon$, where $n=1, 2, \dots$. The same conclusion follows from the inhomogeneous term in Eq. (4.122). The function $F(1+a)$ obtains additional poles due to the Γ -functions in the denominator of Eq. (4.123). Therefore, the solution to Eq. (4.124) can be sought for in the form of an infinite series of poles:

$$F(1+a) = \sum_{n=1}^{\infty} f_n^{(1)} \left(\frac{1}{n+a+\varepsilon} + \frac{1}{n-a-2\varepsilon} \right) + \sum_{n=1}^{\infty} f_n^{(2)} \left(\frac{1}{n+a} + \frac{1}{n-a-3\varepsilon} \right). \quad (4.125)$$

Notice that Eq. (4.125) satisfies Eq. (4.124a). We may now substitute Eq. (4.125) into the following equation coming from Eq. (4.124b):

$$(a-1+3\varepsilon)F(1+a) = -aF(a) - \left[\frac{1}{a+\varepsilon} + \frac{1}{a-1+2\varepsilon} \right]. \quad (4.126)$$

Comparing the terms $1/(n+a+\varepsilon)$ and $1/(n+a)$, we obtain the following equations for the functions $f_n^{(i)}$ ($i=1, 2$):

$$-(n+1-2\varepsilon)(1-\delta_n^0)f_n^{(1)} = (n+\varepsilon)f_{n+1}^{(1)} - \delta_n^0, \quad (4.127a)$$

$$-(n+1-3\varepsilon)(1-\delta_n^0)f_n^{(2)} = nf_{n+1}^{(2)}. \quad (4.127b)$$

In the case $n \geq 1$, these equations simplify as:

$$f_n^{(1)} = -f_{n+1}^{(1)} \frac{n+\varepsilon}{n+1-2\varepsilon}, \quad f_n^{(2)} = -f_{n+1}^{(2)} \frac{n}{n+1-3\varepsilon}, \quad (4.128)$$

and their solution reads:

$$f_n^{(1)} = (-1)^n c_1(\varepsilon) \frac{\Gamma(n+1-2\varepsilon)}{\Gamma(n+\varepsilon)}, \quad f_n^{(2)} = (-1)^n c_2(\varepsilon) \frac{\Gamma(n+1-3\varepsilon)}{\Gamma(n)}. \quad (4.129)$$

In the case $n=0$, Eqs. (4.127) only fix the function $c_1(\varepsilon)$:

$$c_1(\varepsilon) = -\frac{\Gamma(\varepsilon)}{\Gamma(2-2\varepsilon)}. \quad (4.130)$$

²²We would like to note that the inhomogeneous terms in Eq. (11) of [57] and in Eq. (2.14) of [139] have wrong signs. Moreover, the r.h.s. of Eqs. (14) and (15) of [57] and also the r.h.s of Eqs. (2.17) and (2.18) of [139] should have the additional sign “-”.

In order to find c_2 , we compare the obtained solution with the known one for a particular value of a , e.g., $a = 0$. On the one hand, Eqs. (4.123) and (3.42) yield:

$$F(1) = \frac{1}{\varepsilon(1-2\varepsilon)} - \frac{1}{\varepsilon(1-2\varepsilon)} \frac{\Gamma^2(1+\varepsilon)\Gamma(1-\varepsilon)\Gamma(1-3\varepsilon)}{\Gamma^2(1-2\varepsilon)\Gamma(1+2\varepsilon)}. \quad (4.131)$$

On the other hand, from (4.125) for $a = 0$ and (4.130) we have:

$$\begin{aligned} F(1) &= -\frac{\Gamma(\varepsilon)}{\Gamma(2-2\varepsilon)} \sum_{n=1}^{\infty} (-1)^n \frac{\Gamma(n+1-2\varepsilon)}{\Gamma(n+\varepsilon)} \left(\frac{1}{n+\varepsilon} + \frac{1}{n-2\varepsilon} \right) + \\ &+ c_2(\varepsilon) \sum_{n=1}^{\infty} (-1)^n \frac{\Gamma(n+1-3\varepsilon)}{\Gamma(n)} \left(\frac{1}{n} + \frac{1}{n-3\varepsilon} \right). \end{aligned} \quad (4.132)$$

Since

$$\begin{aligned} \sum_{n=1}^{\infty} (-1)^n \frac{\Gamma(n+1-2\varepsilon)}{\Gamma(n+\varepsilon)} \left(\frac{1}{n+\varepsilon} + \frac{1}{n-2\varepsilon} \right) &= \sum_{n=1}^{\infty} (-1)^n \frac{\Gamma(n+1-2\varepsilon)}{\Gamma(n+1+\varepsilon)} + \sum_{n=1}^{\infty} (-1)^n \frac{\Gamma(n-2\varepsilon)}{\Gamma(n+\varepsilon)} \\ &= -\sum_{n=2}^{\infty} (-1)^n \frac{\Gamma(n-2\varepsilon)}{\Gamma(n+\varepsilon)} + \sum_{n=1}^{\infty} (-1)^n \frac{\Gamma(n-2\varepsilon)}{\Gamma(n+\varepsilon)} \\ &= -\frac{\Gamma(1-2\varepsilon)}{\Gamma(1+\varepsilon)}, \end{aligned} \quad (4.133)$$

and

$$\begin{aligned} \sum_{n=1}^{\infty} (-1)^n \frac{\Gamma(n+1-3\varepsilon)}{\Gamma(n)} \left(\frac{1}{n} + \frac{1}{n-3\varepsilon} \right) &= \sum_{n=1}^{\infty} (-1)^n \frac{\Gamma(n+1-3\varepsilon)}{\Gamma(n+1)} + \sum_{n=1}^{\infty} (-1)^n \frac{\Gamma(n-3\varepsilon)}{\Gamma(n)} \\ &= -\sum_{n=2}^{\infty} (-1)^n \frac{\Gamma(n-3\varepsilon)}{\Gamma(n)} + \sum_{n=1}^{\infty} (-1)^n \frac{\Gamma(n-3\varepsilon)}{\Gamma(n)} \\ &= -\Gamma(1-3\varepsilon), \end{aligned} \quad (4.134)$$

then Eq. (4.132) may be written as:

$$F(1) = \frac{1}{\varepsilon(1-2\varepsilon)} - c_2(\varepsilon)\Gamma(1-3\varepsilon). \quad (4.135)$$

Comparing (4.131) and (4.135) then yields:

$$c_2(\varepsilon) = +\frac{\Gamma(\varepsilon)\Gamma(1-\varepsilon)\Gamma(1+\varepsilon)}{\Gamma(2-2\varepsilon)\Gamma(1-2\varepsilon)\Gamma(1+2\varepsilon)}. \quad (4.136)$$

As a result, we have:

$$\begin{aligned} C_D[I(1+a)] &= -2 \frac{\Gamma^2(1-\varepsilon)\Gamma(-a-\varepsilon)\Gamma(a+2\varepsilon)\Gamma(\varepsilon)}{\Gamma(a+1)\Gamma(1-3\varepsilon-a)\Gamma(2-2\varepsilon)} \left[\sum_{n=1}^{\infty} (-1)^n \frac{\Gamma(n+1-2\varepsilon)}{\Gamma(n+\varepsilon)} \left(\frac{1}{n+a+\varepsilon} \right. \right. \\ &\left. \left. + \frac{1}{n-a-2\varepsilon} \right) - \frac{\Gamma(1-\varepsilon)\Gamma(1+\varepsilon)}{\Gamma(1-2\varepsilon)\Gamma(1+2\varepsilon)} \sum_{n=1}^{\infty} (-1)^n \frac{\Gamma(n+1-3\varepsilon)}{\Gamma(n)} \left(\frac{1}{n+a} + \frac{1}{n-a-3\varepsilon} \right) \right]. \end{aligned} \quad (4.137)$$

Ultimately, in order to ascertain the validity of the solution (4.137), one has to be convinced that it is impossible to add an arbitrary solution of the homogeneous equation. Indeed, such a solution vanishes at integer points, is an analytic function and exponentially bounded on the imaginary axis. Hence, due to the Carlson theorem [172], it is identically zero.

The last sum in (4.137) is equal to $-\Gamma(1+a)\Gamma(1-a-3\varepsilon)$. Thus, Eq. (4.137) can be also rewritten as:

$$C_D[F(1+a)] = -2 \frac{\Gamma^2(1-\varepsilon)\Gamma(\varepsilon)}{\Gamma(2-2\varepsilon)} \left[\frac{\Gamma(-a-\varepsilon)\Gamma(a+2\varepsilon)}{\Gamma(a+1)\Gamma(1-3\varepsilon-a)} \sum_{n=1}^{\infty} (-1)^n \frac{\Gamma(n+1-2\varepsilon)}{\Gamma(n+\varepsilon)} \right. \\ \left. \times \left(\frac{1}{n+a+\varepsilon} + \frac{1}{n-a-2\varepsilon} \right) + \frac{\Gamma(1-\varepsilon)\Gamma(1+\varepsilon)\Gamma(-a-2\varepsilon)\Gamma(a+2\varepsilon)}{\Gamma(1-2\varepsilon)\Gamma(1+2\varepsilon)} \right], \quad (4.138)$$

which exactly coincides with Eq. (3.57) after the appropriate change of variables. Hence, the functional equation method shows that diagram $F(1+a)$ is expressible as a combination of Γ -functions together with two hypergeometric functions of argument “-1” thereby proving the result advertised in Eq. (3.57).

The result of Eq. (4.138) for $F(1+a_5\varepsilon)$ can be expanded in series in ε . This provides additional information and gives a possibility to construct the ε -expansion for the general case $\alpha_i = 1 + a_i\varepsilon$ ($i = 1, 2, 3, 4, 5$).

4.6.2 Expansion of $I(1+a_5\varepsilon)$

The important master integral $I(1+a_5\varepsilon)$ can be calculated using Eq. (4.138). After a little algebra, we have for its coefficient function:

$$C_D[I(1+a_5\varepsilon)] = \frac{\hat{K}_2}{1-2\varepsilon} \left[A_0\zeta_2 + A_1\zeta_4\varepsilon + A_2\zeta_5\varepsilon^2 + [A_3\zeta_6 - A_4\zeta_3^2]\varepsilon^3 \right. \\ \left. + [A_5\zeta_7 - A_6\zeta_3\zeta_4]\varepsilon^4 + O(\varepsilon^5) \right], \quad (4.139)$$

with

$$\begin{aligned} A_0 &= 6, \\ A_1 &= 9, \\ A_2 &= 42 + 45a_5 + 15a_5^2, \\ A_3 &= \frac{5}{2}(A_2 - 6), \\ A_4 &= 46 + 45a_5 + 15a_5^2, \\ A_5 &= 294 + \frac{2223}{4}a_5 + \frac{3183}{8}a_5^2 + \frac{567}{4}a_5^3 + \frac{189}{8}a_5^4, \\ A_6 &= 3(A_4 - 1), \end{aligned} \quad (4.140)$$

where \hat{K}_n was defined in Eq. (4.92). Notice that, when $a_5 = 0$, we recover the result in (3.43).

4.7 Final results for $J(D, p, 1 + a_1\varepsilon, 1 + a_2\varepsilon, 1 + a_3\varepsilon, 1 + a_4\varepsilon, 1 + a_5\varepsilon)$

Using the methods reviewed so far: integration by parts, the method of uniqueness, functional equations together with various transformations of the considered diagram, Kazakov found several terms of ε -expansion of the two-loop master integral $J(D, p, 1 + a_1\varepsilon, 1 + a_2\varepsilon, 1 + a_3\varepsilon, 1 + a_4\varepsilon, 1 + a_5\varepsilon)$. The result reads [57]:

$$C_D[I(1 + a_1\varepsilon, 1 + a_2\varepsilon, 1 + a_3\varepsilon, 1 + a_4\varepsilon, 1 + a_5\varepsilon)] = \frac{\hat{K}_2}{1 - 2\varepsilon} \left[A_0\zeta_2 + A_1\zeta_4\varepsilon + A_2\zeta_5\varepsilon^2 \right. \\ \left. + [A_3\zeta_6 - A_4\zeta_3^2]\varepsilon^3 + [A_5\zeta_7 - A_6\zeta_3\zeta_4]\varepsilon^4 + O(\varepsilon^5) \right], \quad (4.141)$$

with

$$\begin{aligned} A_0 &= 6, \\ A_1 &= 9, \\ A_2 &= 42 + \sum_{i=1}^2 A_{2,i}, \\ A_3 &= \frac{5}{2}(A_2 - 6), \\ A_4 &= 46 + \sum_{i=1}^3 A_{4,i}, \\ A_5 &= 294 + \sum_{i=1}^4 A_{5,i}, \\ A_6 &= 3(A_4 - 1), \end{aligned} \quad (4.142)$$

where \hat{K}_n was defined in (4.92) and

$$\begin{aligned} A_{2,1} &= 30\bar{A}_1 + 45a_5, \\ A_{4,1} &= 42\bar{A}_1 + 45a_5, \\ A_{5,1} &= 402\bar{A}_1 + \frac{2223}{4}a_5, \\ A_{2,2} &= 10\bar{A}_2 + 15a_5^2 + 15\bar{A}_1a_5 + 10(a_1a_2 + a_3a_4 + a_1a_4 + a_2a_3) + 5(a_1a_3 + a_2a_4), \\ A_{4,2} &= 14\bar{A}_2 + 15a_5^2 + 33\bar{A}_1a_5 + 50(a_1a_2 + a_3a_4) + 14(a_1a_4 + a_2a_3) + \\ &+ 31(a_1a_3 + a_2a_4), \\ A_{4,3} &= 6a_5\bar{A}_2 + 6a_5^2\bar{A}_1 + 24a_5(a_1a_2 + a_3a_4) + 12a_5(a_1a_3 + a_2a_4) + \\ &+ 12(a_1a_2a_3 + a_1a_2a_4 + a_1a_3a_4 + a_2a_3a_4) + 12(a_1^2a_2 + a_1a_2^2 + a_3^2a_4 + a_3a_4^2) + \\ &+ 6(a_1^2a_3 + a_1a_3^2 + a_2^2a_4 + a_2a_4^2), \\ A_{5,2} &= 260\bar{A}_2 + \frac{3183}{8}a_5^2 + 516\bar{A}_1a_5 + 386(a_1a_2 + a_3a_4 + a_1a_4 + a_2a_3) + \\ &+ \frac{575}{2}(a_1a_3 + a_2a_4), \end{aligned}$$

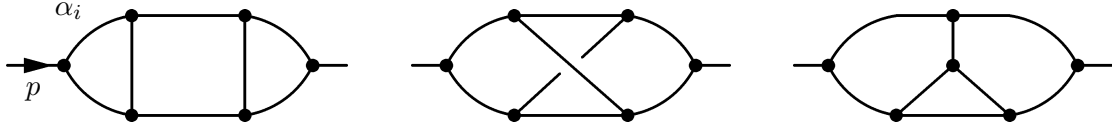


Figure 7: Three-loop scalar massless propagator-type diagrams.

$$\begin{aligned}
A_{5,3} &= 84 \bar{A}_3 + \frac{567}{4} a_5^3 + \frac{945}{4} a_5 \bar{A}_2 + 252 a_5^2 \bar{A}_1 + \frac{693}{2} a_5 (a_1 a_2 + a_3 a_4 + a_1 a_4 + a_2 a_3) + \\
&+ \frac{945}{4} a_5 (a_1 a_3 + a_2 a_4) + 210 (a_1 a_2 a_3 + a_1 a_2 a_4 + a_1 a_3 a_4 + a_2 a_3 a_4) + \\
&+ 168 (a_1^2 a_2 + a_1 a_2^2 + a_3^2 a_4 + a_3 a_4^2 + a_1^2 a_4 + a_1 a_4^2 + a_2^2 a_3 + a_2 a_3^2) \\
&+ \frac{441}{4} (a_1^2 a_3 + a_1 a_3^2 + a_2^2 a_4 + a_2 a_4^2), \\
A_{5,4} &= 14 \bar{A}_4 + \frac{189}{8} a_5^4 + 42 a_5 \bar{A}_3 + \frac{189}{4} a_5^3 \bar{A}_1 + \frac{525}{8} a_5^2 \bar{A}_2 + \\
&+ \frac{357}{4} a_5^2 (a_1 a_2 + a_3 a_4 + a_1 a_4 + a_2 a_3) + \\
&+ \frac{105}{2} a_5^2 (a_1 a_3 + a_2 a_4) + \frac{357}{4} a_5 (a_1 a_2 a_3 + a_1 a_2 a_4 + a_1 a_3 a_4 + a_2 a_3 a_4) + \\
&+ 84 a_5 (a_1^2 a_2 + a_1 a_2^2 + a_3^2 a_4 + a_3 a_4^2 + a_1^2 a_4 + a_1 a_4^2 + a_2^2 a_3 + a_2 a_3^2) \\
&+ \frac{189}{4} a_5 (a_1^2 a_3 + a_1 a_3^2 + a_2^2 a_4 + a_2 a_4^2) + \\
&+ 28 (a_1^3 a_2 + a_1 a_2^3 + a_3^3 a_4 + a_3 a_4^3 + a_1^3 a_4 + a_1 a_4^3 + a_2^3 a_3 + a_2 a_3^3) \\
&+ 14 (a_1^3 a_3 + a_1 a_3^3 + a_2^3 a_4 + a_2 a_4^3) + \\
&+ 42 (a_1^2 a_2^2 + a_3^2 a_4^2 + a_1^2 a_4^2 + a_2^2 a_3^2) + \frac{189}{8} (a_1^2 a_3^2 + a_2^2 a_4^2) + \\
&+ 42 (a_1^2 a_2 a_3 + a_1^2 a_2 a_4 + a_1^2 a_3 a_4 + a_2^2 a_1 a_4 + a_2^2 a_1 a_3 + a_2^2 a_3 a_4 + \\
&+ a_3^2 a_1 a_4 + a_3^2 a_2 a_4 + a_3^2 a_1 a_2 + a_4^2 a_2 a_3 + a_4^2 a_1 a_3 + a_4^2 a_1 a_2) + \frac{315}{4} a_1 a_2 a_3 a_4, \quad (4.143)
\end{aligned}$$

and $\bar{A}_n = a_1^n + a_2^n + a_3^n + a_4^n$. We would like to note that for $a_2 = a_3 = a_5 = 0$ (respectively, $a_1 = a_2 = a_3 = a_4 = 0$) Eqs. (4.141)-(4.143) transform to the ones of (4.90)-(4.92) (respectively, to the ones of (4.139)-(4.140)).

4.8 Three-loop master integrals

At three loops there are three generic topologies of massless propagator-type diagrams, see Fig. 7. For some special values of the indices, these diagrams are primitively two-loop and can therefore be computed with the help of the results derived so far. Let's consider for instance the following two basic massless integrals:

$$J_1(D, p, \alpha_1, \alpha_2, \alpha_3, \alpha_4, \alpha_5, \alpha_6, \alpha_7) = \text{diagram} \quad , \quad (4.144a)$$

$$J_2(D, p, \alpha_1, \alpha_2, \alpha_3, \alpha_4, \alpha_5, \alpha_6, \alpha_7) = \text{Diagram} , \quad (4.144b)$$

which can be obtained for some special values of the indices of the last (benz) diagram in Fig. 7 and which are actually related to each other (see below).

When all line indices are equal to 1, the first three-loop master, $J_1(D, p, 1, 1, 1, 1, 1, 1, 1)$, can be expressed in the following form (with the help of the IBP procedure for the upper triangle with the vertical line being distinguished):

$$\text{Diagram} (D-4) = 2 \text{Diagram} - \text{Diagram} - \text{Diagram} . \quad (4.145)$$

The last term in the rhs contains the two-loop internal diagram $I(1)$, which has the p -dependence given by $1/p^{2(1+2\varepsilon)}$. So, the last term can be represented as $C_D[I(1)]G(2, 1+2\varepsilon)/p^{2(1+3\varepsilon)}$. Thus, the rhs of eq. (4.145) can be transformed into the form:

$$G(2, 1) \text{Diagram} - G(2, 1+2\varepsilon) \text{Diagram} ,$$

i.e., the first three-loop master integral can be expressed in terms of the two-loop master ones. Performing various transformations on the integral, Kazakov managed to derive its ε -expansion which takes the form [57]:²³

$$\begin{aligned} & C_D[J_1(D, p, 1 + a_1\varepsilon, 1 + a_2\varepsilon, 1 + a_3\varepsilon, 1 + a_4\varepsilon, 1 + a_5\varepsilon, \varepsilon + a_6\varepsilon, 1 + a_7\varepsilon)] \\ &= \frac{\hat{K}_3}{1-2\varepsilon} \left[B_0\zeta_5 + [B_1\zeta_6 + B_2\zeta_3^2]\varepsilon + [B_3\zeta_7 + B_4\zeta_3\zeta_4]\varepsilon^2 + O(\varepsilon^3) \right], \end{aligned} \quad (4.146)$$

with

$$B_0 = 20, \quad B_1 = 50, \quad B_2 = 20 + 6\bar{B}, \quad B_4 = 3B_2, \quad B_3 = 380 + 7 \sum_{i=1}^2 B_{3,i}, \quad (4.147)$$

where $\bar{B} = a_4 + a_5 + a_6 + a_7$ and

$$\begin{aligned} B_{3,1} &= \frac{1}{4}\bar{B} + 24(a_1 + a_3) + 32a_2 + 17(a_4 + a_5) + 33(a_6 + a_7), \\ B_{3,2} &= \frac{1}{8}\bar{B}^2 + 6(a_1^2 + a_3^2) + 8a_2^2 + 4(a_4^2 + a_5^2) + 8(a_6^2 + a_7^2) + 8(a_1 + a_3)a_2 \\ &+ 2(a_1a_4 + a_3a_5) + 6(a_1a_5 + a_3a_4) + 10(a_1a_6 + a_3a_7) + 6(a_1a_7 + a_3a_6) \\ &+ 4a_1a_3 + 4(a_4 + a_5)a_2 + 12(a_6 + a_7)a_2 + 2a_4a_5 + 4(a_4a_6 + a_5a_7) \\ &+ 6(a_4a_7 + a_5a_6) + 10a_6a_7. \end{aligned} \quad (4.148)$$

²³Similar results have been recently published in Ref. [173].

The results for the second three-loop master integral $J_2(D, p, \alpha_1, \alpha_2, \alpha_3, \alpha_4, \alpha_5, \alpha_6, \alpha_7)$ can be obtained in the following way:

$$\begin{aligned}
 \text{Diagram 1} & \stackrel{(\text{FT})}{=} \frac{\prod_{k=1}^7 a(\alpha_k)}{a\left(\sum_{k=1}^7 \alpha_k - 3D/2\right)} \text{Diagram 2} \\
 & \stackrel{(\text{D})}{=} \frac{\prod_{k=1}^7 a(\alpha_k)}{a\left(\sum_{k=1}^7 \alpha_k - 3D/2\right)} \text{Diagram 3} ,
 \end{aligned}$$

i.e., by first transforming the considered diagram to x -space with the help of a Fourier transform and later returning to p -space using the dual transformation. So, we can express the coefficient function for the second three-loop master integral through the one of the first three-loop master integral $J_1(D, p, \alpha_1, \alpha_2, \alpha_3, \alpha_4, \alpha_5, \alpha_6, \alpha_7)$, *i.e.*,

$$C_D[J_2(D, p, \alpha_1, \alpha_2, \alpha_3, \alpha_4, \alpha_5, \alpha_6, \alpha_7)] = \frac{\prod_{i=1}^7 a(\alpha_i)}{a\left(\sum_{i=1}^7 \alpha_i - 3D/2\right)} C_D[J_1(D, p, \tilde{\alpha}_1, \tilde{\alpha}_2, \tilde{\alpha}_3, \tilde{\alpha}_4, \tilde{\alpha}_5, \tilde{\alpha}_6, \tilde{\alpha}_7)]. \quad (4.149)$$

The expansion for $C_D[J_2(D, p, 1 + a_1\varepsilon, 1 + a_2\varepsilon, 1 + a_3\varepsilon, 1 + a_4\varepsilon, 1 + a_5\varepsilon, 1 + a_6\varepsilon, 1 + a_7\varepsilon)]$ can therefore be obtained from Eqs. (4.146) and (4.148) with the help of the replacement $a_i \rightarrow -(a_i + 1)$ ($i = 1, \dots, 7$). Of course, the coefficient $\prod_{i=1}^7 a(1 + a_i\varepsilon)/a\left(1 + \left(\sum_{i=1}^7 a_i + 3\right)\varepsilon\right)$ should also be taken into account.

5 More examples of calculations

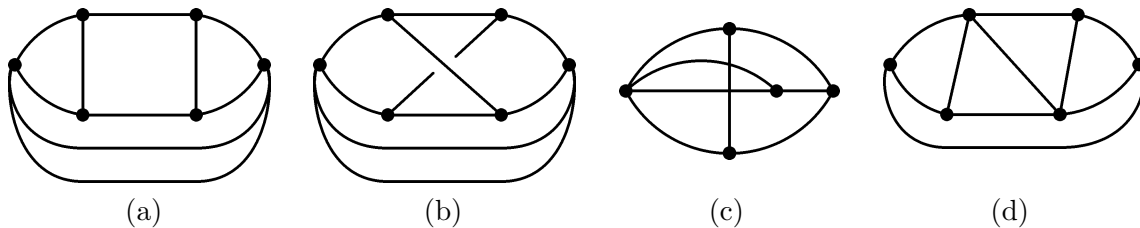
We shall now consider the Φ^4 -model and give some additional examples of concrete calculations. Using a combination of the methods presented in the last section, and following Kazakov, we will show that, up to five loops, the singular part of several complicated diagrams may be calculated exactly by reducing them to the two-loop massless propagator-type diagram.

5.1 Three and four loop calculations in the Φ^4 -model

In order to compute the three- and four-loop β -function of the Φ^4 -model one has, in particular, to calculate the singular parts of the following vertex diagrams:

$$\begin{aligned}
 \text{Diagram 4} & , \quad \text{Diagram 5} , \quad (5.150)
 \end{aligned}$$

where all lines have index 1. It is well known that the singular (UV) contributions of a diagram do not depend on masses and external momenta (and, in the $\overline{\text{MS}}$ scheme, on γ_E and ζ_2 as well)

Figure 8: The four most complicated 5-loop diagrams of the Φ^4 -model.

[31]. This observation is at the basis of the so-called infrared rearrangement (IRR) method [46] which, simply stated, allows to set some external momenta to zero in order to extract ε -poles. For the above diagrams, one may proceed in the following way:

$$\text{Sing} \left[\begin{array}{c} \text{Diagram (a)} \end{array} \right] = \text{Sing} \left[\begin{array}{c} \text{Diagram (b)} \end{array} \right] = \frac{1}{3\varepsilon} \text{Finite} \left[\begin{array}{c} \text{Diagram (c)} \end{array} \right] = \frac{2}{\varepsilon} \zeta_3. \quad (5.151a)$$

$$\text{Sing} \left[\begin{array}{c} \text{Diagram (d)} \end{array} \right] = \text{Sing} \left[\begin{array}{c} \text{Diagram (e)} \end{array} \right] = \frac{1}{4\varepsilon} \text{Finite} \left[\begin{array}{c} \text{Diagram (f)} \end{array} \right] = \frac{5}{\varepsilon} \zeta_5, \quad (5.151b)$$

where the vertex diagrams were reduced to p-type ones and the results of the previous section were used to compute the finite parts of the massless two-loop and three-loop V-shaped p-type diagrams.

5.2 Five loop calculations in the Φ^4 -model

Following Kazakov, we may even go further and apply the described techniques to five-loop renormalization-group calculations in the Φ^4 -model. In this connection, let's recall that the five-loop anomalous dimensions and beta-function in this model in the MS-scheme were calculated long time ago in [55]. The full computation required the evaluation of about 120 diagrams. All but four were calculated analytically using integration by parts. For the remaining four most complicated diagrams, see Fig. 8, an expansion in Gegenbauer polynomials provides the result in the form of a triple infinite convergent series. Computer summation of the series made it possible to achieve good accuracy. However, it is understandable that one would like to obtain an analytic evaluation of these contributions. In order to test the possibilities of the considered above methods, we will present the calculation some of these complicated diagrams. As it was shown in [39], already in [55], it proved to be possible to sum the series for diagram “a” analytically and express the obtained result in terms of ζ_5 and ζ_6 . The results for the other diagrams have also been obtained by Kazakov in [39, 56, 57].

In the following, we will focus on a detailed computation of diagrams “a” and “d”.

5.2.1 Diagram “a”

For diagram “a” (where all indices are equal to 1) the problem is equivalent to calculating the diagram:

$$I_a = \text{Diagram} ,$$

with $O(\varepsilon)$ accuracy.

Applying the IBP procedure to the right triangle with the vertical distinguished line, we first obtain the following relation:

$$\text{Diagram} (D-4) = 2 \left[\text{Diagram}_1 - \text{Diagram}_2 \right] . \quad (5.152)$$

To evaluate the second diagram in the rhs of Eq. (5.152), it is convenient to consider the second three loop master integral $J_2(D, p, \alpha_1, \alpha_2, \alpha_3, \alpha_4, \alpha_5, \alpha_6, \alpha_7)$ with $\alpha_i = 1$ ($i = 1, \dots, 7$). We may then apply the IBP procedure to this diagram twice: for the right triangle with the upper distinguished line and for the middle triangle with the upper distinguished line. The corresponding results read:

$$p \text{Diagram} (D-4) = 2 \text{Diagram}_1 - \text{Diagram}_2 - p^2 \text{Diagram}_3 , \quad (5.153a)$$

$$\text{Diagram} (D-4) = 2 \left[\text{Diagram}_4 - \text{Diagram}_5 \right] . \quad (5.153b)$$

Taking the combination of these two equations, we obtain, for the second diagram in the rhs of (5.152), the following result:

$$\text{Diagram}_2 = \frac{1}{p^2} \left[4 \text{Diagram}_1 - 3 \text{Diagram}_4 \right] . \quad (5.154)$$

Then, substituting back the result of Eq. (5.154) in the rhs of Eq. (5.152) and calculating the remaining one-loop parts, yields, for rhs of (5.152):

$$\frac{2G(D, 2, 1)}{p^2} \left[\text{Diagram}_1 p^{2\varepsilon} - 4 \text{Diagram}_1 + 3 \text{Diagram}_4 \right] .$$

Evaluating the two-loop master integrals appearing in this equation using the expansions provided by Eqs. (4.90) and (4.139), we obtain the expression of the diagram I_a with an accuracy even reaching $O(\varepsilon^2)$:

$$\text{Diagram} = \frac{\hat{K}_3}{1-2\varepsilon} \left[20\zeta_5 + [50\zeta_6 + 44\zeta_3^2]\varepsilon + [317\zeta_7 + 132\zeta_3\zeta_4]\varepsilon^2 + O(\varepsilon^3) \right] \frac{1}{p^{2(2+3)\varepsilon}} . \quad (5.155)$$

Taking into account of the two additional loops produces an additional factor:

$$G(D, 1, 2 + 3\varepsilon)G(D, 1, 1 + 4\varepsilon) = -\frac{1}{20\varepsilon^2} \frac{1}{(1 + 3\varepsilon)(1 - 6\varepsilon)} \frac{\Gamma^2(1 - \varepsilon)\Gamma(1 - 4\varepsilon)\Gamma(1 + 5\varepsilon)}{\Gamma(1 + 3\varepsilon)\Gamma(1 - 6\varepsilon)}. \quad (5.156)$$

Hence, the final result for diagram ‘‘a’’ has the following form:

$$\text{Sing} \left[\text{Diagram} \right] = -\frac{\hat{K}_5}{20(1 - 2\varepsilon)(1 + 3\varepsilon)(1 - 6\varepsilon)} \left[\frac{20}{\varepsilon^2} \zeta_5 + \left[50\zeta_6 + 44\zeta_3^2 \right] \frac{1}{\varepsilon} + 317\zeta_7 + 132\zeta_3\zeta_4 + O(\varepsilon) \right] \frac{1}{p^{10\varepsilon}}. \quad (5.157)$$

5.2.2 Diagram ‘‘d’’

The evaluation of the singular part of diagram ‘‘d’’ (where all indices are equal to 1) is equivalent to calculating the diagram:

$$I_d = \text{Diagram}, \quad (5.158)$$

with $O(\varepsilon^0)$ accuracy. Indeed, the additional loop provides the factor: $G(1, 1 + 4\varepsilon) = \Gamma(1 + \varepsilon)/(5\varepsilon) + O(\varepsilon^0)$.

In order to proceed with the computation, it is firstly convenient to transform the considered diagram to x -space by Fourier transform and then to return to p -space using the dual transformation:

$$\text{Diagram} \stackrel{\text{(Du)}}{=} \text{Diagram}_0 \stackrel{\text{(F)}}{=} \text{Diagram}_p + O(\varepsilon). \quad (5.159)$$

Since the considered accuracy is $O(\varepsilon^0)$, we may as well consider the following diagram:

$$\text{Diagram}_p \quad (5.160)$$

Applying the IBP procedure for the right triangle with the vertical distinguished line, we have the following relation:

$$\text{Diagram}_p \quad (D - 4) = 2 \text{Diagram}_1 - \text{Diagram}_2 - \text{Diagram}_3 \quad (5.161)$$

The first diagram in the rhs of the above equation can be simplified as follows: ²

$$\text{Diagram}_1 = G(D, 2, 1) \text{Diagram}_2 \quad (5.162)$$

On the other hand, the last diagram can be represented as:

$$\begin{array}{c} \text{Diagram 1} \\ \text{2} \end{array} = G(D, 2, 1 + \varepsilon) \begin{array}{c} \text{Diagram 2} \\ \text{1} \end{array}, \quad (5.163)$$

because the diagram contains an internal three-loop one with p -dependence of the form: $\sim 1/p^{2(1+\varepsilon)}$. Finally, the right upper triangle of the second diagram in the rhs of Eq. (5.161) is unique; so, we have:

$$\begin{array}{c} \text{Diagram 1} \\ \text{2} \end{array} = G(D, 2, 1) \begin{array}{c} \text{Diagram 2} \\ \text{1} \end{array}. \quad (5.164)$$

Combining the above results yields the following expression for the diagram of Eq. (5.161):

$$\begin{array}{c} \text{Diagram 1} \\ p \end{array} \times (D-4) = G(D, 2, 1) \left[2 \begin{array}{c} \text{Diagram 2} \\ \text{1} \end{array} - \begin{array}{c} \text{Diagram 3} \\ \text{1} \end{array} - \frac{G(D, 2, 1 + \varepsilon)}{G(D, 2, 1)} \begin{array}{c} \text{Diagram 4} \\ \text{1} \end{array} \right]. \quad (5.165)$$

Notice that the ratio $G(D, 2, 1 + \varepsilon)/G(D, 2, 1) = 1 + O(\varepsilon^3)$ so it can be replaced by 1 and Eq. (5.165) may be further simplified as:

$$\begin{array}{c} \text{Diagram 1} \\ p \end{array} \times (D-4) = G(D, 2, 1) \left[2 \begin{array}{c} \text{Diagram 2} \\ \text{1} \end{array} - \begin{array}{c} \text{Diagram 3} \\ \text{1} \end{array} - \begin{array}{c} \text{Diagram 4} \\ \varepsilon \end{array} \right]. \quad (5.166)$$

Evaluating the three-loop master integrals in the rhs of Eq. (5.166) with the help of Eqs. (4.146) and (4.148), yields the following result for the considered diagram:

$$\begin{array}{c} \text{Diagram 1} \\ p \end{array} = \begin{array}{c} \text{Diagram 2} \\ \text{1} \end{array} + O(\varepsilon) = \frac{441}{8} \zeta_7 \frac{1}{p^{2(1+4\varepsilon)}} + O(\varepsilon). \quad (5.167)$$

Hence, the singular part of diagram “d” reads:

$$\text{Sing} \left[\begin{array}{c} \text{Diagram 1} \\ p \end{array} \right] = \frac{441}{40\varepsilon} \zeta_7 \frac{1}{p^{10\varepsilon}} + O(\varepsilon^0). \quad (5.168)$$

6 Conclusion

In the present article, we have reviewed several powerful multi-loop techniques devoted to the *analytical* calculations of massless Feynman diagrams: integration by parts [44, 45] (and similar approach in coordinate space [37, 51]), the method of uniqueness [37, 38, 39, 56] (see also Vassiliev’s book [51]), Kazakov’s functional equations [57] (see also Kazakov’s lectures [139]) and the Gegenbauer polynomial technique [46, 61]. We would like to note that there is another powerful technique [58] (see also an extension in [59]) which is based on difference equations connecting Feynman diagrams in D and $(D + 2)$ dimensions; this technique is very popular now (see the recent Ref. [174] for short review of the application of the approach) but its consideration is beyond the scope of our present paper. Based on the method of uniqueness, we have shown various possibilities to transform the basic two-loop diagram to ones with different powers of propagators. The full set of such transformations can be found in Refs. [37, 150, 47, 48] and in the book [51]. Our review closely followed the nice lectures of Kazakov which were published in [139]. But contrary to the lectures [139] as well as the original papers [37, 38, 39, 56], we presented all our results in momentum space, which is more popular at the present time.

As concrete examples of analytic calculations, we presented the evaluations of two-, three-, four- and even five-loop Feynman integrals of rather complicated topologies. The five-loop diagrams considered in detail in Sec. 5.2, are part of the set of the four most complicated Feynman integrals which were calculated firstly numerically [55] and later analytically [39, 56, 57] in order to evaluate the 5-loop correction to the β -function of the Φ^4 -model in $D = 4$ dimensions. That the presented purely analytical techniques allow to compute such complicated diagrams is quite suggestive of their power and efficiency.

Moreover, the considered methods may be applied to a wide range of models across various fields. In particular, they can be of crucial importance for odd-dimensional models and/or to evaluate Feynman integrals with propagators having nonzero indices, *i.e.*, nontrivial powers of their momenta, all the more that, precisely in these cases, the most popular modern computer programs undergo strong restrictions. Let’s add that diagrams with non-trivial indices generally appear upon considering high orders of perturbation theory where such indices come from calculations of subgraphs. However, in some effective field theories, such propagators appear already at the leading order of some expansion parameter. One example is reduced QED (see, for example, [125]-[129]), which can be considered as describing the ultrarelativistic limit of planar Dirac liquids. The second one [133]-[135] is the $1/N$ -expansion of three-dimensional QED with N -species of fermions. Both of these models contain photon propagators of rather specific forms. Their accurate study with the help of the methods reviewed in this manuscript could reveal some of their duality [136] and, as a consequence, some relation between the results for these two different models (see [175] for a review). Among other recent achievements of these techniques, let’s briefly mention: their application to models with broken-Lorentz invariance [130, 131], the calculation of the critical index η of the Φ^3 -model at four-loops [176], the computation of the anomalous dimension of double trace operators in hexagonal fishnet models [177], and more to come in the next years.

In closing, we hope that our review will be useful to both experts in calculations as well as to novices interested in the methods of analytical calculations of Feynman diagrams.

Acknowledgements

We are very grateful to David Broadhurst, John Gracey, Valery Gusynin and Mikhail Kompaniets for their comments. The work of A.V.K. was supported in part by the Russian Foundation for Basic Research (Grant No.16-02-00790-a).

7 Appendix A. Gegenbauer polynomial technique

This Appendix is devoted to a short presentation of the Gegenbauer polynomial technique. The latter should be considered as the effective (but rather cumbersome) method for calculating dimensionally regularized Feynman diagrams. In its modern form, it has been introduced by Chetyrkin, Kataev and Tkachov [46]. Later, subtle and important improvements were brought up by Kotikov [61] and we shall follow this reference in our brief review of the technique.

Hereafter we will use the variables x, y, \dots , which are usually used in coordinate space. But we can also think about the variables x, y, \dots as being some momenta. Thus, all formulae in this Appendix are also applicable in the momentum space. Such type of ‘‘duality’’ has already been considered in Sec. 4.5.

7.1 Presentation of the method

The basic motivation for this technique lays in the fact that, in multi-loop computations, the complicated part of the integration is often the one over the angular variables. This task is considerably simplified by expanding some of the propagators in the integrand in terms of the Gegenbauer polynomials (the so-called multipole expansion):

$$\frac{1}{(x_1 - x_2)^{2\lambda}} = \sum_{n=0}^{\infty} C_n^\lambda(\hat{x}_1 \cdot \hat{x}_2) \left[\frac{(x_1^2)^{n/2}}{(x_2^2)^{n/2+\lambda}} \Theta(x_2^2 - x_1^2) + (x_1^2 \leftrightarrow x_2^2) \right], \quad (\text{A1})$$

where C_n^λ is the Gegenbauer polynomial of degree n and $\hat{x} = x/\sqrt{x^2}$, and then using the orthogonality relation of Gegenbauer polynomials on the unit D -dimensional sphere:

$$\frac{1}{\Omega_D} \int d_D \hat{x} C_n^\lambda(\hat{z} \cdot \hat{x}) C_m^\lambda(\hat{x} \cdot \hat{z}) = \delta_{n,m} \frac{\lambda \Gamma(n+2\lambda)}{\Gamma(2\lambda) (n+\lambda) n!}, \quad \lambda = \frac{D}{2} - 1, \quad (\text{A2})$$

where $d_D \hat{x}$ is the surface element of the unit D -dimensional sphere and $\Omega_D = 2\pi^{D/2}/\Gamma(D/2)$. The Gegenbauer polynomials can be defined from their generating function:

$$\frac{1}{(1 - 2xw + w^2)^\beta} = \sum_{k=0}^{\infty} C_k^\beta(x) w^k \quad C_n^\beta(1) = \frac{\Gamma(n+2\beta)}{\Gamma(2\beta) n!}, \quad (\text{A3})$$

with some additional particular values given by:

$$C_0^\lambda(x) = 1, \quad C_1^\lambda(x) = 2\lambda x, \quad C_2^\lambda(x) = 2\lambda(\lambda+1)x^2 - \lambda. \quad (\text{A4})$$

For our purpose, it is convenient to express the Gegenbauer polynomials in terms of traceless symmetric tensors [61]:

$$C_n^\lambda(\hat{x} \cdot \hat{z}) (x^2 z^2)^{n/2} = S_n(\lambda) x^{\mu_1 \mu_2 \dots \mu_n} z^{\mu_1 \mu_2 \dots \mu_n}, \quad S_n(\lambda) = \frac{2^n \Gamma(n+\lambda)}{n! \Gamma(\lambda)}. \quad (\text{A5})$$

From Eq. (A5) for $x = z$ and the last equation in (A3), we deduce the following equation for products of traceless tensors:

$$S_n(\lambda) z^{\mu_1 \mu_2 \dots \mu_n} z^{\mu_1 \mu_2 \dots \mu_n} = \frac{\Gamma(n + 2\lambda)}{\Gamma(2\lambda) n!} z^{2n}. \quad (\text{A6})$$

With the help of Eq. (A5), Eq. (A1) can be rewritten as:

$$\frac{1}{(x_1 - x_2)^{2\lambda}} = \sum_{n=0}^{\infty} S_n(\lambda) x_1^{\mu_1 \dots \mu_n} x_2^{\mu_1 \dots \mu_n} \left[\frac{1}{(x_2^2)^{n+\lambda}} \Theta(x_2^2 - x_1^2) + (x_1^2 \longleftrightarrow x_2^2) \right]. \quad (\text{A7})$$

Notice that, for a propagator with arbitrary index, Eq. (A1) can be generalized as:

$$\frac{1}{(x_1 - x_2)^{2\beta}} = \sum_{n=0}^{\infty} C_n^\beta(\hat{x}_1 \cdot \hat{x}_2) \left[\frac{(x_1^2)^{n/2}}{(x_2^2)^{n/2+\beta}} \Theta(x_2^2 - x_1^2) + (x_1^2 \longleftrightarrow x_2^2) \right], \quad (\text{A8})$$

where $C_n^\beta(x)$ can then be related to $C_{n-2k}^\lambda(x)$ ($0 \leq k \leq [n/2]$) with the help of:

$$C_n^\delta(x) = \sum_{k=0}^{[n/2]} C_{n-2k}^\lambda(x) \frac{(n - 2k + \lambda)\Gamma(\lambda)}{k!\Gamma(\delta)} \frac{\Gamma(n + \delta - k)\Gamma(k + \delta - \lambda)}{\Gamma(n - k + \lambda + 1)\Gamma(\delta - \lambda)}. \quad (\text{A9})$$

Moreover, the series appearing upon expanding the propagators and after performing all integrations may sometimes be resummed in the form of a generalized hypergeometric function ${}_3F_2$ of unit argument. There is a very useful transformation property relating such hypergeometric functions. Even though not directly connected with Gegenbauer polynomials, we mention it here:

$$\begin{aligned} {}_3F_2(a, b, c; e, f; 1) &= \frac{\Gamma(1-a)\Gamma(e)\Gamma(f)\Gamma(c-b)}{\Gamma(e-b)\Gamma(f-b)\Gamma(1+b-a)\Gamma(c)} \\ &\times {}_3F_2(b, b-e+1, b-f+1; 1+b-c, 1+b-a; 1) + (b \longleftrightarrow c). \end{aligned} \quad (\text{A10})$$

Of peculiar importance is the case where $e = b + 1$ in which case the ${}_3F_2$ function can be expressed in terms of another ${}_3F_2$ plus a term involving only products of Gamma functions:

$$\begin{aligned} \sum_{p=0}^{\infty} \frac{\Gamma(p+a)\Gamma(p+c)}{p!\Gamma(p+f)} \frac{1}{p+b} &= \frac{\Gamma(a)\Gamma(1-a)\Gamma(b)\Gamma(c-b)}{\Gamma(f-b)\Gamma(1+b-a)} \\ - \frac{\Gamma(1-a)\Gamma(a)}{\Gamma(f-c)\Gamma(1+c-f)} \sum_{p=0}^{\infty} \frac{\Gamma(p+c-f+1)\Gamma(p+c)}{p!\Gamma(p+1+c-a)} \frac{1}{p+c-b}. \end{aligned} \quad (\text{A11})$$

7.2 One-loop integral

Let's consider some simple examples in order to illustrate the method. We start with the one-loop massless p-type diagram with two arbitrary indices in x -space (transformation rules between x -space and p -space are provided in Sec. 4.5):

$$J(D, z, \alpha, \beta) = \int \frac{d^D x}{x^{2\alpha}(x-z)^{2\beta}}, \quad d^D x = \frac{1}{2} x^{2\lambda} dx^2 d_D \hat{x}. \quad (\text{A12})$$

Combining Eqs. (A8) and (A9), the integral can be separated into a radial and an angular part as follows:

$$J(D, z, \alpha, \beta) = \frac{1}{2} \sum_{n=0}^{\infty} \sum_{k=0}^{[n/2]} \int_0^{\infty} dx^2 (x^2)^{\lambda-\alpha} \left[\frac{(x^2)^{n/2}}{(z^2)^{n/2+\beta}} \Theta(z^2 - x^2) + (x^2 \leftrightarrow y^2) \right] \\ \times \underbrace{\int_{\Omega_D} d\hat{x} C_{n-2k}^{\lambda}(\hat{x} \cdot \hat{z})}_{\delta_{n,2k}} \frac{(n-2k+\lambda)\Gamma(\lambda)}{k!\Gamma(\beta)} \frac{\Gamma(n+\beta-k)\Gamma(k+\beta-\lambda)}{\Gamma(n+\lambda+1-k)\Gamma(\beta-\lambda)}, \quad (\text{A13})$$

where the orthogonality relation, Eq. (A2) has been used to compute the angular part. It then follows that n must be an even integer: $n = 2p$ and $k = [n/2] = p$. The remaining radial integrals are easily performed. The resulting expression can be conveniently written as a sum of two one-fold series:

$$J(D, z, \alpha, \beta) = \frac{\pi^{D/2}}{(z^2)^{\alpha+\beta-\lambda-1}} \frac{1}{\Gamma(\beta)\Gamma(\beta-\lambda)} \\ \times \sum_{p=0}^{\infty} \frac{\Gamma(p+\beta)\Gamma(p+\beta-\lambda)}{p!\Gamma(p+\lambda+1)} \left[\frac{1}{p+\alpha+\beta-1-\lambda} + \frac{1}{p-\alpha+\lambda+1} \right]. \quad (\text{A14})$$

This expression can be further simplified by transforming the first sum with the help of Eq. (A11) with $a = \beta - \lambda$, $b = \alpha + \beta - 1 - \lambda$, $c = \beta$ and $f = \lambda + 1$. Indeed, this yields:

$$\sum_{p=0}^{\infty} \frac{\Gamma(p+\beta)\Gamma(p+\beta-\lambda)}{p!\Gamma(p+\lambda+1)} \frac{1}{p+\alpha+\beta-1-\lambda} = \quad (\text{A15}) \\ \frac{\Gamma(\beta-\lambda)\Gamma(1+\lambda-\alpha)\Gamma(1+\lambda-\beta)\Gamma(\alpha+\beta-1-\lambda)}{\Gamma(\alpha)\Gamma(2+2\lambda-\alpha-\beta)} - \sum_{p=0}^{\infty} \frac{\Gamma(p+\beta)\Gamma(p+\beta-\lambda)}{p!\Gamma(p+\lambda+1)} \frac{1}{p-\alpha+1+\lambda},$$

and the sum on the lhs is simply the opposite of the second sum in $J(D, z, \alpha, \beta)$. Hence, the sum of the two one-fold series reduces to a product of Γ -functions and we recover the well-known result:

$$J(D, z, \alpha, \beta) = \frac{\pi^{D/2}}{(z^2)^{\alpha+\beta-\lambda-1}} G(D, \alpha, \beta), \quad G(D, \alpha, \beta) = \frac{a(\alpha)a(\beta)}{a(\alpha+\beta-1-\lambda)}, \quad (\text{A16})$$

where $a(\alpha) = \Gamma(D/2 - \alpha)/\Gamma(\alpha)$ and which was given in Eq. (2.17) in p -space.

7.3 One-loop integral with traceless products

We may next generalize this result to the case where a traceless product appears in the numerator:

$$J^{\mu_1 \cdots \mu_n}(D, z, \alpha, \beta) = \int d^D x \frac{x^{\mu_1 \cdots \mu_n}}{x^{2\alpha}(x-z)^{2\beta}}, \quad d^D x = \frac{1}{2} x^{2\lambda} dx^2 d_D \hat{x}. \quad (\text{A17})$$

Dimensional analysis suggests that this integral should have the form:

$$J^{\mu_1 \cdots \mu_n}(D, z, \alpha, \beta) = \pi^{D/2} \frac{z^{\mu_1 \cdots \mu_n}}{(z^2)^{\alpha+\beta-\lambda-1}} G^{(n,0)}(\alpha, \beta), \quad (\text{A18})$$

where the coefficient function, $G^{(n,0)}(\alpha, \beta)$, is yet to be determined. In order to do so, we consider the scalar function:

$$z^{\mu_1 \cdots \mu_n} J^{\mu_1 \cdots \mu_n}(D, z, \alpha, \beta) = \pi^{D/2} \frac{z^{2n}}{(z^2)^{\alpha+\beta-\lambda-1}} \frac{\Gamma(\lambda)\Gamma(n+2\lambda)}{2^n \Gamma(2\lambda)\Gamma(n+\lambda)} G^{(n,0)}(\alpha, \beta), \quad (\text{A19})$$

where Eqs. (A18) and (A6) have been used. The corresponding integral can be evaluated by using the relation between traceless products and Gegenbauer polynomials, Eq. (A5):

$$z^{\mu_1 \cdots \mu_n} J^{\mu_1 \cdots \mu_n}(D, z, \alpha, \beta) = \int d^D x \frac{z^{\mu_1 \cdots \mu_n} x^{\mu_1 \cdots \mu_n}}{x^{2\alpha}(x-z)^{2\beta}} = \frac{n!\Gamma(\lambda)}{2^n \Gamma(n+\lambda)} \int d^D x \frac{C_n(\hat{z} \cdot \hat{x}) (x^2 z^2)^{n/2}}{x^{2\alpha}(x-z)^{2\beta}}, \quad (\text{A20})$$

and then expanding the propagator in Gegenbauer polynomials as before. This yields:

$$z^{\mu_1 \cdots \mu_n} J^{\mu_1 \cdots \mu_n}(D, z, \alpha, \beta) = \frac{n!\Gamma(\lambda)}{2^n \Gamma(n+\lambda)} \frac{1}{2} \sum_{p=0}^{\infty} \sum_{k=0}^{[p/2]} \int dx^2 (x^2)^{\lambda-\alpha} \left[\frac{(x^2)^{\frac{p+n}{2}}}{(y^2)^{\frac{p-n}{2}+\beta}} \Theta(z^2 - x^2) + (x^2 \leftrightarrow y^2) \right] \\ \times \int d_D \hat{x} C_n(\hat{z} \cdot \hat{x}) C_{p-2k}^\lambda(\hat{x} \cdot \hat{z}) \frac{(p-2k+\lambda)\Gamma(\lambda)}{k!\Gamma(\beta)} \frac{\Gamma(p+\beta-k)\Gamma(k+\beta-\lambda)}{\Gamma(p+\lambda+1-k)\Gamma(\beta-\lambda)}. \quad (\text{A21})$$

The angular integral is non-zero for $2k = p - n$ which implies that p must have the same parity as n and $p \geq n$. Separate analysis of the even and odd n cases yield, after some simple manipulations:

$$z^{\mu_1 \cdots \mu_n} J^{\mu_1 \cdots \mu_n}(D, z, \alpha, \beta) = \pi^{D/2} \frac{z^{2n}}{(z^2)^{\alpha+\beta-\lambda-1}} \frac{\Gamma(\lambda)\Gamma(n+2\lambda)}{2^n \Gamma(2\lambda)\Gamma(n+\lambda)} \times \\ \times \sum_{m=0}^{\infty} B(m, n|\beta, \lambda) \left(\frac{1}{m+\alpha+\beta-1-\lambda} + \frac{1}{m+n-\alpha+\lambda+1} \right), \quad (\text{A22})$$

where:

$$B(m, n|\beta, \lambda) = \frac{\Gamma(m+n+\beta)}{m!\Gamma(m+n+\lambda+1)\Gamma(\beta)} \frac{\Gamma(m+\beta-\lambda)}{\Gamma(\beta-\lambda)}. \quad (\text{A23})$$

Comparing Eqs. (A22) and (A18), we see that the coefficient function equals the sum of two one-fold series:

$$G^{(n,0)}(D, \alpha, \beta) = \sum_{m=0}^{\infty} B(m, n|\beta, \lambda) \left(\frac{1}{m+\alpha+\beta-1-\lambda} + \frac{1}{m+n-\alpha+\lambda+1} \right). \quad (\text{A24})$$

Such a series representation reduces to a product of Γ -functions upon using the transformation properties of hypergeometric functions:

$$G^{(n,0)}(D, \alpha, \beta) = \frac{a_n(\alpha)a_0(\beta)}{a_n(\alpha+\beta-\lambda-1)}, \quad a_n(\alpha) = \frac{\Gamma(n+D/2-\alpha)}{\Gamma(\alpha)}, \quad (\text{A25})$$

in accordance with Eq. (2.21).

7.4 One-loop integral with Heaviside functions

The above results yield *integration rules for Feynman integrals involving traceless products and Heaviside functions* which were given in Ref. [61]. From Eq. (A22) we indeed recover the basic results of this reference:

$$\int d^D x \frac{x^{\mu_1 \dots \mu_n}}{x^{2\alpha}(x-y)^{2\beta}} \Theta(x^2 - y^2) = \pi^{D/2} \frac{y^{\mu_1 \dots \mu_n}}{(y^2)^{\alpha+\beta-\lambda-1}} \sum_{m=0}^{\infty} \frac{B(m, n|\beta, \lambda)}{m + \alpha + \beta - 1 - \lambda}$$

$$\stackrel{(\beta=\lambda)}{=} \pi^{D/2} \frac{y^{\mu_1 \dots \mu_n}}{(y^2)^{\alpha-1}} \frac{1}{\Gamma(\lambda)} \frac{1}{(\alpha-1)(n+\lambda)}, \quad (\text{A26})$$

and

$$\int d^D x \frac{x^{\mu_1 \dots \mu_n}}{x^{2\alpha}(x-y)^{2\beta}} \Theta(y^2 - x^2) = \pi^{D/2} \frac{y^{\mu_1 \dots \mu_n}}{(y^2)^{\alpha+\beta-\lambda-1}} \sum_{m=0}^{\infty} \frac{B(m, n|\beta, \lambda)}{m + n - \alpha + 1 + \lambda}$$

$$\stackrel{(\beta=\lambda)}{=} \pi^{D/2} \frac{y^{\mu_1 \dots \mu_n}}{(y^2)^{\alpha-1}} \frac{1}{\Gamma(\lambda)} \frac{1}{(n+\lambda+1-\alpha)(n+\lambda)}, \quad (\text{A27})$$

where the peculiar case $\beta = \lambda$ has been explicitly displayed. The following more complicated cases are also useful (see [61]):

$$\int d^D x \frac{x^{\mu_1 \dots \mu_n}}{x^{2\alpha}(x-y)^{2\beta}} \Theta(x^2 - z^2) = \pi^{D/2} y^{\mu_1 \dots \mu_n} \left[\frac{\Theta(y^2 - z^2)}{(y^2)^{\alpha+\beta-\lambda-1}} G^{n,0}(\alpha, \beta) \right.$$

$$\left. + \sum_{m=0}^{\infty} \frac{B(m, n|\beta, \lambda)}{(z^2)^{\alpha+\beta-\lambda-1}} \left(\left(\frac{y^2}{z^2} \right)^m \frac{\Theta(z^2 - y^2)}{m + \alpha + \beta - 1 - \lambda} - \left(\frac{z^2}{y^2} \right)^{m+n+\beta} \frac{\Theta(y^2 - z^2)}{m - \alpha + n + 1 + \lambda} \right) \right]$$

$$\stackrel{(\beta=\lambda)}{=} \pi^{D/2} \frac{1}{\Gamma(\lambda)} y^{\mu_1 \dots \mu_n} \left[\frac{\Theta(y^2 - z^2)}{(y^2)^{\alpha-1}} \frac{1}{(\alpha-1)(n+\lambda+1-\alpha)} \right.$$

$$\left. + \frac{1}{(z^2)^{\alpha-1}} \frac{1}{n+\lambda} \left(\frac{\Theta(z^2 - y^2)}{\alpha-1} - \left(\frac{z^2}{y^2} \right)^{n+\lambda} \frac{\Theta(y^2 - z^2)}{n+1+\lambda-\alpha} \right) \right], \quad (\text{A28})$$

and

$$\int d^D x \frac{x^{\mu_1 \dots \mu_n}}{x^{2\alpha}(x-y)^{2\beta}} \Theta(z^2 - x^2) = \pi^{D/2} y^{\mu_1 \dots \mu_n} \left[\frac{\Theta(z^2 - y^2)}{(y^2)^{\alpha+\beta-\lambda-1}} G^{n,0}(\alpha, \beta) \right.$$

$$\left. - \sum_{m=0}^{\infty} \frac{B(m, n|\beta, \lambda)}{(z^2)^{\alpha+\beta-\lambda-1}} \left(\left(\frac{y^2}{z^2} \right)^m \frac{\Theta(z^2 - y^2)}{m + \alpha + \beta - 1 - \lambda} - \left(\frac{z^2}{y^2} \right)^{m+n+\beta} \frac{\Theta(y^2 - z^2)}{m - \alpha + n + 1 + \lambda} \right) \right]$$

$$\stackrel{(\beta=\lambda)}{=} \pi^{D/2} \frac{1}{\Gamma(\lambda)} y^{\mu_1 \dots \mu_n} \left[\frac{\Theta(z^2 - y^2)}{(y^2)^{\alpha-1}} \frac{1}{(\alpha-1)(n+\lambda+1-\alpha)} \right.$$

$$\left. - \frac{1}{(z^2)^{\alpha-1}} \frac{1}{n+\lambda} \left(\frac{\Theta(z^2 - y^2)}{\alpha-1} - \left(\frac{z^2}{y^2} \right)^{n+\lambda} \frac{\Theta(y^2 - z^2)}{n+1+\lambda-\alpha} \right) \right] / \quad (\text{A29})$$

With these rules in hand, the Gegenbauer polynomials technique allows to compute the massless p-type two-loop master integral with up three arbitrary indices as a linear combination of up to four hypergeometric functions ${}_3F_2$ of argument 1, a result which can be found in Ref. [61]. In particular, the method provides an alternative representation for the integral $I(1+a)$ found in the previous section with functional equations (see Eq. (4.138)).

7.5 Application to $I(1+a)$

Here we reconsider the simple but very important example of: $I(1+a) = J(D, p, 1, 1, 1, 1, 1+a)$ (see Eq. (3.28)). Applying the rules of the previous paragraph, its coefficient function $C_D[I(1+a)]$ can be expressed as:

$$C_D[I(a+1)] = 2 \frac{\Gamma^2(1-\varepsilon)\Gamma(-\varepsilon-a)\Gamma(a+2\varepsilon)}{\Gamma(2-2\varepsilon)\Gamma(1-3\varepsilon-a)} \left[\frac{\pi\Gamma(1-a-3\varepsilon)\Gamma(1-a-2\varepsilon)\Gamma(a+2\varepsilon)}{\Gamma(1-\varepsilon)\Gamma(1/2-a-2\varepsilon)\Gamma(1/2+2\varepsilon+a)} - \sum_{n=1}^{\infty} \frac{\Gamma(n+1-2\varepsilon)}{\Gamma(n+1+a)} \frac{1}{n+a+1+\varepsilon} \right], \quad (\text{A30})$$

which coincides with Eq. (3.58) after changing of variables.

So, using the method of Gegenbauer polynomials, the results for $I(1+a)$ can be expressed as a combination of Γ -functions together with one hypergeometric function with the arguments “1”. Such result can be successfully used for an efficient ε -expansion of the diagram. Moreover, the combination of the two results (4.138) and (A30) provides the advertised relation (3.59) between two hypergeometric functions of argument “-1” and one hypergeometric function of argument “1”. Such a relation is absent in standard textbooks and was recently proven exactly in [137].

8 References

- [1] S.-I. Tomonaga, “On a relativistically invariant formulation of the quantum theory of wave fields,” *Prog. Theor. Phys.* **1** (1946) 27; Z. Koba, T. Tati, and S.-I. Tomonaga, “On a Relativistically Invariant Formulation of the Quantum Theory of Wave Fields. II: Case of Interacting Electromagnetic and Electron Fields” *Prog. Theor. Phys.* (1947) 2; S. I. Tomonaga and J. R. Oppenheimer, “On Infinite Field Reactions in Quantum Field Theory,” *Phys. Rev.* **74** (1948) 224.
- [2] J. S. Schwinger, “Quantum electrodynamics. I: A covariant formulation,” *Phys. Rev.* **74** (1948) 1439; “Quantum electrodynamics. II: Vacuum polarization and selfenergy,” *Phys. Rev.* **75** (1948) 651; “Quantum electrodynamics. III: The electromagnetic properties of the electron: Radiative corrections to scattering,” *Phys. Rev.* **76** (1949) 790.
- [3] R. P. Feynman, “Relativistic cutoff for quantum electrodynamics,” *Phys. Rev.* **74** (1948) 1430; “Space-time approach to quantum electrodynamics,” *Phys. Rev.* **76** (1949) 769; “Mathematical formulation of the quantum theory of electromagnetic interaction,” *Phys. Rev.* **80** (1950) 440.
- [4] F. J. Dyson, “The Radiation Theories of Tomonaga, Schwinger, and Feynman,” *Phys. Rev.* **75** (1949) 486.
- [5] M. Gell-Mann and F. E. Low, “Quantum electrodynamics at small distances,” *Phys. Rev.* **95** (1954) 1300.
- [6] E. C. G. Stueckelberg and A. Petermann, “La normalisation des constantes dans la théorie des quanta. Normalization of constants in the quanta theory,” *Helv. Phys. Acta* **26** (1953) 499.

-
- [7] N. N. Bogolyubov and D. V. Shirkov, “Charge renormalization group in quantum field theory,” *Nuovo Cim.* **3** (1956) 845.
- [8] N. N. Bogoliubov and O. S. Parasiuk, “On the Multiplication of the causal function in the quantum theory of fields,” *Acta Math.* **97** (1957) 227.
- [9] K. Hepp, “Proof of the Bogolyubov-Parasiuk theorem on renormalization,” *Commun. Math. Phys.* **2** (1966) 301.
- [10] W. Zimmermann, ‘Convergence of Bogoliubov’s method of renormalization in momentum space,’ *Communications in Mathematical Physics* **15** (1969) 208; W. Zimmermann, in “Lectures on elementary particle and quantum field theory”, 1970. Brandies University Summer Institute in Theoretical Physics (MIT Press Cambridge, Massachusetts).
- [11] N. N. Bogolyubov and D. V. Shirkov, “Introduction To The Theory Of Quantized Fields,” *Intersci. Monogr. Phys. Astron.* **3** (1959) 1.
- [12] C. N. Yang and R. L. Mills, “Conservation of Isotopic Spin and Isotopic Gauge Invariance,” *Phys. Rev.* **96** (1954) 191.
- [13] S. Glashow, “Partial Symmetries of Weak Interactions,” *Nucl. Phys.* **22** (1961) 579; A. Salam and J. C. Ward, “Electromagnetic and Weak Interactions,” *Phys. Lett.* **13** (1964) 168; S. Weinberg, “A Model of Leptons,” *Phys. Rev. Lett.* **19** (1967) 1264.
- [14] G. ’t Hooft, “Renormalizable Lagrangians for Massive Yang-Mills Fields,” *Nucl. Phys. B* **35** (1971) 167.
- [15] G. ’t Hooft and M. J. G. Veltman, “Regularization and Renormalization of Gauge Fields,” *Nucl. Phys. B* **44** (1972) 189.
- [16] C. G. Bollini and J. J. Giambiagi, “Dimensional Renormalization: The Number of Dimensions as a Regularizing Parameter,” *Nuovo Cim. B* **12** (1972) 20.
- [17] G. M. Cicuta and E. Montaldi, “Analytic renormalization via continuous space dimension,” *Lett. Nuovo Cim.* **4** (1972) 329.
- [18] J. F. Ashmore, “A Method of Gauge Invariant Regularization,” *Lett. Nuovo Cim.* **4** (1972) 289.
- [19] G. ’t Hooft, “Dimensional regularization and the renormalization group,” *Nucl. Phys. B* **61** (1973) 455.
- [20] H. D. Politzer, “Reliable Perturbative Results for Strong Interactions?,” *Phys. Rev. Lett.* **30** (1973) 1346.
- [21] D. J. Gross and F. Wilczek, “Ultraviolet Behavior of Nonabelian Gauge Theories,” *Phys. Rev. Lett.* **30** (1973) 1343.
- [22] G. ’t Hooft, “A Planar Diagram Theory for Strong Interactions,” *Nucl. Phys. B* **72** (1974) 461.

-
- [23] E. Brézin and S. R. Wadia, “The Large N expansion in quantum field theory and statistical physics: From spin systems to two-dimensional gravity,” Singapore, Singapore: World Scientific (1993).
- [24] J. M. Maldacena, “The Large N limit of superconformal field theories and supergravity,” *Int. J. Theor. Phys.* **38** (1999) 1113 [*Adv. Theor. Math. Phys.* **2** (1998) 231] [[arXiv:hep-th/9711200](#)]; S. S. Gubser, I. R. Klebanov and A. M. Polyakov, “Gauge theory correlators from noncritical string theory,” *Phys. Lett. B* **428** (1998) 105 [[arXiv:hep-th/9802109](#)]; E. Witten, “Anti-de Sitter space and holography,” *Adv. Theor. Math. Phys.* **2** (1998) 253 [[arXiv:hep-th/9802150](#)].
- [25] K. G. Wilson, “Renormalization group and critical phenomena. 1. Renormalization group and the Kadanoff scaling picture,” *Phys. Rev. B* **4** (1971) 3174.
- [26] K. G. Wilson, “Renormalization group and critical phenomena. 2. Phase space cell analysis of critical behavior,” *Phys. Rev. B* **4** (1971) 3184.
- [27] K. G. Wilson and M. E. Fisher, “Critical exponents in 3.99 dimensions,” *Phys. Rev. Lett.* **28** (1972) 240.
- [28] E. Brézin, J. C. Le Guillou and J. Zinn-Justin, “Wilson’s theory of critical phenomena and Callan-Symanzik equations in 4-epsilon dimensions,” *Phys. Rev. D* **8** (1973) 434; “Addendum to Wilson’s theory of critical phenomena and Callan-Symanzik equations in 4-epsilon dimensions,” *Phys. Rev. D* **9** (1974) 1121.
- [29] J. Zinn-Justin, “Quantum Field Theory and Critical Phenomena,” Clarendon Press, 2002.
- [30] H. E. Stanley, “Spherical model as the limit of infinite spin dimensionality,” *Phys. Rev.* **176** (1968) 718.
- [31] A. A. Vladimirov, “Method for Computing Renormalization Group Functions in Dimensional Renormalization Scheme,” *Theor. Math. Phys.* **43** (1980) 417 [*Teor. Mat. Fiz.* **43** (1980) 210].
- [32] K. G. Chetyrkin and F. V. Tkachov, “Infrared R Operation And Ultraviolet Counterterms In The Ms Scheme,” *Phys. Lett. B* **114** (1982) 340.
- [33] K. G. Chetyrkin and V. A. Smirnov, “R* Operation Corrected,” *Phys. Lett. B* **144** (1984) 419.
- [34] V. A. Smirnov and K. G. Chetyrkin, “R* Operation in the Minimal Subtraction Scheme,” *Theor. Math. Phys.* **63** (1985) 462 [*Teor. Mat. Fiz.* **63** (1985) 208].
- [35] K. G. Chetyrkin, “Combinatorics of \mathbf{R} -, \mathbf{R}^{-1} -, and \mathbf{R}^* -operations and asymptotic expansions of feynman integrals in the limit of large momenta and masses,” [arXiv:1701.08627 \[hep-th\]](#).
- [36] M. D’Eramo, G. Parisi and L. Peliti, “Theoretical Predictions For Critical Exponents At The Lambda Point Of Bose Liquids,” *Lett. Nuovo Cim.* **2** (1971) 878.

- [37] A. N. Vasiliev, Y. M. Pismak and J. R. Honkonen, “ $1/N$ Expansion: Calculation of the Exponents η and ν in the Order $1/N^2$ for Arbitrary Number of Dimensions,” *Theor. Math. Phys.* **47** (1981) 465 [*Teor. Mat. Fiz.* **47** (1981) 291].
- [38] N. I. Usyukina, “Calculation Of Many Loop Diagrams Of Perturbation Theory,” *Theor. Math. Phys.* **54** (1983) 78 [*Teor. Mat. Fiz.* **54** (1983) 124].
- [39] D. I. Kazakov, “Calculation Of Feynman Integrals By The Method Of ‘uniqueness’,” *Theor. Math. Phys.* **58** (1984) 223 [*Teor. Mat. Fiz.* **58** (1984) 343] [*inspires*].
- [40] D. I. Kazakov and A. V. Kotikov, “The Method of Uniqueness: Multiloop Calculations in QCD,” *Theor. Math. Phys.* **73** (1988) 1264 [*Teor. Mat. Fiz.* **73** (1987) 348].
- [41] D. I. Kazakov and A. V. Kotikov, “Total α_s Correction to Deep Inelastic Scattering Cross-section Ratio, $R = \sigma^{-1} / \sigma^{-t}$ in QCD. Calculation of Longitudinal Structure Function,” *Nucl. Phys. B* **307** (1988) 721; Erratum: [*Nucl. Phys. B* **345** (1990) 299].
- [42] A. V. Kotikov, “The Calculation of Moments of Structure Function of Deep Inelastic Scattering in QCD,” *Theor. Math. Phys.* **78** (1989) 134 [*Teor. Mat. Fiz.* **78** (1989) 187].
- [43] A. N. Vasiliev, Y. M. Pismak and J. R. Honkonen, “ $1/n$ Expansion: Calculation Of The Exponent η In The Order $1/n^{**3}$ By The Conformal Bootstrap Method,” *Theor. Math. Phys.* **50** (1982) 127 [*Teor. Mat. Fiz.* **50** (1982) 195].
- [44] F. V. Tkachov, “A Theorem on Analytical Calculability of Four Loop Renormalization Group Functions,” *Phys. Lett. B* **100** (1981) 65.
- [45] K. G. Chetyrkin and F. V. Tkachov, “Integration by Parts: The Algorithm to Calculate beta Functions in 4 Loops,” *Nucl. Phys. B* **192** (1981) 159.
- [46] K. G. Chetyrkin, A. L. Kataev and F. V. Tkachov, “New Approach to Evaluation of Multiloop Feynman Integrals: The Gegenbauer Polynomial x Space Technique,” *Nucl. Phys. B* **174** (1980) 345.
- [47] D. J. Broadhurst, “Exploiting the 1.440 Fold Symmetry of the Master Two Loop Diagram,” *Z. Phys. C* **32** (1986) 249.
- [48] D. T. Barfoot and D. J. Broadhurst, “ $Z(2) \times S(6)$ Symmetry of the Two Loop Diagram,” *Z. Phys. C* **41** (1988) 81.
- [49] J. C. Collins, “Renormalization : An Introduction to Renormalization, The Renormalization Group, and the Operator Product Expansion,” Cambridge Monographs on Mathematical Physics, 1986.
- [50] H. Kleinert and V. Schulte-Frohlinde, “Critical Properties of Φ^4 -theories,” World Scientific, 2001.
- [51] A.N.Vasil’ev, “The Field Theoretic Renormalization Group in Critical Behavior theory and Stochastic Dynamics,” Chapman & Hall/CRC, 2004.

-
- [52] A. G. Grozin, “Lectures on QED and QCD: Practical Calculation and Renormalization of One- and Multi-loop Feynman Diagrams,” World Scientific, 2007 [[arXiv:hep-ph/0508242](#)].
- [53] V. A. Smirnov, “Analytic Tools for Feynman Integrals,” Springer Tracts in Modern Physics, Springer Berlin Heidelberg, 2013.
- [54] O. V. Tarasov, A. A. Vladimirov and A. Y. Zharkov, “The Gell-Mann-Low Function of QCD in the Three Loop Approximation,” *Phys. Lett. B* **93** (1980) 429.
- [55] S. G. Gorishnii, S. A. Larin, F. V. Tkachov and K. G. Chetyrkin, “Five Loop Renormalization Group Calculations in the $g\phi^4$ in Four-dimensions Theory,” *Phys. Lett.* **132B** (1983) 351.
- [56] D. I. Kazakov, “The Method Of Uniqueness, A New Powerful Technique For Multiloop Calculations,” *Phys. Lett. B* **133** (1983) 406.
- [57] D. I. Kazakov, “Multiloop Calculations: Method of Uniqueness and Functional Equations,” *Theor. Math. Phys.* **62** (1985) 84 [*Teor. Mat. Fiz.* **62** (1984) 127] [[inspires](#)].
- [58] O. V. Tarasov, “Connection between Feynman integrals having different values of the space-time dimension,” *Phys. Rev. D* **54** (1996) 6479 [[hep-th/9606018](#)]; “Generalized recurrence relations for two loop propagator integrals with arbitrary masses,” *Nucl. Phys. B* **502** (1997) 455 [[hep-ph/9703319](#)].
- [59] R. N. Lee, “Space-time dimensionality D as complex variable: Calculating loop integrals using dimensional recurrence relation and analytical properties with respect to D,” *Nucl. Phys. B* **830** (2010) 474 [[arXiv:0911.0252](#) [[hep-ph](#)]].
- [60] J. A. Gracey, “On the evaluation of massless Feynman diagrams by the method of uniqueness,” *Phys. Lett. B* **277** (1992) 469.
- [61] A. V. Kotikov, “The Gegenbauer polynomial technique: The Evaluation of a class of Feynman diagrams,” *Phys. Lett. B* **375** (1996) 240 [[arXiv:hep-ph/9512270](#)].
- [62] D. J. Broadhurst, J. A. Gracey and D. Kreimer, “Beyond the triangle and uniqueness relations: Nonzeta counterterms at large N from positive knots,” *Z. Phys. C* **75** (1997) 559 [[arXiv:hep-th/9607174](#)].
- [63] E. E. Boos and A. I. Davydychev, “A Method of evaluating massive Feynman integrals,” *Theor. Math. Phys.* **89** (1991) 1052 [*Teor. Mat. Fiz.* **89** (1991) 56].
- [64] A. V. Kotikov, “Differential equations method: New technique for massive Feynman diagrams calculation,” *Phys. Lett. B* **254** (1991) 158.
- [65] A. V. Kotikov, “Differential equations method: The Calculation of vertex type Feynman diagrams,” *Phys. Lett. B* **259** (1991) 314.
- [66] A. V. Kotikov, “Differential equation method: The Calculation of N point Feynman diagrams,” *Phys. Lett. B* **267** (1991) 123; Erratum: [*Phys. Lett. B* **295** (1992) 409]; “New method of massive N point Feynman diagrams calculation,” *Mod. Phys. Lett. A* **6** (1991) 3133.

- [67] D. J. Broadhurst and A. V. Kotikov, “Compact analytical form for nonzeta terms in critical exponents at order $1/N^{**3}$,” *Phys. Lett. B* **441** (1998) 345 [[arXiv:hep-th/9612013](#)].
- [68] D. J. Broadhurst, “Where do the tedious products of zeta’s come from?,” *Nucl. Phys. Proc. Suppl.* **116** (2003) 432 [[arXiv:hep-ph/0211194](#)].
- [69] I. Bierenbaum and S. Weinzierl, “The Massless two loop two point function,” *Eur. Phys. J. C* **32** (2003) 67 [[arXiv:hep-ph/0308311](#)].
- [70] F. Brown, “The Massless higher-loop two-point function,” *Commun. Math. Phys.* **287** (2009) 925 [[arXiv:0804.1660](#) [[math.AG](#)]].
- [71] F. C. S. Brown, “On the periods of some Feynman integrals,” [arXiv:0910.0114](#) [[math.AG](#)].
- [72] H. Kleinert, J. Neu, V. Schulte-Frohlinde, K. G. Chetyrkin and S. A. Larin, “Five loop renormalization group functions of $O(n)$ symmetric ϕ^{**4} theory and epsilon expansions of critical exponents up to ϵ^{**5} ,” *Phys. Lett. B* **272** (1991) 39 Erratum: [*Phys. Lett. B* **319** (1993) 545].
- [73] J. A. Gracey, “Electron mass anomalous dimension at $O(1/(Nf(2)))$ in quantum electrodynamics,” *Phys. Lett. B* **317** (1993) 415 [[arXiv:hep-th/9312055](#)].
- [74] A. N. Vasiliev, S. E. Derkachov, N. A. Kivel and A. S. Stepanenko, “The $1/n$ expansion in the Gross-Neveu model: Conformal bootstrap calculation of the index eta in order $1/n^{**3}$,” *Theor. Math. Phys.* **94**, 127 (1993) [*Teor. Mat. Fiz.* **94**, 179 (1993)].
- [75] J. A. Gracey, “The Conformal bootstrap equations for the four Fermi interaction in arbitrary dimensions,” *Z. Phys. C* **59** (1993) 243.
- [76] N. A. Kivel, A. S. Stepanenko and A. N. Vasiliev, “On calculation of $(2+\epsilon)$ RG functions in the Gross-Neveu model from large N expansions of critical exponents,” *Nucl. Phys. B* **424** (1994) 619 [[arXiv:hep-th/9308073](#)].
- [77] J. A. Gracey, “Computation of critical exponent eta at $O(1/N(f)^{**2})$ in quantum electrodynamics in arbitrary dimensions,” *Nucl. Phys. B* **414** (1994) 614 [[arXiv:hep-th/9312055](#)].
- [78] D. Kreimer, “On the Hopf algebra structure of perturbative quantum field theories,” *Adv. Theor. Math. Phys.* **2** (1998) 303 [[arXiv:q-alg/9707029](#)].
- [79] A. Connes and D. Kreimer, “Hopf algebras, renormalization and noncommutative geometry,” *Commun. Math. Phys.* **199** (1998) 203 [[arXiv:hep-th/9808042](#)].
- [80] P. Cartier, “A mad day’s work: from Grothendieck to Connes and Kontsevich The evolution of concepts of space and symmetry,” *Bull. Amer. Math. Soc.* **38** (2001), 389.
- [81] M. Kontsevich, “Operads and Motives in Deformation Quantization,” *Lett. Math. Phys.* **48** (1999)35 [[arXiv:math/9904055](#) [[math.QA](#)]].
- [82] A. Connes and M. Marcolli, “Renormalization and motivic galois theory,” [math/0409306](#) [[math-nt](#)].

-
- [83] D. J. Broadhurst, “The Master Two Loop Diagram With Masses,” *Z. Phys. C* **47** (1990) 115.
- [84] M. J. G. Veltman, SCHOONSHIP (1963).
- [85] A. C. Hearn, REDUCE.
- [86] J. A. M. Vermaseren, “New features of FORM,” [math-ph/0010025](#); FORM.
- [87] C. W. Bauer, A. Frink and R. Kreckel, “Introduction to the GiNaC framework for symbolic computation within the C++ programming language,” *J. Symb. Comput.* **33** (2000) 1 [[cs/0004015 \[cs-sc\]](#)].
- [88] S. Wolfram, “Mathematica: a system for doing mathematics by computer,” (1991) Addison-Wesley Pub. Co., Advanced Book Program
- [89] S. Weinzierl, “Computer algebra in particle physics,” [hep-ph/0209234](#).
- [90] P. Nogueira, “Automatic Feynman graph generation,” *J. Comput. Phys.* **105** (1993) 279 [[inspirehep/315611](#)].
- [91] T. Seidensticker, “Automatic application of successive asymptotic expansions of Feynman diagrams,” [hep-ph/9905298](#).
- [92] S. Laporta, “High precision calculation of multiloop Feynman integrals by difference equations,” *Int. J. Mod. Phys. A* **15** (2000) 5087 [[hep-ph/0102033](#)].
- [93] P. A. Baikov, “Explicit solutions of the three loop vacuum integral recurrence relations,” *Phys. Lett. B* **385** (1996) 404 [[hep-ph/9603267](#)].
- [94] C. Studerus, “Reduze-Feynman Integral Reduction in C++,” *Comput. Phys. Commun.* **181** (2010) 1293 [[arXiv:0912.2546 \[physics.comp-ph\]](#)].
- [95] A. von Manteuffel and C. Studerus, “Reduze 2 - Distributed Feynman Integral Reduction,” [arXiv:1201.4330 \[hep-ph\]](#).
- [96] A. V. Smirnov, “Algorithm FIRE – Feynman Integral REduction,” *JHEP* **0810** (2008) 107 [[arXiv:0807.3243 \[hep-ph\]](#)].
- [97] P. Maierhoefer, J. Usovitsch and P. Uwer, “Kira - A Feynman Integral Reduction Program,” [arXiv:1705.05610 \[hep-ph\]](#).
- [98] R. N. Lee, “LiteRed 1.4: a powerful tool for reduction of multiloop integrals,” *J. Phys. Conf. Ser.* **523** (2014) 012059 [[arXiv:1310.1145 \[hep-ph\]](#)].
- [99] T. Binoth and G. Heinrich, “An automatized algorithm to compute infrared divergent multiloop integrals,” *Nucl. Phys. B* **585** (2000) 741 [[hep-ph/0004013](#)].
- [100] C. Bogner and S. Weinzierl, “Resolution of singularities for multi-loop integrals,” *Comput. Phys. Commun.* **178** (2008) 596 [[arXiv:0709.4092 \[hep-ph\]](#)].
- [101] C. Bogner, “Mathematical aspects of Feynman integrals,” PhD, Mainz (2009).

- [102] E. Panzer, “Algorithms for the symbolic integration of hyperlogarithms with applications to Feynman integrals,” *Comput. Phys. Commun.* **188** (2015) 148 [arXiv:1403.3385 [hep-th]].
- [103] E. Panzer, “Feynman integrals and hyperlogarithms,” PhD, Humboldt-Universität zu Berlin [arXiv:1506.07243 [math-ph]].
- [104] A. Georgoudis, V. Goncalves, E. Panzer and R. Pereira, “Five-loop massless propagator integrals,” arXiv:1802.00803 [hep-th].
- [105] O. Schnetz, “Graphical functions and single-valued multiple polylogarithms,” *Commun. Num. Theor. Phys.* **08** (2014) 589 [arXiv:1302.6445 [math.NT]].
- [106] M. Golz, E. Panzer and O. Schnetz, “Graphical functions in parametric space,” *Lett. Math. Phys.* **107** (2017) no.6, 1177 [arXiv:1509.07296 [math-ph]].
- [107] D. V. Batkovich and M. Kompaniets, “Toolbox for multiloop Feynman diagrams calculations using R^* operation,” *J. Phys. Conf. Ser.* **608** (2015) no.1, 012068 [arXiv:1411.2618 [hep-th]].
- [108] F. Herzog and B. Ruijl, “The R^* -operation for Feynman graphs with generic numerators,” *JHEP* **1705** (2017) 037 [arXiv:1703.03776 [hep-th]].
- [109] J. A. Gracey, T. Luthe and Y. Schroder, “Four loop renormalization of the Gross-Neveu model,” *Phys. Rev. D* **94** (2016) no.12, 125028 [arXiv:1609.05071 [hep-th]].
- [110] J. A. Gracey, “Large N critical exponents for the chiral Heisenberg Gross-Neveu universality class,” arXiv:1801.01320 [hep-th].
- [111] L. N. Mihaila, N. Zerf, B. Ihrig, I. F. Herbut and M. M. Scherer, “Gross-Neveu-Yukawa model at three loops and Ising critical behavior of Dirac systems,” *Phys. Rev. B* **96** (2017) no.16, 165133 [arXiv:1703.08801 [cond-mat.str-el]].
- [112] N. Zerf, L. N. Mihaila, P. Marquard, I. F. Herbut and M. M. Scherer, “Four-loop critical exponents for the Gross-Neveu-Yukawa models,” *Phys. Rev. D* **96** (2017) no.9, 096010 [arXiv:1709.05057 [hep-th]].
- [113] P. A. Baikov, K. G. Chetyrkin and J. H. Kühn, “Five-Loop Running of the QCD coupling constant,” *Phys. Rev. Lett.* **118** (2017) no.8, 082002 [arXiv:1606.08659 [hep-ph]].
- [114] T. Luthe, A. Maier, P. Marquard and Y. Schröder, “Five-loop quark mass and field anomalous dimensions for a general gauge group,” *JHEP* **1701** (2017) 081 [arXiv:1612.05512 [hep-ph]].
- [115] T. Luthe, A. Maier, P. Marquard and Y. Schröder, “Complete renormalization of QCD at five loops,” *JHEP* **1703** (2017) 020 [arXiv:1701.07068 [hep-ph]].
- [116] F. Herzog, B. Ruijl, T. Ueda, J. A. M. Vermaseren and A. Vogt, “The five-loop beta function of Yang-Mills theory with fermions,” *JHEP* **1702** (2017) 090 [arXiv:1701.01404 [hep-ph]].

-
- [117] K. G. Chetyrkin, G. Falcioni, F. Herzog and J. A. M. Vermaseren, “Five-loop renormalisation of QCD in covariant gauges,” *JHEP* **1710** (2017) 179; Addendum: [*JHEP* **1712** (2017) 006] [[arXiv:1709.08541](#) [hep-ph]].
- [118] T. Luthe, A. Maier, P. Marquard and Y. Schroder, “The five-loop Beta function for a general gauge group and anomalous dimensions beyond Feynman gauge,” *JHEP* **1710** (2017) 166 [[arXiv:1709.07718](#) [hep-ph]].
- [119] D. V. Batkovich, K. G. Chetyrkin and M. V. Kompaniets, “Six loop analytical calculation of the field anomalous dimension and the critical exponent η in $O(n)$ -symmetric ϕ^4 model,” *Nucl. Phys. B* **906** (2016) 147 [[arXiv:1601.01960](#) [hep-th]].
- [120] M. Kompaniets and E. Panzer, “Renormalization group functions of ϕ^4 theory in the MS-scheme to six loops,” *PoS LL* **2016** (2016) 038 [[arXiv:1606.09210](#) [hep-th]].
- [121] M. V. Kompaniets and E. Panzer, “Minimally subtracted six loop renormalization of $O(n)$ -symmetric ϕ^4 theory and critical exponents,” *Phys. Rev. D* **96** (2017) no.3, 036016 [[arXiv:1705.06483](#) [hep-th]].
- [122] O. Schnetz, “Numbers and Functions in Quantum Field Theory,” *Phys. Rev. D* **97** (2018) no.8, 085018 [[arXiv:1606.08598](#) [hep-th]].
- [123] C. Marboe and V. Velizhanin, “Twist-2 at seven loops in planar $\mathcal{N} = 4$ SYM theory: full result and analytic properties,” *JHEP* **1611** (2016) 013 [[arXiv:1607.06047](#) [hep-th]].
- [124] C. Bogner, S. Borowka, T. Hahn, G. Heinrich, S. P. Jones, M. Kerner, A. von Manteuffel, M. Michel, E. Panzer and V. Papara, “Loopedia, a Database for Loop Integrals,” *Comput. Phys. Commun.* **225** (2018) 1 [[arXiv:1709.01266](#) [hep-ph]].
- [125] S. Teber, “Electromagnetic current correlations in reduced quantum electrodynamics,” *Phys. Rev. D* **86** (2012) 025005 [[arXiv:1204.5664](#) [hep-ph]].
- [126] A. V. Kotikov and S. Teber, “Note on an application of the method of uniqueness to reduced quantum electrodynamics,” *Phys. Rev. D* **87** (2013) 087701 [[arXiv:1302.3939](#) [hep-ph]].
- [127] A. V. Kotikov and S. Teber, “Two-loop fermion self-energy in reduced quantum electrodynamics and application to the ultrarelativistic limit of graphene,” *Phys. Rev. D* **89** (2014) 065038 [[arXiv:1312.2430](#) [hep-ph]].
- [128] S. Teber, “Two-loop fermion self-energy and propagator in reduced QED_{3,2},” *Phys. Rev. D* **89** (2014) 067702 [[arXiv:1402.5032](#) [hep-ph]].
- [129] S. Teber and A. V. Kotikov, “Field theoretic renormalization study of reduced quantum electrodynamics and applications to the ultrarelativistic limit of Dirac liquids,” *Phys. Rev. D* **97** (2018) no.7, 074004 [[arXiv:1801.10385](#) [hep-th]].
- [130] S. Teber and A. V. Kotikov, “Interaction corrections to the minimal conductivity of graphene via dimensional regularization,” *Europhys. Lett.* **107** (2014) 57001 [[arXiv:1407.7501](#) [cond-mat.mes-hall]].

- [131] S. Teber and A. V. Kotikov, “Field theoretic renormalization study of interaction corrections to the universal ac conductivity of graphene,” [arXiv:1802.09898 \[cond-mat.mes-hall\]](#).
- [132] S. Teber and A. V. Kotikov, “The method of uniqueness and the optical conductivity of graphene: new application of a powerful technique for multi-loop calculations,” *Theoretical and Mathematical Physics* **190** (2017) 446 [*Teor. Mat. Fiz.* **190** (2017) no.3, 519] [[arXiv:1602.01962 \[hep-th\]](#)].
- [133] A. V. Kotikov, “Critical behavior of 3D electrodynamics,” *JETP Lett.* **58** (1993) 731 [*Zh. Eksp. Teor. Fiz.* **58** (1993) 785]. “On the Critical Behavior of (2+1)-Dimensional QED,” *Phys. Atom. Nucl.* **75** (2012) 890 [[arXiv:1104.3888 \[hep-ph\]](#)].
- [134] A. V. Kotikov, V. I. Shilin and S. Teber, “Critical behaviour of (2 + 1)-dimensional QED: $1/N_f$ -corrections in the Landau gauge,” *Phys. Rev. D* **94** (2016) 056009 [[arXiv:1605.01911 \[hep-th\]](#)].
- [135] A. V. Kotikov and S. Teber, “Critical behavior of (2 + 1)-dimensional QED: $1/N_f$ corrections in an arbitrary nonlocal gauge,” *Phys. Rev. D* **94** (2016) no.11, 114011 [[arXiv:1609.06912 \[hep-th\]](#)].
- [136] A. V. Kotikov and S. Teber, “Critical behaviour of reduced QED_{4,3} and dynamical fermion gap generation in graphene,” *Phys. Rev. D* **94** (2016) no.11, 114010 [[arXiv:1610.00934 \[hep-th\]](#)].
- [137] A. V. Kotikov and S. Teber, “New results for a two-loop massless propagator-type Feynman diagram,” *Teor. Mat. Fiz.* **194** (2018) no.2, 331 [[arXiv:1611.07240 \[hep-th\]](#)].
- [138] H. A. Chawdhry, M. A. Lim and A. Mitov, “Two-loop five-point massless QCD amplitudes within the IBP approach,” [arXiv:1805.09182 \[hep-ph\]](#).
- [139] D. I. Kazakov, “Analytical Methods For Multiloop Calculations: Two Lectures On The Method Of Uniqueness,” *JINR-E2-84-410*.
- [140] G. Leibbrandt, “Introduction to the Technique of Dimensional Regularization,” *Rev. Mod. Phys.* **47** (1975) 849.
- [141] S. Narison, “Techniques of Dimensional Renormalization and Applications to the Two Point Functions of QCD and QED,” *Phys. Rept.* **84** (1982) 263.
- [142] W. B. Kilgore, “Regularization Schemes and Higher Order Corrections,” *Phys. Rev. D* **83** (2011) 114005 [[arXiv:1102.5353 \[hep-ph\]](#)].
- [143] G. Passarino and M. J. G. Veltman, “One Loop Corrections for e+ e- Annihilation Into mu+ mu- in the Weinberg Model,” *Nucl. Phys. B* **160** (1979) 151.
- [144] A. Denner, “Techniques for calculation of electroweak radiative corrections at the one loop level and results for W physics at LEP-200,” *Fortsch. Phys.* **41** (1993) 307 [[arXiv:0709.1075 \[hep-ph\]](#)].
- [145] V. Shtabovenko, R. Mertig and F. Orellana, “New Developments in FeynCalc 9.0,” *Comput. Phys. Commun.* **207** (2016) 432 [[arXiv:1601.01167 \[hep-ph\]](#)].

-
- [146] R. Mertig, M. Bohm and A. Denner, “FEYN CALC: Computer algebraic calculation of Feynman amplitudes,” *Comput. Phys. Commun.* **64** (1991) 345.
- [147] T. Hahn and M. Perez-Victoria, “Automatized one loop calculations in four-dimensions and D-dimensions,” *Comput. Phys. Commun.* **118**, 153 (1999) [[hep-ph/9807565](#)].
- [148] T. Hahn, “Generating Feynman diagrams and amplitudes with FeynArts 3,” *Comput. Phys. Commun.* **140** (2001) 418 [[hep-ph/0012260](#)].
- [149] T. Hahn, “New features in FormCalc 4,” *Nucl. Phys. Proc. Suppl.* **135**, 333 (2004) [[hep-ph/0406288](#)]. [[hep-ph/0406288](#)].
- [150] S. G. Gorishnii and A. P. Isaev, “On an Approach to the Calculation of Multiloop Massless Feynman Integrals,” *Theor. Math. Phys.* **62** (1985) 232 [*Teor. Mat. Fiz.* **62** (1985) 345].
- [151] N. I. Usyukina, “On a Representation for Three Point Function,” *Teor. Mat. Fiz.* **22** (1975) 300.
- [152] E. E. Boos and A. I. Davydychev, “A Method of the Evaluation of the Vertex Type Feynman Integrals,” *Moscow Univ. Phys. Bull.* **42N3** (1987) 6 [*Vestn. Mosk. Univ. Fiz. Astron.* **28N3** (1987) 8].
- [153] A. I. Davydychev, “Some exact results for N point massive Feynman integrals,” *J. Math. Phys.* **32** (1991) 1052 [[pdf](#)].
- [154] A. I. Davydychev, “Recursive algorithm of evaluating vertex type Feynman integrals,” *J. Phys. A* **25** (1992) 5587 [[pdf](#)].
- [155] A. I. Davydychev and J. B. Tausk, “Two loop selfenergy diagrams with different masses and the momentum expansion,” *Nucl. Phys. B* **397** (1993) 123 [[pdf](#)].
- [156] P. A. Baikov and K. G. Chetyrkin, “Four Loop Massless Propagators: An Algebraic Evaluation of All Master Integrals,” *Nucl. Phys. B* **837** (2010) 186 [[arXiv:1004.1153](#) [[hep-ph](#)]].
- [157] A. G. Grozin, “Massless two-loop self-energy diagram: Historical review,” *Int. J. Mod. Phys. A* **27** (2012) 1230018 [[arXiv:1206.2572](#) [[hep-ph](#)]].
- [158] L. Adams, C. Bogner, E. Chaubey, A. Schweitzer and S. Weinzierl, “Differential equations for Feynman integrals beyond multiple polylogarithms,” [arXiv:1712.03532](#) [[hep-ph](#)].
- [159] M. Hidding and F. Moriello, “All orders structure and efficient computation of linearly reducible elliptic Feynman integrals,” [arXiv:1712.04441](#) [[hep-ph](#)]; L. Adams, E. Chaubey and S. Weinzierl, “The planar double box integral for top pair production with a closed top loop to all orders in the dimensional regularisation parameter,” [arXiv:1804.11144](#) [[hep-ph](#)].
- [160] J. Fleischer, A. V. Kotikov and O. L. Veretin, “Analytic two loop results for selfenergy type and vertex type diagrams with one nonzero mass,” *Nucl. Phys. B* **547** (1999) 343 [[hep-ph/9808242](#)].

- [161] A. Kotikov, J. H. Kuhn and O. Veretin, “Two-Loop Formfactors in Theories with Mass Gap and Z-Boson Production,” *Nucl. Phys. B* **788** (2008) 47 [[hep-ph/0703013](#)].
- [162] A. V. Kotikov and L. N. Lipatov, “NLO corrections to the BFKL equation in QCD and in supersymmetric gauge theories,” *Nucl. Phys. B* **582** (2000) 19 [[hep-ph/0004008](#)].
- [163] A. V. Kotikov and L. N. Lipatov, “DGLAP and BFKL evolution equations in the N=4 supersymmetric gauge theory,” [[hep-ph/0112346](#)]; “DGLAP and BFKL equations in the $N = 4$ supersymmetric gauge theory,” *Nucl. Phys. B* **661** (2003) 19 Erratum: [*Nucl. Phys. B* **685** (2004) 405] [[hep-ph/0208220](#)].
- [164] A. V. Kotikov, “The Property of maximal transcendentality in the N=4 Supersymmetric Yang-Mills,” In *Diakonov, D. (ed.): Subtleties in quantum field theory* 150-174 [[arXiv:1005.5029](#) [[hep-th](#)]]; “The property of maximal transcendentality: Calculation of anomalous dimensions in the $\mathcal{N} = 4$ SYM and master integrals,” *Phys. Part. Nucl.* **44** (2013) 374; “The property of maximal transcendentality: calculation of master integrals,” *Theor. Math. Phys.* **176** (2013) 913 [[arXiv:1212.3732](#) [[hep-ph](#)]]; “The property of maximal transcendentality: calculation of Feynman integrals,” *Theor. Math. Phys.* **190** (2017) no.3, 391 [[arXiv:1601.00486](#) [[hep-ph](#)]].
- [165] M. Y. Kalmykov, B. A. Kniehl, B. F. L. Ward and S. A. Yost, “Hypergeometric functions, their epsilon expansions and Feynman diagrams,” [arXiv:0810.3238](#) [[hep-th](#)]; M. Y. Kalmykov and B. A. Kniehl, “‘Sixth root of unity’ and Feynman diagrams: Hypergeometric function approach point of view,” *Nucl. Phys. Proc. Suppl.* **205-206** (2010) 129 [[arXiv:1007.2373](#) [[math-ph](#)]].
- [166] A. P. Isaev, “Multiloop Feynman integrals and conformal quantum mechanics,” *Nucl. Phys. B* **662** (2003) 461 [[hep-th/0303056](#)].
- [167] D. I. Kazakov and A. V. Kotikov, “Correction to DIS Cross-section Ratio $R = \Sigma^{-1} / \sigma^{-t}$ in QCD,” *Yad. Fiz.* **46** (1987) 1767.
- [168] P. Heslop and V. V. Tran, “Multi-Particle Amplitudes from the Four-Point Correlator in Planar N=4 SYM,” [arXiv:1803.11491](#) [[hep-th](#)].
- [169] A. V. Kotikov, “New method of massive Feynman diagrams calculation,” *Mod. Phys. Lett. A* **6** (1991) 677.
- [170] A. V. Kotikov, “New method of massive Feynman diagrams calculation. Vertex type functions,” *Int. J. Mod. Phys. A* **7** (1992) 1977.
- [171] J. M. Henn and J. C. Plefka, “Scattering Amplitudes in Gauge Theories,” *Lect. Notes Phys.* **883** (2014) pp.1.
- [172] F. Carlson, “Sur une classe de séries de Taylor” Dissertation, Uppsala, Sweden (1914).
- [173] E. Panzer, “On the analytic computation of massless propagators in dimensional regularization,” *Nucl. Phys. B* **874**, 567 (2013) [[arXiv:1305.2161](#) [[hep-th](#)]].

-
- [174] R. N. Lee and K. T. Mingulov, “DREAM, a program for arbitrary-precision computation of dimensional recurrence relations solutions, and its applications,” [arXiv:1712.05173 \[hep-ph\]](#).
- [175] S. Teber, “Field theoretic study of electron-electron interaction effects in Dirac liquids”, Habilitation, Sorbonne Université (2017).
- [176] A. L. Pismensky, “Calculation of critical index η of the φ^3 -theory in four-loop approximation by the conformal bootstrap technique,” *Int. J. Mod. Phys. A* **30** (2015) no.24, 1550138 [[arXiv:1511.03211 \[hep-th\]](#)].
- [177] O. Mamroud and G. Torrents, “RG stability of integrable fishnet models,” *JHEP* **1706** (2017) 012 [[arXiv:1703.04152 \[hep-th\]](#)].